CHAPTER 5 GENERALISATION OF DEPOSITION

Introduction

There is a difference between deposition modelling and long-range transport modelling, i.e. the focus of the two is different: deposition modelling is aimed at estimating the input to ecosystems as accurately as possible; long-range transport modelling, on the other hand, is aimed at determining the distribution of pollutants (concentration and deposition) based on emission estimates and dispersion calculations. In long-range transport modelling, deposition is a loss term in which the accuracy needed is dependent on the modelled scale. When both the pollution distribution and the deposition needs to be known as accurately as possible, a compromise is required on the detail some of the aspects will be modelled in order to take the main processes determining transport and deposition into account. In applying abatement strategies on a national or European scale, it is desirable to know both the deposition and the distribution of pollution as accurately as possible. When emission abatement strategies are based on the critical load concept, the deposition has to be determined on the ecosystem level. Desired emission reductions based on the target levels should be known per country and/or per individual source or activity. Therefore, long-range transport modelling and ecosystem-scale deposition modelling should be linked. In this chapter we will show two examples of this combination in the Netherlands and in Europe. The deposition model used here to determine the deposition in the Netherlands is DEADM (Dutch Empirical Acid Deposition Model) and in Europe, the EDACS model (Estimation of Deposition of Acidifying Components in Europe). Wet deposition in these models is estimated using interpolation of wet deposition measurements. Dry deposition is determined using the inferential technique (Hicks *et al*, 1987). The dry deposition flux is inferred from interpolated concentrations and land-use-specific dry deposition velocities. The resistance framework used in the inferential technique is already extensively described in Chapter 4 and will not be explained here. First, we will explain the need for local-scale modelling. The application and results for the Netherlands will be given followed by a discussion on the European application and results. At the end of this chapter, a section will be devoted to the variation in deposition over several years. Current deposition estimates will be compared to an estimate of the 'natural background deposition' and to historical deposition measurements.

5.1 LOCAL-SCALE DEPOSITION MAPS, WHAT'S THE USE?

The need for small-scale deposition data for many parts of Europe is obvious from the strong variations in deposition observed within a grid due to variation in concentration and receptor characteristics. Concentrations might vary strongly in or near source regions. This is especially the case for gases emitted from low-level sources, such as ammonia and nitrogen oxides. Strong variations in deposition are also a consequence of variation in landscape and surface roughness.

There is a need to identify ecosystems with high local deposition and low critical loads. Most very sensitive ecosystems are located near source areas for the Netherlands. This is illustrated in Table 5.1 where 10 x 10 km grid total acid deposition loads (Erisman, 1992; 1993a) are averaged for each median value critical load for these grids (Hettelingh *et al.*, 1991). The table shows the correlation between critical loads and acid loads. It is obvious that areas in the Netherlands with low critical loads often have the highest acid deposition. For nitrogen species, this situation will be even more pronounced, at least for the Netherlands or other regions with small nature conservation areas and scattered sources or source areas of ammonia.

TABLE 5.1 Number of grid cells (10 x 10 km) in the Netherlands with median critical loads, divided into classes, and the average and standard deviation of the acid loads for the grid cells in each class

Median critical load (mol H^+ ha^{-1} a^{-1})	Acid deposition (mol H^+ ha^{-1} a^{-1})	Standard deviation of acid deposition	Number of grid cells
< 1000	4450	1180	100
1000 - 1500	4730	1480	167
1500 - 2400	4010	970	43
2400 - 3000	4000	890	29
> 3000	3540	770	98

If 1 or 5 percentile critical load values are used instead of median values, the anti-correlation between critical loads and actual loads will be even higher. Another similar problem is the correlation between low critical loads for sulphur and nitrogen to forest soils, and the high deposition of these pollutants to forest ecosystems. These problems are not overcome by the use of so-called filtering factors. Filtering factors are estimated as throughfall deposition divided by open field wet deposition, obtained from different throughfall measurements in European forests. This implies that the filtering factor accounts for the dry deposition onto the forest and that there is a relation between dry deposition and wet deposition. Both assumptions are not valid, as is explained in Chapter 6.2. The use of filtering factors can lead to serious errors. This is demonstrated by comparing deposition to ecosystems within EMEP

grids in the Netherlands (obtained using filtering factors) with the small-scale estimates by Erisman (1993a), cf. Figure 5.1. This figure clearly shows the large variation of deposition of sulphur and nitrogen species within an EMEP (150 x 150 km) grid cell. Generally, this will mean that by taking measures based on exceedances estimated on large grids corrected with filtering factors, the deposition reduction will not lead to the necessary reduction.

The appropriate exceedance maps will be obtained when deposition estimates are available at least on the same scale as the critical loads, i.e. generally in the order of 10 x 10 km to 50 x 50 km resolution.

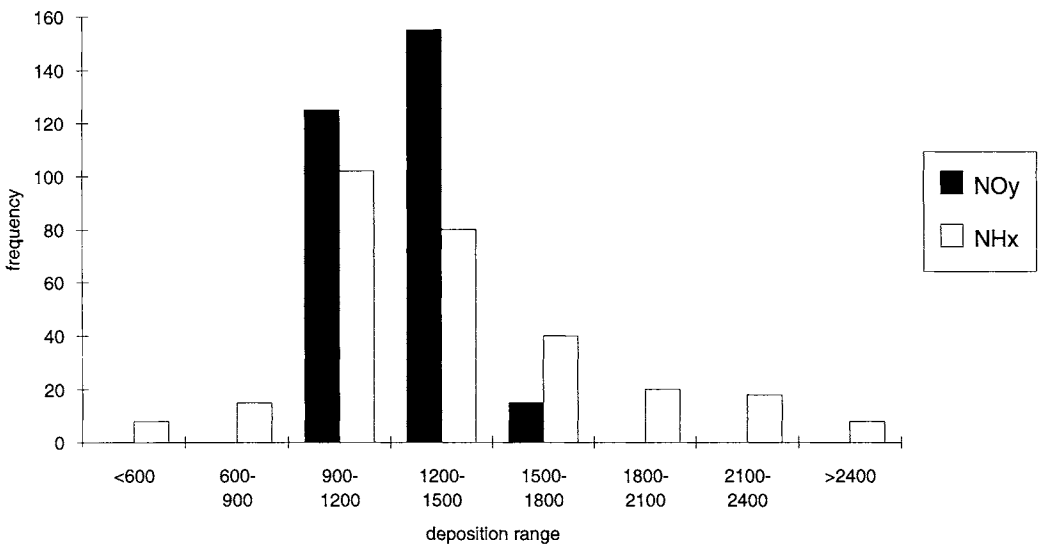

FIGURE 5.1 Frequency distribution of deposition on a small scale (5 x 5 km) within an EMEP grid (150 x 150 km) for nitrogen compounds. Using EMEP model results together with the appropriate filtering factor, we estimate total nitrogen deposition to this grid at 1650 mol ha^{-1} a^{-1}.

5.2 DEPOSITION MODELLING IN THE NETHERLANDS

5.2.1 DEADM

The Dutch Empirical Acid Deposition Model (DEADM) to describe the deposition of acidifying components on a small scale in the Netherlands has been developed and extensively evaluated (Erisman, 1992; 1993a; 1993b). The model has a wet and dry deposition module. Wet deposition fluxes are obtained directly from precipitation measurements at 14 monitoring locations in the Netherlands. Annual average wet deposition fluxes for each monitoring station are interpolated on a 10 x 10 km grid above the Netherlands. Dry deposition is inferred from measured air concentrations, meteorological parameters, surface resistances and surface roughness. Air concentrations (SO_2, NO, NO_2, HNO_2, HNO_3, HCl and aerosols) and meteorological parameters (global radiation, temperature, wind direction/speed, precipitation) are obtained from the National Air Quality Monitoring Network and extended with measurements made by other institutes. For NH_3 and NH_4 air concentrations, results of model calculations are used (Asman and Van Jaarsveld, 1992). These were calculated for each 5 x 5 km grid over the Netherlands using emission estimates for the Netherlands (Van der Hoek, 1994) and Europe (Asman, 1992) and seasonal and daily variations in the emission (Asman, 1992). Annual average values are used as input for DEADM, together with monthly and daily variations in concentration obtained from the monitoring network (Van Elzakker *et al.*, 1994). Relative monthly variations were estimated for highly polluted areas (annual concentration above 15 $\mu g\ m^{-3}$) and less polluted areas (annual concentration below 15 $\mu g\ m^{-3}$) from data from the eight sites of the ammonia concentration monitoring network. Also, average daily variations were derived for each month. These could be explained by the monthly average concentration, temperature and wind speed variations during the day, again for highly polluted areas (72% variance accounted for) and less polluted areas (83% variance accounted for) (Bleeker and Erisman, 1994). The monthly average concentration and the daily variation in concentration for each grid cell can thus be estimated. The average daily variation in V_d was estimated for each month using the resistance analogy (see below). The average daily variations of V_d were multiplied by the average daily variations in concentration for each grid to estimate monthly and annual average fluxes.

Detailed land-use information is used to characterise roughness lengths and to determine surface resistances, together with other surface conditions. The roughness length for forests is related to tree species, mean tree height and crown coverage of the forest stand; this was estimated separately for summer and winter months (Erisman, 1990; 1992). Wind and concentration fields were obtained for every two hours via extrapolation of the measurements at each individual station, or from model results (in the case of ammonia) to a height of 50 m and subsequent interpolation onto a grid system reaching across the Netherlands. The 50-m height is chosen because it is assumed that at this height concentration and wind speed are not substantially influenced by surface characteristics. For each 1 x 1 km grid, u_* and L are

calculated using the meteorological data and the schemes provided by Beljaars and Holtslag (1990). From u_* and L, R_a and R_b can be estimated. With the land-use information and estimation of the surface condition (wet/dry, stomata open or closed, etc.), component-specific surface resistances or surface-exchange parametrisations (see section 4.2) and, subsequently, dry deposition velocities are determined (Erisman, 1993a, Erisman *et al.*, 1994) for each 1 x 1 km grid in the Netherlands. Accordingly, two-hour averaged fluxes are calculated by multiplying V_d with the concentrations. Total annual deposition is calculated by summing the average dry and wet deposition obtained in each time step.

The Netherlands is divided in 20 so-called acidification areas as shown in Figure 5.2. Deposition is determined for each acidification area. These areas are also used in the Dutch Acidification System (DAS) model used for scenario analysis and policy development (Heij and Schneider, 1991).

1 = Groningen
2 = Friesland
3 = Drenthe
4 = W/NO-Overijssel
5 = ZO-Overijssel
6 = NW-Gelderland
7 = NO-Gelderland
8 = Z-Gelderland
9 = Utrecht
10 = N-Noord Holland
11 = Z-Noord Holland, Flevopolder
12 = N-Zuid Holland
13 = Z-Zuid Holland
14 = Zeeland
15 = W-Noord Brabant
16 = Midden-Noord Brabant
17 = NO-Noord Brabant
18 = ZO-Noord Brabant
19 = N-Limburg
20 = Z/Midden Limburg

FIGURE 5.2 Distribution of the acidification areas over the Netherlands.

The deposition of acidifying components in the Netherlands was calculated with the DEADM model for the years 1980 to 1993. Total potential acid, the maximum acid load to soils, or the amount of acidifying components removed from the atmosphere by deposition, is defined as (see also Chapter 1):

$$\text{Total potential acid} = 2\text{SOx} + \text{NOy} + \text{NHx} \qquad [5.1]$$

This is the maximum load as it is assumed that NH_3 and NH_4 are completely nitrified in the soil (Van Breemen *et al.*, 1982). Furthermore, it is assumed that deposited neutralised aerosols lead to acidification. HCl, organic acids, PAN, H_2S and HF are not taken into account. These are considered of minor importance for the present potential acid deposition loads.

5.2.2 WET DEPOSITION

The concentrations of components in precipitation are monitored in the LML on a monthly basis (KNMI/RIVM, 1987; RIVM, 1989). The amount of precipitation is monitored at the same locations using official rain gauges of KNMI. Up to 1988, precipitation samples were collected using bulk samplers. At the beginning of 1988 these were replaced by wet-only samplers. In wet-only samplers dry deposition onto the funnel during dry periods is excluded. Corrections for the dry deposition to bulk samplers have been estimated on the basis of parallel measurements done with the two samplers. In this study the main focus is on the estimation of *potential acid* deposition. As the wet deposition fluxes measured also contain dissolved neutral salts, their contribution to the ion composition of the sample have to be identified and subtracted from the total.

Dry deposition in bulk samplers
If open samplers are used, dry deposition onto the funnels of the device influences the results (see section 3.1). For the monthly open field measurements it was found that in the Netherlands an average of 25% of the wet deposition fluxes of SO_4^{2-} and NH_4 measured by open samplers was due to dry deposition, whereas for NO_3^- this was only 15% (Ridder *et al.*, 1984). The 1980 - 1987 data from bulk samplers were therefore corrected by these correction factors.

Neutral salts
The potential acid deposition from precipitation can be calculated from the volume weighted average deposition of $H^+ + 2\ NH_4^+$, where NH_4^+ originates both from gaseous NH_3 and particulate NH_4^+ dissolved in rain water. Particulate NH_4^+ can be associated to both SO_4^{2-} and NO_3^-, but their origins in terms of source contributions cannot be ascertained. However, when the molar equivalent ratio of NH_4^+ to that of $NO_3^- + SO_4^{2-}$ is near to one, which is the case under Dutch circumstances, the origin can be obtained from the amount of SO_4^{2-} and NO_3^- in the samples. In this procedure, the sulphate levels are corrected for the (neutral) sea salt contribution. Buijsman (1990) in comparing fluxes of potential acid calculated by $H^+ + 2\ NH_4^+$ and $2\ SO_4^{2-} + NO_3^- + NH_4^+$ showed that the agreement was very good, provided a correction was also made for the Ca^{2+} contribution to the neutralisation of the sample:

$$\text{Total potential acid} = NH_4^+ + NO_3^- + 2\ SO_4^{2-} - 2\ Ca^{2+} \qquad [5.2]$$

The Cl^- compound in precipitation is almost completely associated to Na^+ and is therefore of sea-salt origin.

In order to determine the relative source contributions to the total potential acid by SO_4^{2-}, NO_3^- and NH_4^+, the origin of Ca^{2+} in the samples has to be identified. Unfortunately, Buijsman (1990) does not refer to the source or form of Ca^{2+} in the samples. The source of Ca^{2+} can either be dissolved aerosol in rain, or dry deposition of road dust or sea salt onto the funnels. The large correction factor for open samplers of 0.45 (Table 3.1) suggests that dry deposition is the most important source in open samplers. The contribution of Ca^{2+} to SO_4^{2-}, NO_3^- and Cl^- in rain water was investigated by Slanina *et al.* (1982) using a cluster analysis on 24-hour averaged rain samples. At two locations, near to the coast and in the centre of the Netherlands, results from eight wet-only samplers were investigated. From the results it was estimated that for the continental location, 11% of SO_4^{2-} and 22% of NO_3^- is related to Ca^{2+}. For the coastal site this is 11% and 0%, respectively, for SO_4^{2-} and NO_3^-. No Ca^{2+} seems to be connected to Cl^- (Slanina *et al.*, 1990). Information on the contribution of $CaCO_3$ to the amount of Ca^{2+} in precipitation could not be found in the literature. In this study, Ca^{2+} was only attributed to sulphate and nitrate. Taking yearly average fluxes at these sites, as reported by Slanina (1985) for the continental site and by RIVM (1989) for a coastal site, it was estimated that for the coastal site 50% of Ca^{2+} originates from SO_4^{2-} and 50% from NO_3^-, whereas all Ca^{2+} originates from SO_4^{2-} at the continental site. These are all results obtained from wet-only measurements not influenced by dry deposition.

Calculation procedure

The procedure for correcting fluxes of SO_4^{2-} and NO_3^- for Ca^{2+} and sea salt (SO_4^{2-}), as followed here, is first correcting Ca^{2+}, Na^+, SO_4^{2-} and NO_3^- for dry deposition contribution (open samplers) and then applying the correction to Ca^{2+} and sea salt (0.06 times the Na^+ concentration based on the concentration ratio of SO_4^{2-} and Na^+ in sea water). This leads to the following equations on molar basis for coastal sites:

$$[SO_4^{2-}]_c = d1 * SO_4^{2-} - 0.5 * d2 * Ca^{2+} - 0.06 * d3 * Na^+ \quad [5.3]$$
$$[NO_3^-]_c = d4 * NO_3^- - 0.5 * d2 * Ca^{2+}$$
$$[NH_4^+]_c = d5 * NH_4^+$$

and for continental sites:

$$[SO_4^{2-}]_c = d1 * SO_4^{2-} - d2 * Ca^{2+} - 0.06 * d3 * Na^+ \quad [5.4]$$
$$[NO_3^-]_c = d4 * NO_3^-$$
$$[NH_4^+]_c = d5 * NH_4^+$$

where the subscript *c* denotes corrected fluxes and *d1* to *d5* the appropriate dry deposition factors listed in Table 3.1. For those years where wet-only samplers were used (from 1988 onwards), the dry deposition factors in Eqn. (5.3) and (5.4) are taken as 1.

Wet deposition estimates
The yearly average wet deposition fluxes for each monitoring station in the Netherlands (20 stations in 1980 and 14 in 1987 and successive years) were calculated by multiplying the concentrations by the amount of rain measured with the official KNMI rain gauges. The fluxes were interpolated onto a 10 x 10 km grid reaching across the country. In this way local fluxes were estimated assuming that the amount and composition of precipitation is independent on the structure of the surface. Furthermore, it was assumed that rain-out of gases from local sources is negligible.

The wet deposition maps for the Netherlands in 1993 are shown in Figures 5.3 for SOx, NOy, NHx and potential acid, respectively. Wet deposition fluxes for the years 1980-1993 are presented in Table 5.2. The average wet deposition fluxes for each acidification region in the Netherlands in 1980 and 1993 are listed in Tables 5.5 and 5.6, respectively, shown later in this chapter.

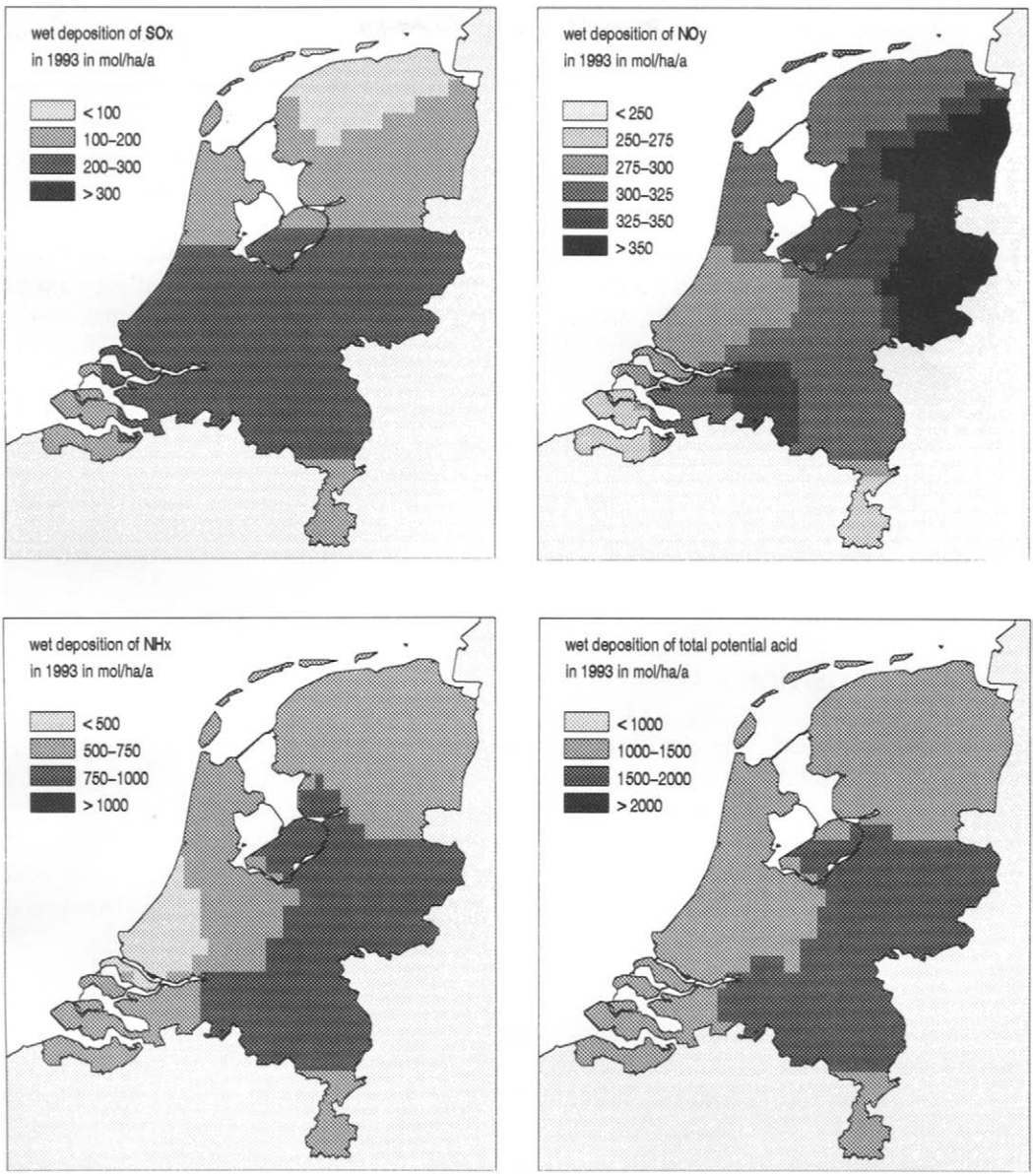

FIGURE 5.3 The spatial distribution of the wet deposition of SOx, NOy, NHx and potential acid in 1993 (mol ha^{-1} a^{-1}).

TABLE 5.2 Country average dry, wet and total deposition of SOx, NOy, NHx, total nitrogen and potential acid in 1980 - 1993 (mol ha^{-1} a^{-1})

	SOx			NOy			NHx			Total N			Total potential acid		
	dry	wet	total	dry	wet	total	dry	wet	total	dry	wet	total	dry	wet	total
1980*	1750	320	2070	480	390	880	1565	640	2205	2045	1030	3075	5545	1670	7215
1981	1750	320	2070	490	390	880	1565	640	2205	2055	1030	3085	5555	1670	7225
1982	1510	295	1805	515	360	875	1600	630	2230	2115	990	3105	5135	1580	6715
1983	1470	275	1705	523	355	885	1560	680	2240	2083	1035	3118	5023	1585	6608
1984	1430	280	1830	530	360	870	1620	665	2285	2150	1025	3175	5010	1585	6595
1985	1550	275	1565	510	350	830	1615	715	2330	2125	1065	3190	5225	1615	6840
1986	1290	275	1435	480	370	840	1475	735	2210	1955	1105	3060	4535	1655	6190
1987	1030	280	1310	455	395	850	1640	760	2400	2095	1155	3250	4155	1715	5870
1988	750	225	975	445	305	750	1555	625	2180	2000	930	2930	3500	1380	4880
1989	620	225	845	455	305	760	1505	625	2130	1960	930	2890	3200	1380	4580
1990	615	225	840	445	290	735	1490	680	2170	1935	970	2905	3165	1420	4585
1991	580	190	770	445	255	700	1580	540	2120	2025	795	2820	3185	1175	4360
1992	555	220	775	420	330	750	1245	680	1925	1665	1010	2675	2775	1450	4225
1993	570	190	760	420	320	740	1320	680	2000	1740	1000	2750	2900	1380	4280

* Data for 1980 not available for wet deposition, SO_2 and NH_3; these data have been taken from 1981.

5.2.3 DRY DEPOSITION

Dry deposition of acidifying components and base cations are calculated for the years 1980-1993 using DEADM. An important input to DEADM for estimating small scale dry deposition fluxes is a land-use map and, derived from this, a roughness length map. The z_0 maps will be used for the dry deposition velocity calculations from the inferential technique on a grid basis. Before describing the results of the dry deposition calculations, we will explain the method to estimate the roughness length for the different monitoring stations and for the Netherlands as a whole.

Roughness length maps

Measurements of meteorological parameters, such as wind speed, u, and wind direction, q, are made at 26 stations in the National Air Quality Monitoring Network LML on a routine basis. To date, z_0 values have been estimated, usually by defining landscape classes for which z_0 values are known (Wieringa, 1981). In this section, z_0 values are estimated for each monitoring station from measurements of the standard deviation of wind direction. The second part of this section describes a method to obtain z_0 maps for across the Netherlands from land-use information. Both estimates are used for extrapolating air quality measurements to areas where measurements are lacking.

Values of z_0 for meteorological stations
The values for u and q averaged over one hour are available for each station, as well as σ_θ averaged both over one hour and the last 10 minutes of the hour, as calculated from 12-s average wind direction measurements. Most measurements are made at 10 m height, except for four locations, where the measuring height is 20 m. The monitoring stations are extensively described in the Technical Report of the National Air Quality Monitoring Network (Elskamp, 1989).

A dataset of 10-min average measurements for each LML monitoring station is available from the beginning of 1987. The dataset used here contains about 26,000 hours of σ_θ measurements for each station. Data with non-neutral stability and low wind speed ($u < 4$ m s^{-1}) were identified and rejected. About 40% of the dataset remained for estimating z_0 values. This dataset was subdivided in subsets for four seasons and four wind direction sectors (90°). For each class, σ_θ was averaged. The z_0 values for each classification were then calculated from the class average σ_θ, using Eqn. (3.30). By first averaging σ_θ and then calculating z_0, statistical errors in the results are reduced. Values for each station per season per wind direction sector are listed in Erisman (1990b).

Figure 5.4 shows the calculated z_0 values for station 103 (Steeg) as a function of wind direction (in this case in the 30^0 sectors) and of season. The seasonal influence on z_0 values is clearly demonstrated, with the highest values in spring and summer and lowest in winter. An average z_0 value of 7 cm was calculated for this location. From the classification by Wieringa (1981), z_0 for this location (agricultural area with homogeneous low crops or pastures with spread roughness elements, like isolated trees, low hedges or isolated farms) should be about 0.1 m, which is in good agreement.

Much research has been done on methods for estimating z_0 values at the meteorological tower of Cabauw, KNMI (see e.g. Beljaars, 1988). Beljaars (1988) compared three methods for estimating z_0 values (based on σ_θ, σ_u [standard deviation of wind speed] and wind profile measurements). His estimates for each 30° wind direction sector for summer and winter months are compared to the estimates from the LML dataset in Figure 5.5. Data observed in summer is in very good agreement and in winter in fair, even though data from different years were compared.

Roughness length maps for the Netherlands
Grid average z_0 values (z_{0t}) have been calculated using the method by Van Dop (1983). This method is based on the assumption that the z_0 of a certain area is determined primarily by the roughest subarea within the area considered. Area-weighted averages of the drag coefficient, c_D, for each individual subarea assumed to be homogeneous are determined for the whole area. The area average drag coefficient is then used to calculate z_{0t}.

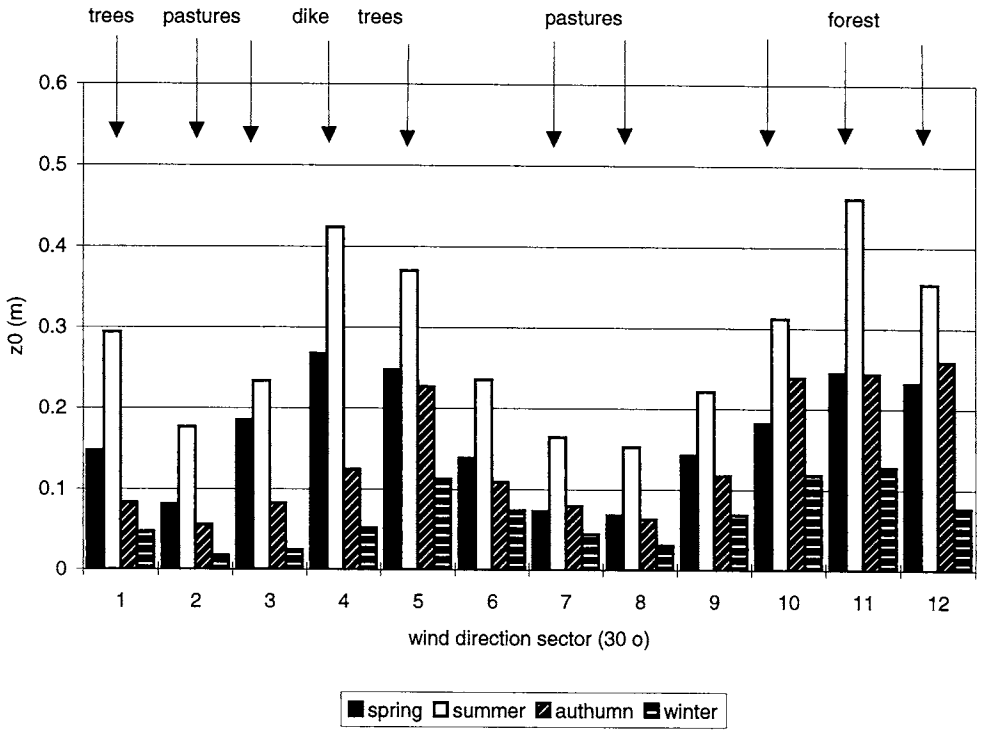

FIGURE 5.4 Values for z_0 as a function of wind direction sector (30^0) and season for the Steeg station (103).

The 10-m drag coefficient for each individual subarea, i, is related to the z_{0i} by (Van Dop, 1983):

$$C_{D,i} = [\frac{0.4}{\ln(\frac{10}{z_{0i}})}]^2 \qquad [5.5]$$

The weighted average C_D for the whole area is calculated from the individual $C_{D,i}$ and the surface area fraction, f_i:

$$C_D = \Sigma_i \; f_i \; C_{D,i} \qquad [5.6]$$

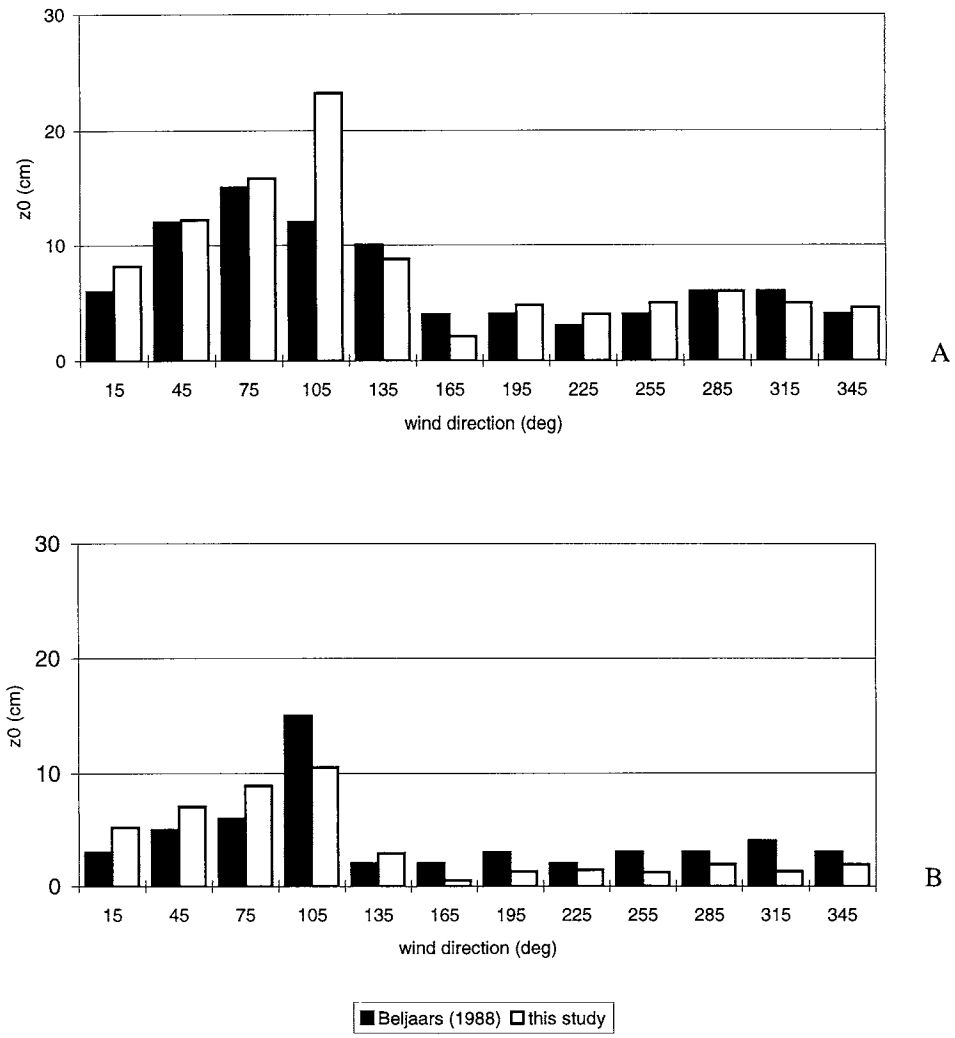

FIGURE 5.5 Values for z_0 as a function of wind direction sector (30^0) for the Cabauw station (620) estimated by Beljaars (1988) and in this study for summer (A) and winter (B) months.

By rearranging Equation (5.5), the average z_0 for this area at 10 m height can be calculated from C_D. The information needed to estimate grid average z_{0t} values from this method are the fraction of the grid covered by the subareas and the z_0 values of these subareas.

A detailed inventory of tree species, height, surface area and crown cover of the Dutch forests is available from the Dutch Forestry Service (SBB, 1985). This inventory was revised and aggregated to classes on a 1 x 1 km grid by Meijers (1990). The following classification was used: closed canopy forests (crown cover > 60%) and open forests (crown cover < 60% and > 20%), subdivided into classes of deciduous and coniferous forests with the average height of the trees and the surface area covered by the canopy. Land-use data for the Netherlands on a 25 x 25 m grid (CBS, 1993) were aggregated to classes on the 1 x 1 km grid for the country. These data have been used for estimating grid average surface resistances according to the parametrisations outlined in Chapter 4. Classes used include open water, forest, bare soil, grassland, agricultural crops, heathland, nature conservation areas and remaining categories. The z_0 values for each individual class were taken from Verver (1986), and Duijm and Van Aalst (1984). It was assumed that z_0 for forests is related to the tree height, h, (Stull, 1988). The classification and z_0 values for each class are listed in Table 5.3. For deciduous forest and agricultural areas, difference between summer and winter was introduced.

Grid average z_{0t} values were calculated from the Eqns. (5.5) and (5.6) and the values in Table 5.3. The z_{0t} values on a 1 x 1 km grid are plotted in Figure 5.6 A and B for z_{0t} values between 0 and 60 cm and greater than 50 cm, respectively. In these maps the forest areas 'Veluwe' and 'Utrechtse Heuvelrug' in the centre of the Netherlands are clearly shown, as well as the urban areas, like Amsterdam, Rotterdam, The Hague, Groningen, etc.

The z_0 values for each LML monitoring station are representative for a measuring height of 10 m and, therefore, represent the roughness characteristics of an area with a radius of about 1 km (100 times the measuring height; Stull, 1988). These values can therefore be compared to the 1 x 1 km averages for the grids in which the LML stations are located (Erisman, 1992). Agreement was found to be reasonable, although large differences can be observed at locations with very small values calculated from σ_θ. These locations are surrounded by pastures only. Measurements at these locations show much lower values than estimated from land use. The reason for this is that the value for agricultural areas (average in the Netherlands) is set to 5-15 cm (see Table 5.3). This is an average value for landscapes consisting of pastures with isolated farms and trees or hedges. When these roughness elements are not present in a landscape, this value will be lower. Large discrepancies are also observed for stations which are surrounded by roughness elements in the near vicinity of the measuring location. No LML wind stations are located in forested or urban areas (see Elskamp, 1989).

TABLE 5.3 Individual roughness elements as z_0 values, with h = the average tree height in m

Classification		z_{0t} (cm)
Surface water (> 25 ha)		1
Surface water (< 25 ha)		8
Agricultural area summer:		15
winter:		5
Urban area		100
Closed canopy forest (> 60% crown coverage):	coniferous:	0.1 h
	deciduous summer:	0.07 h
	winter:	0.05 h
Open canopy forest (> 60% crown coverage):	coniferous:	0.085 h
	deciduous summer:	0.09 h
	winter:	0.06 h

The z_0 values for the 5 x 5 km grids were calculated by taking the 1 x 1 grid z_0 values as individual z_0 values, covering 1 km of the larger grid surfaces. For each grid the drag coefficient and, accordingly, the average z_0 was calculated as described. It must be emphasised that these values are representative for 10 m height, and can be significantly different for other measuring heights. At other heights, roughness elements within a larger or smaller area will be reflected in z_0.

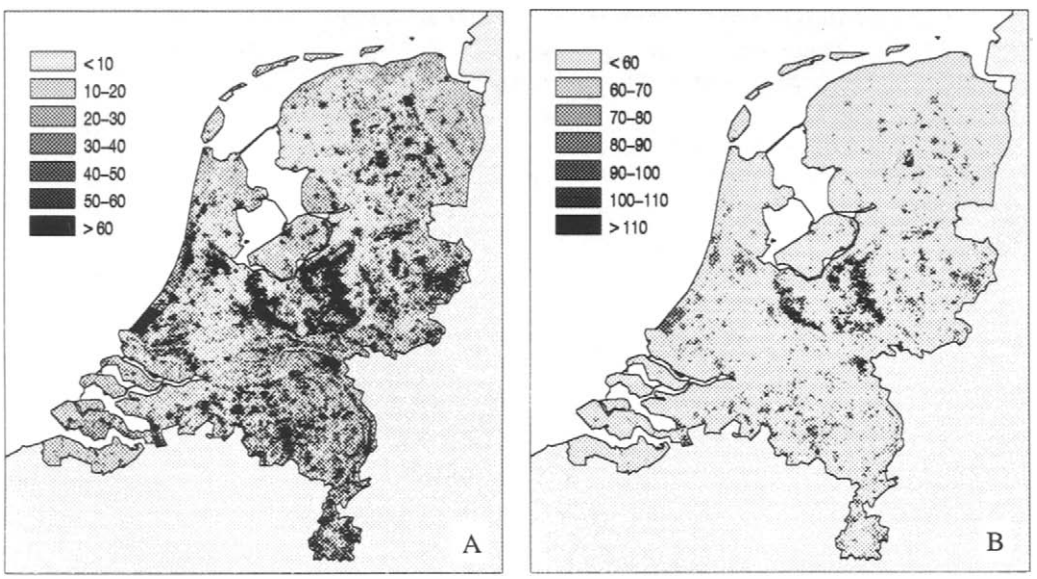

FIGURE 5.6 1 x 1 km grid average z_0 values in the Netherlands: A: 0-60 cm, B: >50 cm.

Dry deposition of acidifying components

The dry deposition of SOx, NOy, NHx, total nitrogen and total potential acid deposition is given in Table 5.2. The spatial distribution of the dry deposition in 1993 is given in Figures 5.7 (A - D) for SOx, NOy, NHx and total potential acid, respectively. These figures show the highest dry deposition of SOx in the large industrial Rijnmond area near the city of Rotterdam on the west coast. Furthermore, there is a gradient with lower dry deposition in the north reaching the highest values in the south of the country. This is mainly the result of the source areas in the neighbouring countries to the east ant the south, such as the Ruhr area in Germany, but also further away in the Black Triangle. Highest dry deposition of NOy is found in the western and central part of the country. Dry deposition of NHx is most pronounced in and near the 'Gelderse Vallei' (in the centre), in the eastern part of the country and in the Peel area to the south.

The average dry deposition of SOx, NOy, NHx in the Netherlands and the total potential acid to deciduous forests, coniferous forests and nature conservation areas are listed in Table 5.4. These estimates are based on 5 x 5 km averages, where the dominant land use is deciduous forest, coniferous forest or nature conservation area. The coverage of deciduous forests over the Netherlands is about 2% of the total land area. For coniferous forests this is 6.2% and for other nature conservation areas, 2.3%. On the average, the dry deposition of SOx to deciduous forests is 28% higher than the average dry deposition of SOx in the Netherlands, whereas the dry deposition to coniferous forests is 42% higher. Dry SOx deposition to forests in the Netherlands is 40% higher than to the 'average' Dutch landscape For NOy, these numbers are 45% higher onto deciduous, 62% higher onto coniferous forests and 58% higher onto forests relative to dry deposition of NOy in the Netherlands. For NHx, the numbers are +2%, +26% and +20%. A higher than country-averaged deposition for forests is caused by the roughness effect on V_d. The location of forests to source areas affects concentrations and may also determine the extent that values are higher.

TABLE 5.4 Average deposition to forests in the Netherlands in 1993 (mol ha^{-1} a^{-1})

	SOx			NOy			NHx			N			Acid		
	dry	wet	total	dry	wet	total	dry	wet	total	dry	wet	total	dry	wet	total
Netherlands	570	190	760	420	320	740	1320	680	2000	1740	1000	2750	2900	1380	4280
Deciduous	730	210	940	610	320	930	1340	740	2080	1950	1060	3010	3420	1490	4910
Coniferous	810	210	1020	680	320	1000	1660	770	2430	2350	1100	3450	3980	1540	5520
Forest (average)	790	210	1000	660	320	980	1580	760	2340	2240	1080	3320	3820	1500	5320

Figure 5.8 shows histograms of the dry deposition of SO_x, NO_y and NH_x to forest, grassland and water. The distribution is determined by taking the deposition to 1 x 1 km grids (5 x 5 km grids for NH_x) where the dominating land use is one of these categories. These distributions show that for all three compounds deposition to forest is higher than that to grass and water.

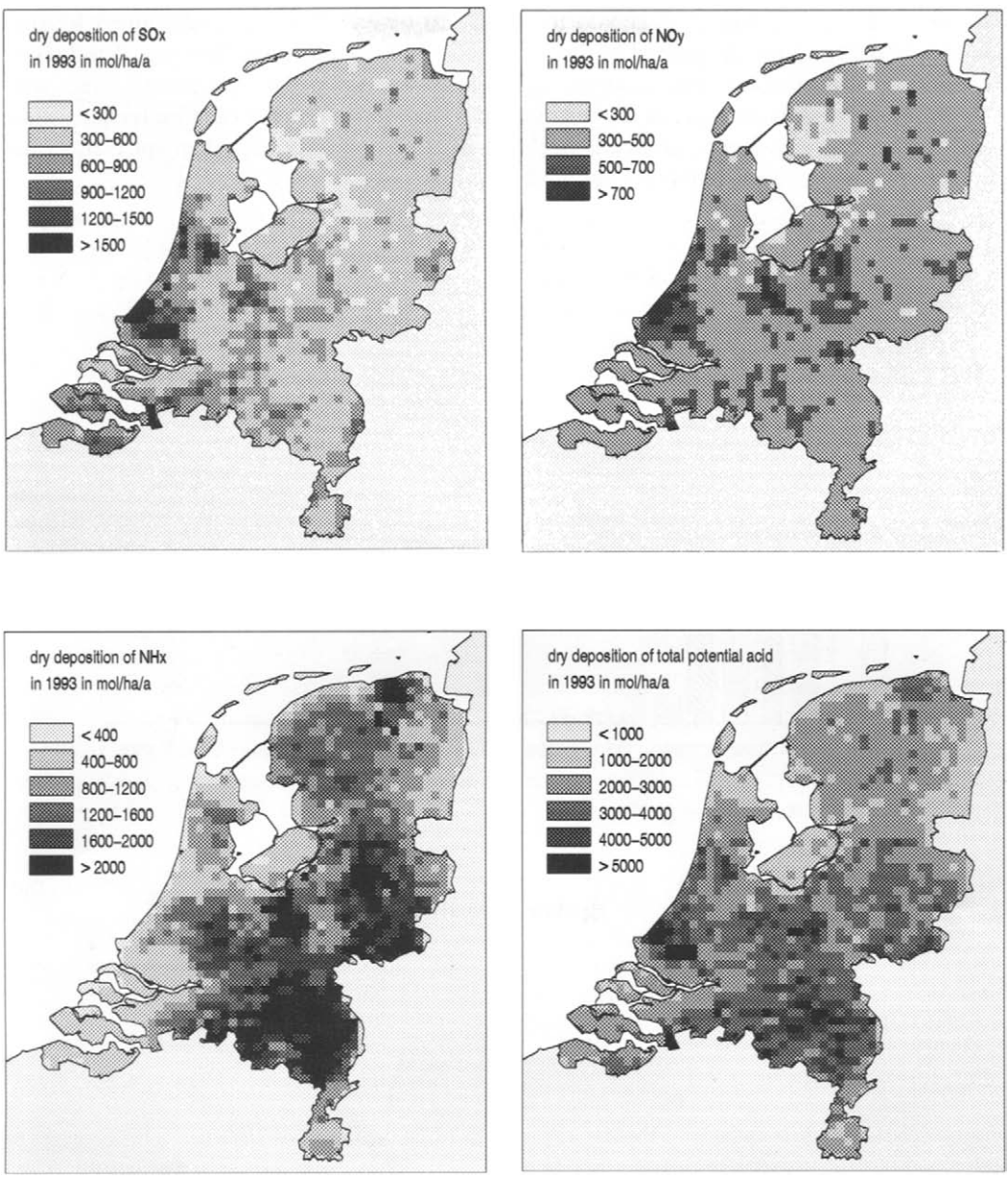

FIGURE 5.7 The spatial distribution of the dry deposition of SOx, NOy, NHx and total potential acid in 1993 (mol ha^{-1} a^{-1}).

Deposition to grass is higher than that to water. The distributions are determined by the roughness effect and the distance of grid cells to sources or source areas. The first determines the difference between the three land-use categories, whereas both the roughness effect and the distance to sources determines the distribution of dry deposition for each individual land-use category. The distance of grid cells to the sources is especially important for NH_x. This can be seen from the distribution in Figure 5.8.

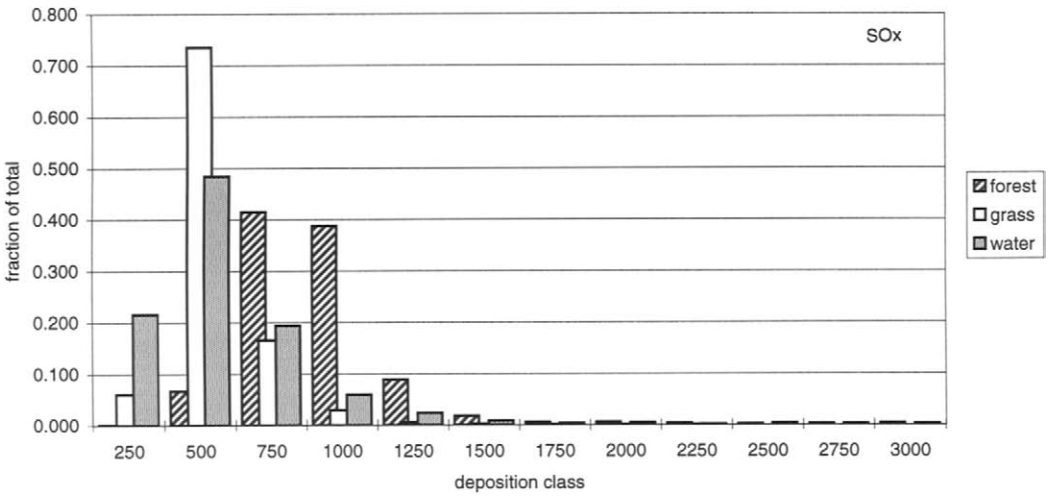

FIGURE 5.8 Distribution of dry deposition SOx to forest, grassland and water in 1993 in the Netherlands.

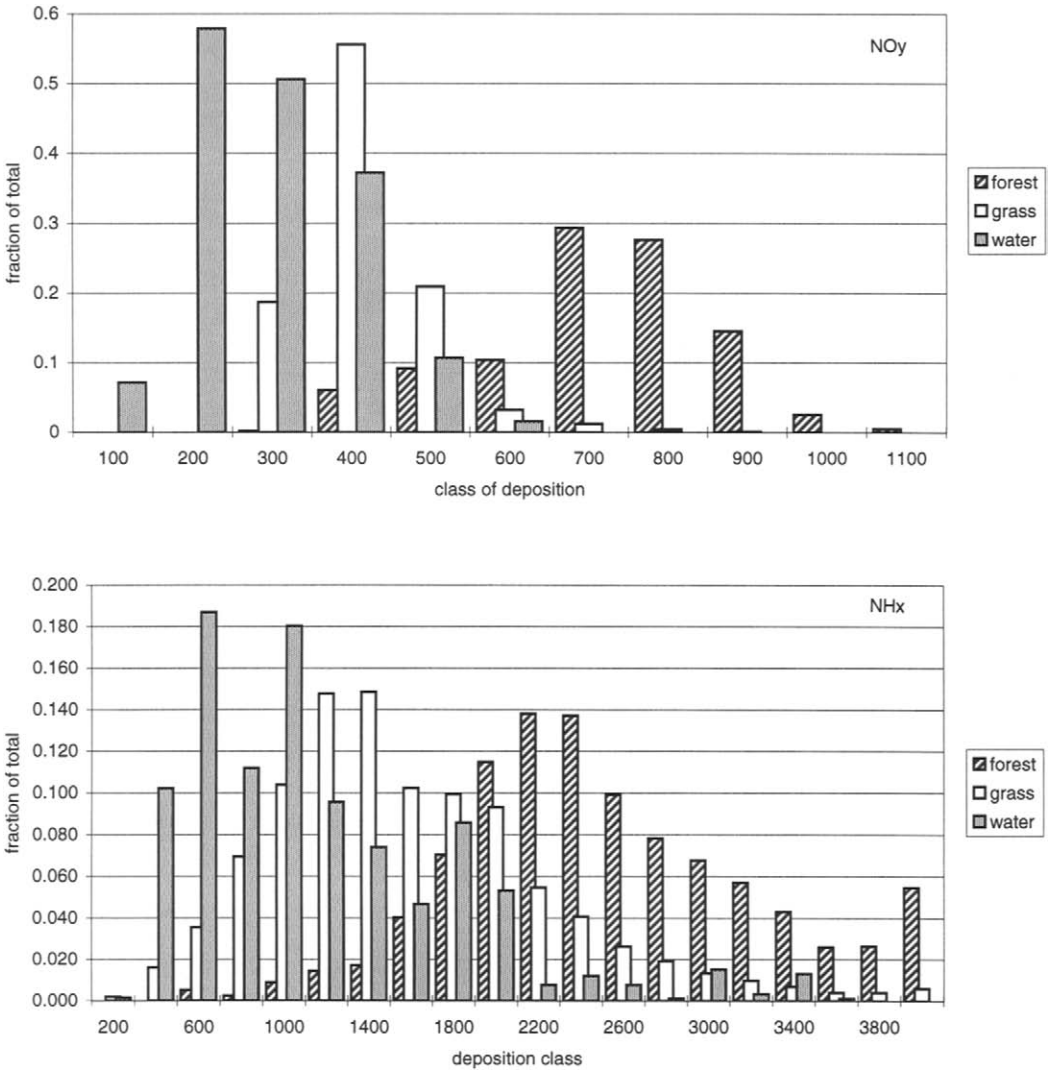

FIGURE 5.8 *(continued)* Distribution of dry deposition of NOy and NHx to forest, grassland and water in 1993 in the Netherlands.

Dry base cation deposition
Up to now there have been no other estimates of the dry deposition of base cations in the Netherlands. The main reason for this is the lack of information on ambient concentrations, both measurements and modelled concentrations. The reason for the lack of the latter is a lack of emission estimates, and the temporal and spatial variation in emissions. Concentrations used here are obtained from wet deposition measurements and scavenging ratios. This method was applied to the Canadian situation (Eder and Dennis, 1990), and evaluated and accordingly applied to the Netherlands and Europe (see section 5.2). An extensive description of this method and the evaluation is found in Erisman *et al.* (1994) and in Chapter 7. Base cation concentrations thus obtained are annual averages on a 10 x 10 km grid across the country. Dry deposition velocities are obtained with DEADM on a 1 x 1 km grid using the parametrisations outlined in section 4.2 for particles.

The first dry deposition results for the Netherlands show the highest input of Na^+ over Ca^{2+}, Mg^{2+} and K^+. Figure 5.9 displays maps of Na^+, K^+, Mg^{2+} and Ca^{2+} dry deposition. Average dry deposition fluxes of acidifying aerosols and base cations for each acidification area are displayed in Table 5.7. Here it is shown that coastal areas receive the highest base cation inputs. Areas with many forests Veluwe and Brabant also receive high inputs. This is in line with what is expected. Na is of sea-salt origin and inputs are high because of the prevailing southwesterly winds over the Netherlands. A gradient can be seen over the country, with the highest inputs near the coast. High inputs of base cations are caused by periods with southwesterly storms. Such periods dominate annual inputs. Forests receive high base-cation inputs as a result of the high dry deposition velocities for large particles. The estimates are in good agreement with those derived from the experiments and model application at the Speulder forest (Erisman *et al.*, 1994; see section 7.3). It might be concluded that the method used to estimate ambient base cation concentrations is accurate enough to provide concentration estimates. However, there is certainly a need to evaluate the scavenging ratios with simultaneous concentration methods in precipitation and air.

Figure 5.10 shows histograms of the dry deposition of Na^+, K^+, Mg^{2+} and Ca^{2+} to forest, grassland and water. The distribution is determined by taking the deposition to 1x1 km grids where the dominating land use is one of these categories. These distributions show that for all four compounds deposition to forest is higher than that to grass and water. Deposition to grass is higher than to water. The distributions are determined by the roughness effect and by the distance of grid cells to sources or source areas. The distribution of forests is broader than that of grassland and of water. This is due to the relatively large range in roughness length values in this land-use class compared to the other two.

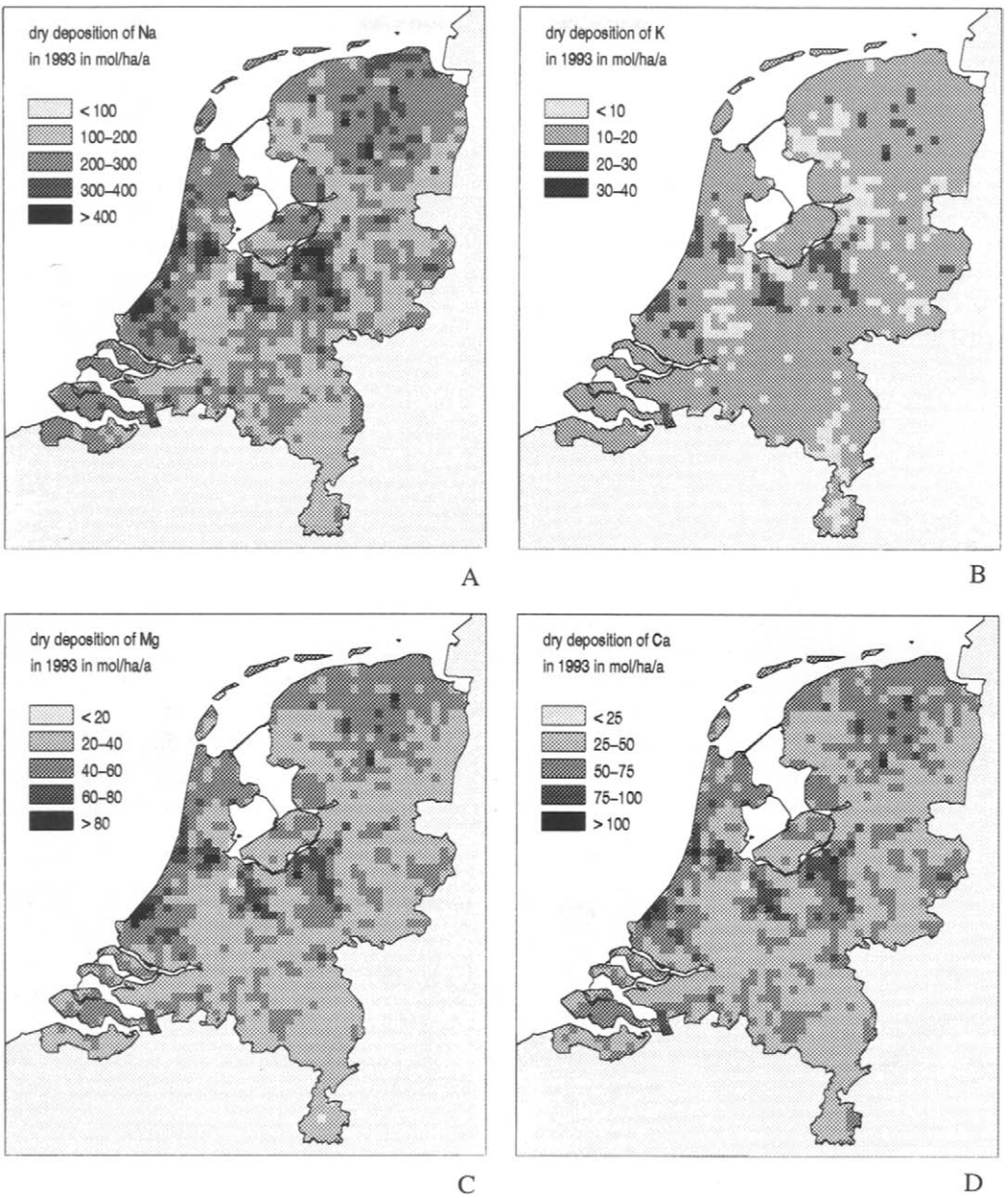

FIGURE 5.9 Maps of the dry deposition of Na^+ (A), K^+ (B), Mg^{2+} (C) and Ca^{2+} (D) in the Netherlands (mol ha^{-1} a^{-1}).

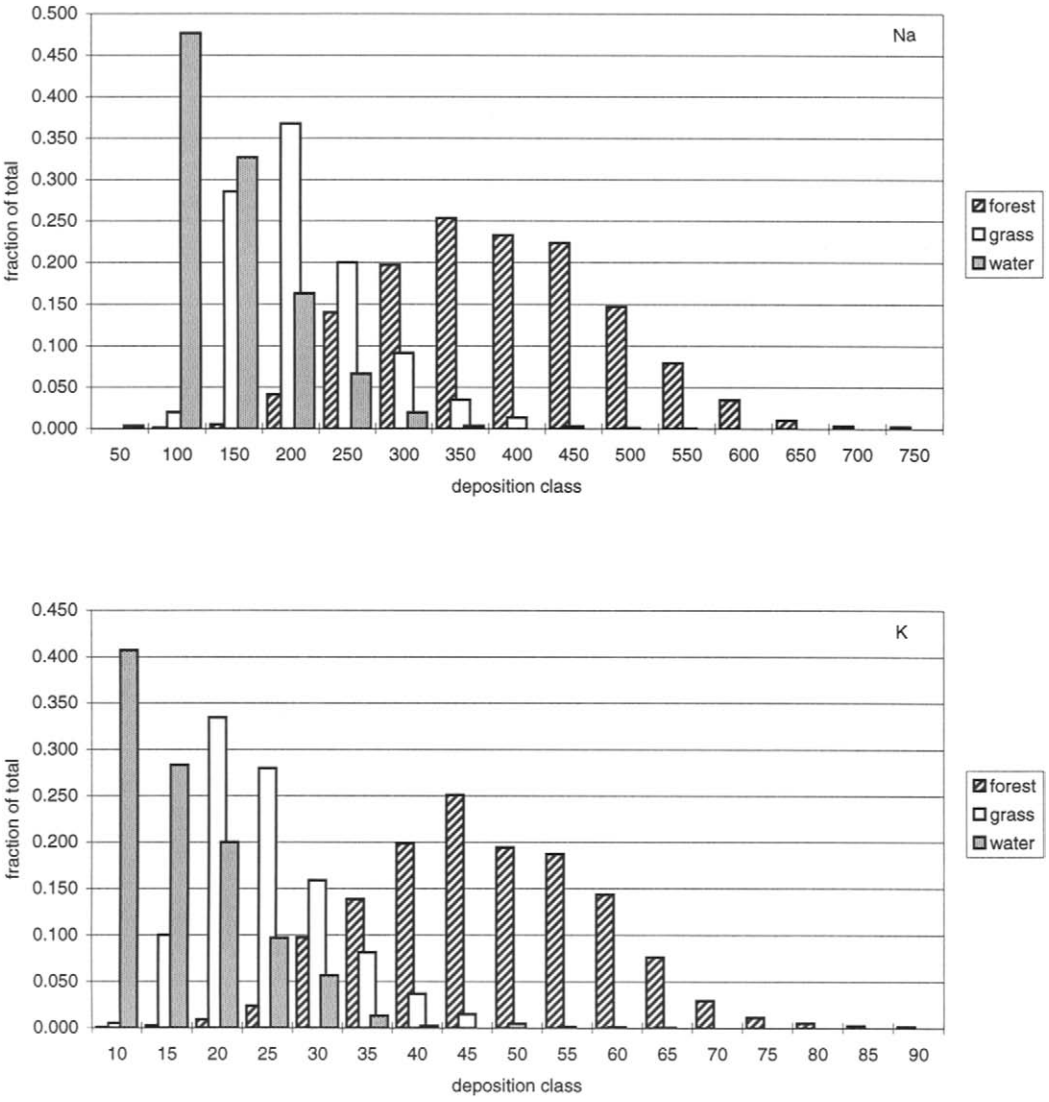

FIGURE 5.10 Distribution of dry deposition distribution of Na^+ and K^+ to forest, grassland and water.

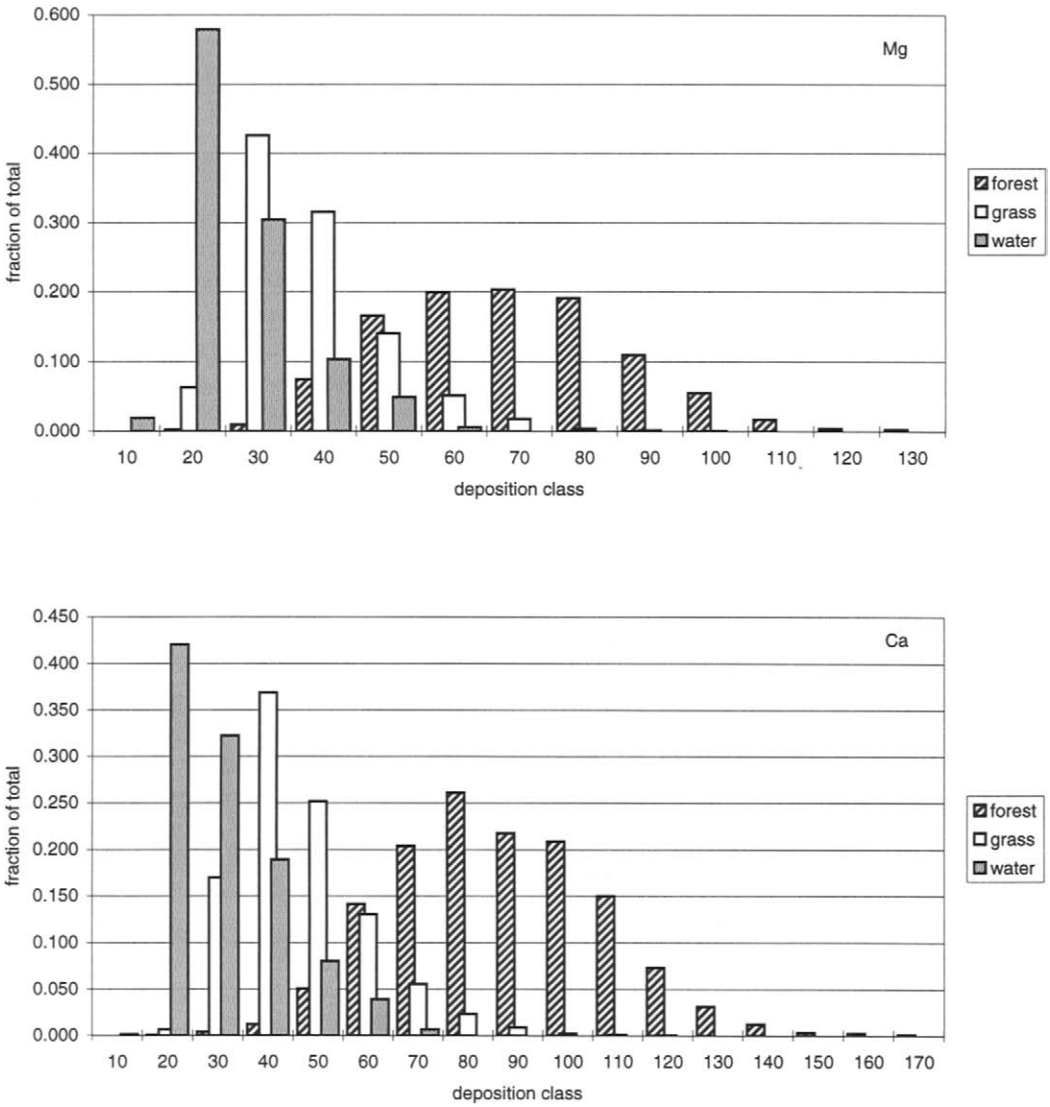

FIGURE 5.10 *(continued)* Distribution of dry deposition Mg^{2+} and Ca^{2+} to forest, grassland and water.

5.2.4 TOTAL DEPOSITION

Acidifying components

Table 5.2 lists the dry, wet and total deposition of SOx, NOy, NHx, total nitrogen and total potential acid for each year averaged over the Netherlands. Figure 5.11 shows the variation in total deposition between 1980 and 1993. The deposition of total potential acid decreased from 7215 mol ha^{-1} a^{-1} in 1980 to 4280 mol ha^{-1} a^{-1} in 1993 (-41%). This decrease is mainly the result of the decrease in dry SO_2 deposition. The dry NH_3 deposition has gradually decreased since 1987, whereas NOy deposition has remained the same over the years. Wet deposition of SOx and NOy has decreased since 1980, whereas that of NHx has remained the same. Trends in wet deposition are lower than those in dry deposition. Over the years wet deposition has become more important in determining total input. This is due to completely different removal mechanisms and source origins. The spatial distribution of the deposition of SOx, NOy, NHx and total potential acid in 1980 and 1993 is shown in Figures 5.12 and 5.13, respectively.

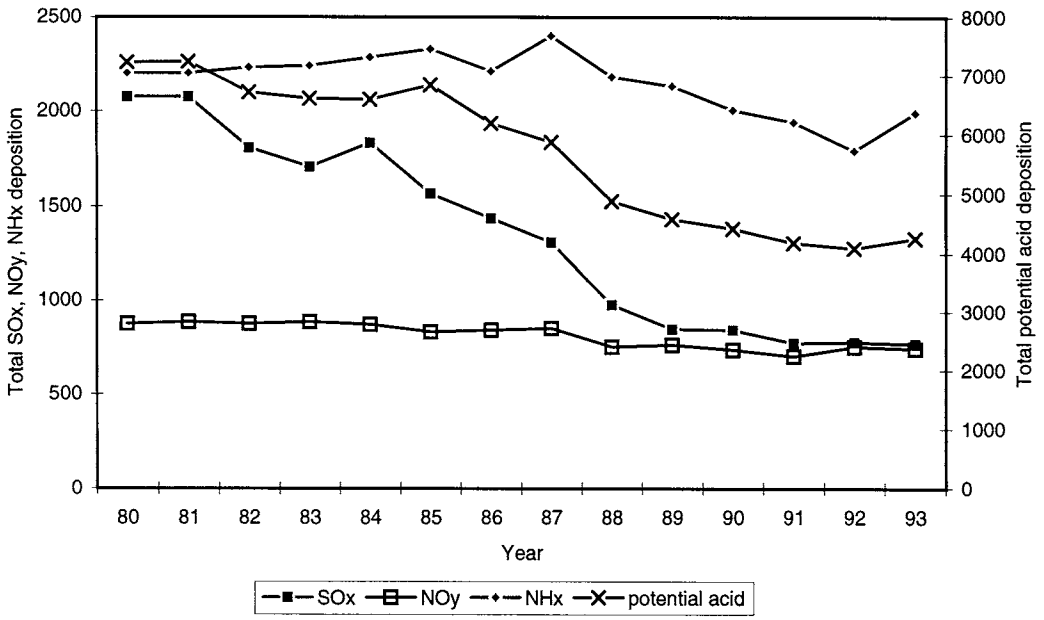

FIGURE 5.11 Variation in total SOx, NOy, NHx and potential acid deposition between 1980 and 1993 (mol ha^{-1} a^{-1}).

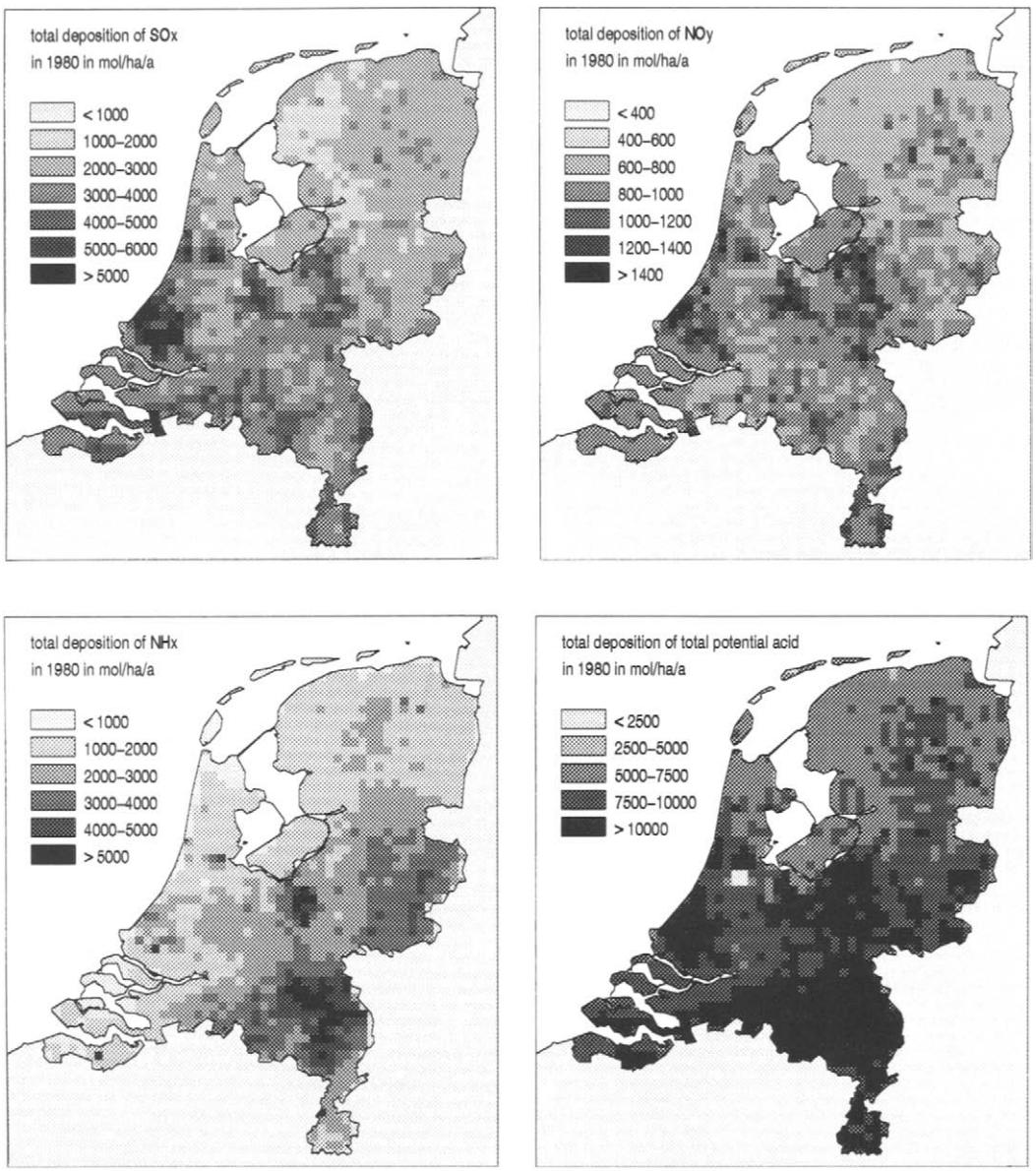

FIGURE 5.12 The spatial distribution of the total deposition of SOx, NOy, NHx and potential acid in 1980 (mol ha^{-1} a^{-1}).

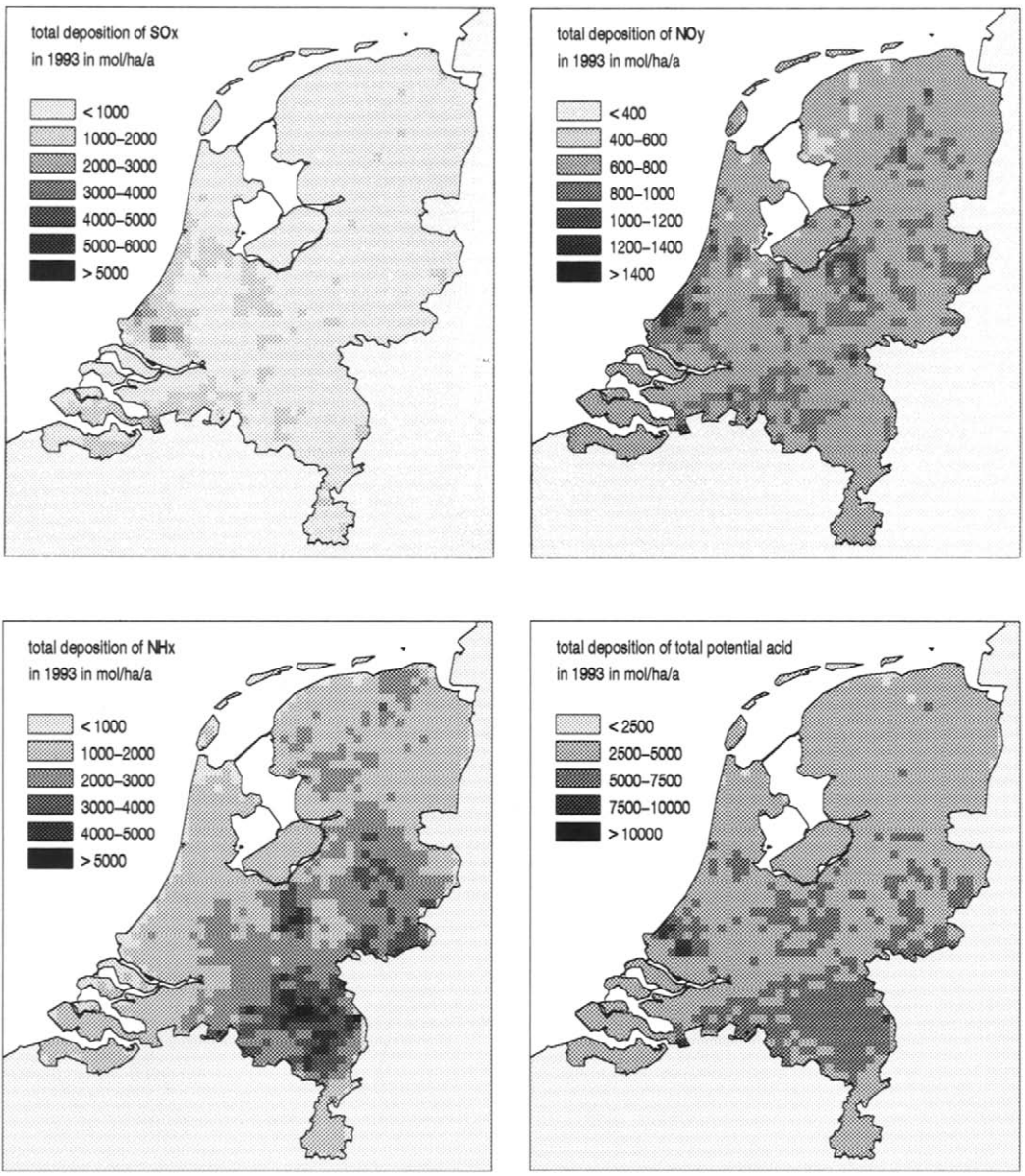

FIGURE 5.13 The spatial distribution of the total deposition of SOx, NOy, NHx and total potential acid in 1993 (mol ha^{-1} a^{-1}).

The deposition for each acidification area in 1980 and 1993 are listed in Tables 5.5 and 5.6, respectively. The total dry deposition accounts for about 68% of the total acid deposition in the Netherlands in 1993; the contribution of dry deposition of the respective components is 75% for SOx, 57% for NOy and 66% for NHx. Local variations are mainly due to variations in dry deposition. These variations are not always fully represented in the figures because of a smoothing introduced by the interpolation of the concentrations from different stations of the monitoring network, and the assumed lack of spatial variation of the HNO_2, HNO_3 and HCl concentrations, and SO_4^{2-} and NO_3^- aerosols.

TABLE 5.5 Deposition of SOx, NOy, NHx, total nitrogen and potential acid for each acidification area in the Netherlands in 1980 (mol ha^{-1} a^{-1})

Acidification area	SOx			NOy			NHx			N			Potential acid		
	dry	wet	total	dry	wet	total	dry	wet	total	dry	wet	total	dry	wet	total
The Netherlands	1750	320	2070	480	390	880	1565	640	2205	2045	1030	3075	5545	1670	7215
Groningen	1450	270	1720	410	350	770	955	590	1545	1365	940	2305	4265	1480	5745
Friesland	1160	230	1390	380	320	710	960	530	1490	1340	850	2190	3660	1310	4970
Drenthe	1510	290	1800	460	370	830	1210	620	1830	1670	990	2660	4690	1570	6260
W/NE Overijssel	1320	280	1600	420	400	820	1380	640	2020	1800	1040	2840	4440	1600	6040
SE Overijssel	1310	320	1630	460	380	850	2565	680	3245	3025	1060	4085	5645	1700	7345
NW Gelderland	1890	360	2250	620	420	1050	2150	790	2940	2770	1210	3980	6550	1930	8480
NE Gelderland	1430	350	1780	460	400	870	2695	760	3455	3155	1160	4315	6015	1860	7875
S Gelderland	2000	370	2370	560	410	970	1955	780	2735	2515	1190	3705	6515	1930	8445
Utrecht	2020	340	2360	610	410	1030	1740	660	2400	2350	1070	3420	6390	1750	8140
N Noord-Holland	1610	240	1850	430	400	830	595	430	1025	1025	830	1855	4245	1310	5555
S Noord-Holland	1800	290	2090	490	420	920	810	630	1440	1300	1050	2350	4900	1630	6530
N Zuid-Holland, Flevopl	2690	330	3020	590	420	1020	1375	550	1925	1965	970	2935	7345	1630	8975
S Zuid-Holland	2550	340	2890	510	420	940	1095	570	1665	1605	990	2595	6705	1670	8375
Zeeland	2010	350	2360	430	460	900	520	510	1030	950	970	1920	4970	1670	6640
W Noord-Brabant	2220	400	2620	470	370	850	1300	700	2000	1770	1070	2840	6210	1870	8080
Mid-Noord-Brabant	1940	400	2340	500	350	860	2185	720	2905	2685	1070	3755	6565	1870	8435
NE Noord-Brabant	1720	350	2070	500	360	860	3685	680	4365	4185	1040	5225	7625	1740	9365
SE Noord-Brabant	1930	340	2270	540	350	890	3225	660	3885	3765	1010	4775	7625	1690	9315
N Limburg	1880	350	2230	530	370	900	3845	690	4535	4375	1060	5435	8135	1760	9895
S-Mid-Limburg	1870	390	2260	520	450	980	1940	770	2710	2460	1220	3680	6200	2000	8200

TABLE 5.6 Deposition of SOx, NOy, NHx, total nitrogen and potential acid deposition for each acidification area in the Netherlands in 1993 (mol ha^{-1} a^{-1})

Acidification areas	SOx			NOy			NHx			N			Potential acid		
	dry	wet	total	dry	wet	total	dry	wet	total	dry	wet	total	dry	wet	total
The Netherlands	570	190	760	420	320	740	1320	680	2000	1740	1000	2750	2900	1380	4280
Groningen	480	120	590	370	340	700	1170	570	1740	1540	910	2440	2490	1140	3630
Friesland	380	110	480	330	320	660	1160	550	1710	1490	880	2370	2240	1090	3330
Drenthe	420	180	600	390	350	740	1040	620	1650	1420	970	2390	2270	1320	3590
W/NE Overijssel	380	190	570	370	340	720	1300	710	2020	1680	1060	2740	2430	1450	3880
SE Overijssel	470	230	700	410	360	780	1600	890	2490	2010	1260	3260	2950	1720	4670
NW Gelderland	510	220	730	500	330	830	1580	790	2370	2080	1120	3200	3110	1550	4660
NE Gelderland	400	240	640	380	360	750	2120	910	3030	2500	1280	3780	3300	1750	5060
S Gelderland	580	230	810	470	310	780	1610	790	2400	2080	1110	3190	3250	1570	4810
Utrecht	690	210	900	500	300	800	1560	620	2180	2050	920	2970	3430	1350	4780
N Noord-Holland	510	130	640	380	320	700	720	530	1250	1100	850	1950	2120	1110	3230
S Noord -Holland	670	190	860	410	320	730	720	640	1360	1130	960	2090	2470	1340	3810
N Zuid-Holland, Flevopl	1030	210	1240	570	300	870	1060	480	1540	1630	780	2400	3690	1200	4890
S Zuid-Holland	940	210	1160	490	300	790	890	510	1400	1380	810	2190	3260	1230	4500
Zeeland	780	190	970	410	270	680	510	570	1080	910	850	1760	2470	1220	3700
W Noord-Brabant	850	240	1080	460	310	770	1050	630	1690	1510	950	2460	3210	1420	4630
Mid-Noord-Brabant	640	260	900	470	330	800	1730	760	2490	2200	1090	3280	3480	1600	5080
NE Noord-Brabant	510	240	750	450	320	770	2460	920	3380	2910	1230	4150	3930	1700	5640
SE Noord-Brabant	610	240	850	450	320	770	2450	920	3370	2900	1240	4140	4130	1720	5840
N Limburg	560	230	790	440	310	750	2440	990	3430	2880	1310	4180	4000	1770	5770
S Mid-Limburg	550	190	750	400	280	690	1420	680	2100	1820	960	2780	2930	1350	4270

Highest deposition of potential acid, up to 15000 mol ha^{-1} a^{-1} in 1980 and up to 10000 mol ha^{-1} a^{-1} was found in the south of the country in 1993. In the centre of the country, where the largest forested area (the Veluwe) is located, deposition reaches similar values. This is the result of the relatively high roughness of the area but also of the large ammonia emission area situated to the west of the Veluwe (the Gelderse Vallei). The variability in spatial distribution of dry deposition is much more pronounced than that of wet deposition. Whereas the influence of z_0 on the deposition velocity is obvious, the influence on the flux is more complex. Regions with high z_0 values show significantly higher fluxes for SOx and NOy than, for example, agricultural areas. The SO_2 concentration pattern over the whole country happens to be positively correlated with areas having high z_0 values, enhancing the correlation between the flux and z_0. The highest NHx concentrations are found in the agricultural areas, where NH_3 emissions are high. There is a large-scale spatial correlation between concentrations of NH_3 and z_0. However, the relation of the NHx flux and z_0 on a small scale is not univocal because areas with the highest concentration (agricultural) show the smallest z_0 values.

The contribution of aerosol to the total deposition in the Netherlands was estimated in the Aerosol project (see also Chapter 2 and section 7.3). Average SO_4^{2-} aerosol input in the

Netherlands is about 9% of the total dry SOx deposition. For forested areas the contribution is much higher; for deciduous forests it is 25% and for coniferous forests, 12%. For NH_4^+, these numbers are 24 and 27% respectively, and for NO_3, 27% and 29%. The contribution of aerosol deposition to the total deposition in the Netherlands is 7% for SO_4^{2-}, 11% for NH_4^+ and 9% for NO_3^-. For deciduous forests these numbers are 14, 15 and 17%, and for coniferous forests 10, 17 and 20%, respectively. It must be kept in mind that the figures for forests heavily depend on the location of forests to source areas and on forest structure characteristics. Furthermore, the estimates for aerosols and NHx are based on 5 x 5 km calculations.

Source contribution and origin of deposition

The source contribution and origin of deposition in the Netherlands is estimated using the TREND model (Van Jaarsveld, 1995; see also Heij and Schneider, 1991). The most accurate calculation of deposition in the Netherlands with the TREND model can be made for the years 1980 and 1993. For these years accurate estimates of emissions and locations of sources are available for the Netherlands and for Europe. The deposition values derived with the TREND model show a fairly good agreement with those calculated with DEADM (see section 6.2).

Relative contributions of foreign emissions per component and for the total deposition in 1980 and 1993 are show in Figure 5.14. In 1993, the Netherlands contributed almost 57% to the deposition in the Netherlands. The contributions to the deposition in the Netherlands of the surrounding countries (Great Britain, France, Belgium, and Germany) are more or less comparable.

Figure 5.15 shows the contribution of the different Dutch source categories to the total deposition and to the deposition of the different compounds for 1980 and 1993. The largest contribution among Dutch source categories to the total deposition in 1993 is from agriculture (61 %). Traffic is the largest contributor to the NOy deposition in the Netherlands. For SOx, industry, traffic and refineries contribute most to the deposition.

Total base cation deposition

Total deposition of base cations, as well as dry and wet deposition, are listed for each acidification area in Table 5.7. In contrast to the acidifying components, dry deposition of base cations is lower than the wet deposition flux. The total base cation flux averaged over the Netherlands relevant to the estimation of buffer capacities or critical loads of ecosystems (K^+ + Ca^{2+} + Mg^{2+}) is 650 mol ha^{-1} a^{-1}. The spatial distribution of Na^+, K^+, Mg^{2+} and Ca^{2+} deposition is given in Figure 5.16. The highest base cation fluxes are found on the north and west coasts of the country.

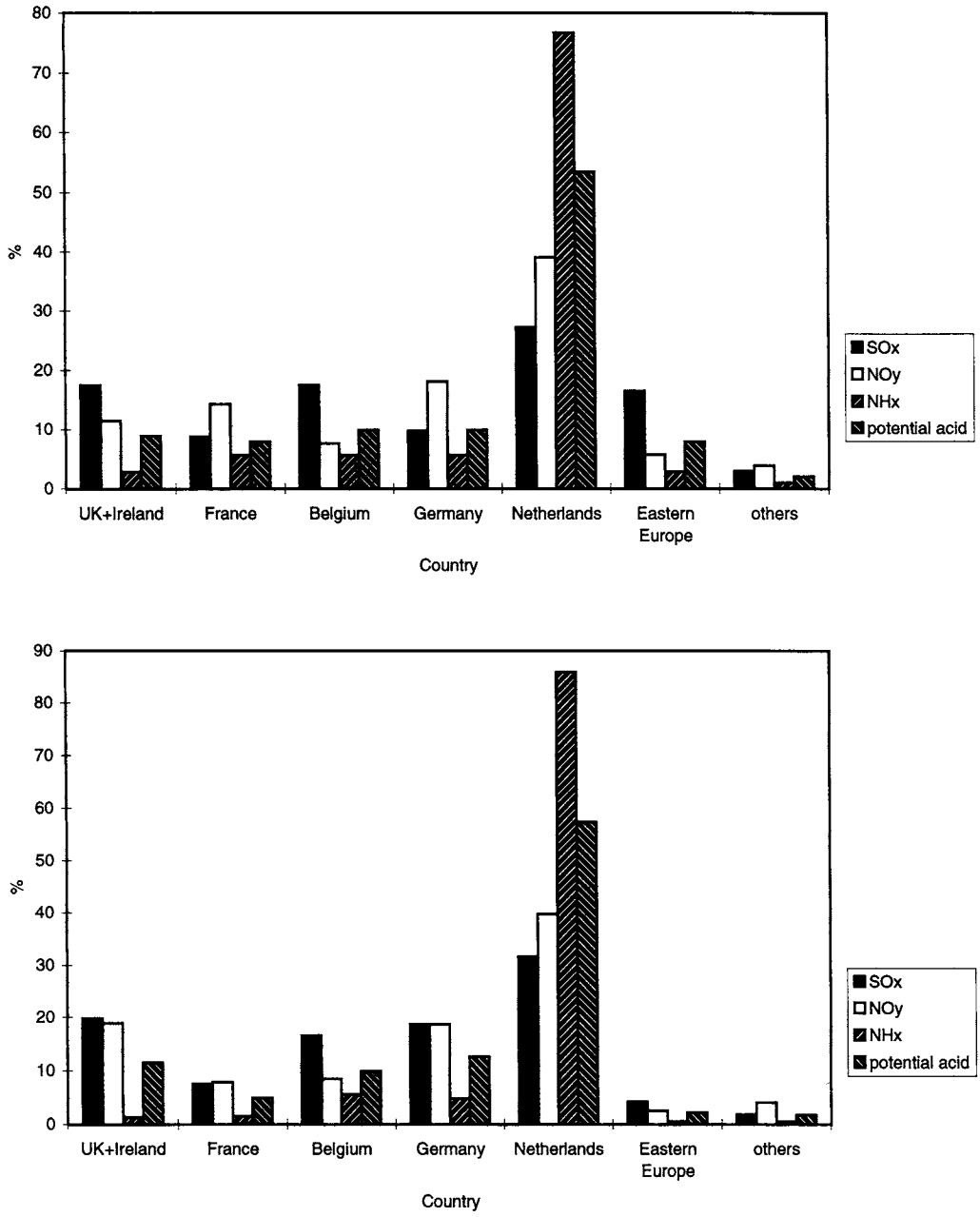

FIGURE 5.14 Contribution of different countries to the deposition in the Netherlands (A) 1980 and (B) 1993.

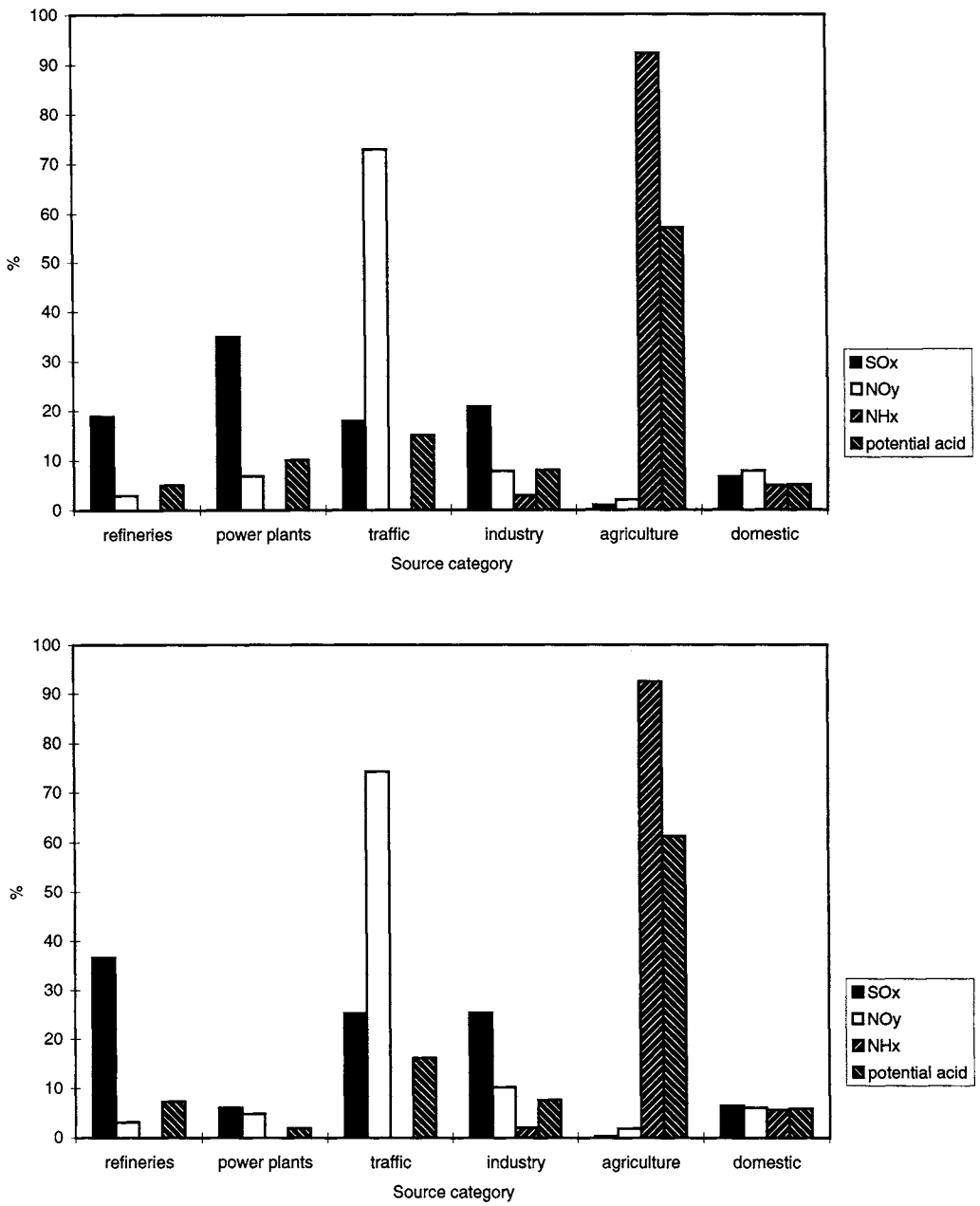

FIGURE 5.15 Source category contribution to the deposition in the Netherlands (A) 1980 and (B) 1993.

TABLE 5.7 Dry, wet and total deposition of base cations for each acidification area in the Netherlands in 1993 (mol ha^{-1} a^{-1})

Acidification area	Na^+			K^+			Mg^{2+}			Ca^{2+}			K^++Ca^{2+}+Mg^{2+}		
	dry	wet	total	dry	wet	total	dry	wet	total	dry	wet	total	dry	wet	total
The Netherlands	230	690	910	10	40	50	40	80	120	50	130	180	190	460	650
Groningen	260	1010	1270	20	50	70	50	130	180	60	130	190	240	570	810
Friesland	230	1060	1290	10	50	60	40	130	170	50	130	180	190	570	760
Drenthe	230	760	1000	10	40	50	40	90	130	50	60	110	190	340	530
W/NE Overijssel	210	580	790	10	40	50	40	70	110	50	50	100	190	280	470
SE Overijssel	210	510	720	10	40	50	40	60	100	50	60	110	190	280	470
NW Gelderland	280	480	750	20	40	60	50	60	110	60	50	110	240	260	500
NE Gelderland	190	480	670	10	40	50	30	60	90	50	60	110	170	280	450
S Gelderland	230	500	730	10	40	50	40	60	100	50	60	110	190	280	470
Utrecht	250	600	850	20	40	60	40	80	120	50	120	170	200	440	640
N Noord-Holland	250	1080	1330	10	50	60	40	130	170	50	90	140	190	490	680
S Noord-Holland	250	620	870	10	40	50	40	80	120	50	70	120	190	340	530
N Zuid-Holland, Flevopl	280	860	1140	20	50	70	50	110	160	60	80	140	240	430	670
S Zuid-Holland	240	870	1100	10	60	70	40	110	150	50	80	130	190	440	630
Zeeland	210	790	1010	10	50	60	40	90	130	50	80	130	190	390	580
W Noord-Brabant	210	710	930	10	50	60	40	80	120	50	60	110	190	330	520
Mid-Noord-Brabant	210	520	720	10	40	50	40	60	100	50	60	110	190	280	470
NE Noord-Brabant	200	390	580	10	40	50	30	50	80	40	50	90	150	240	390
SE Noord-Brabant	200	350	540	10	40	50	30	40	70	50	50	100	170	220	390
N Limburg	180	290	470	10	40	50	30	40	70	40	50	90	150	220	370
S/Mid-Limburg	150	250	400	10	30	40	30	30	60	40	70	110	150	230	380

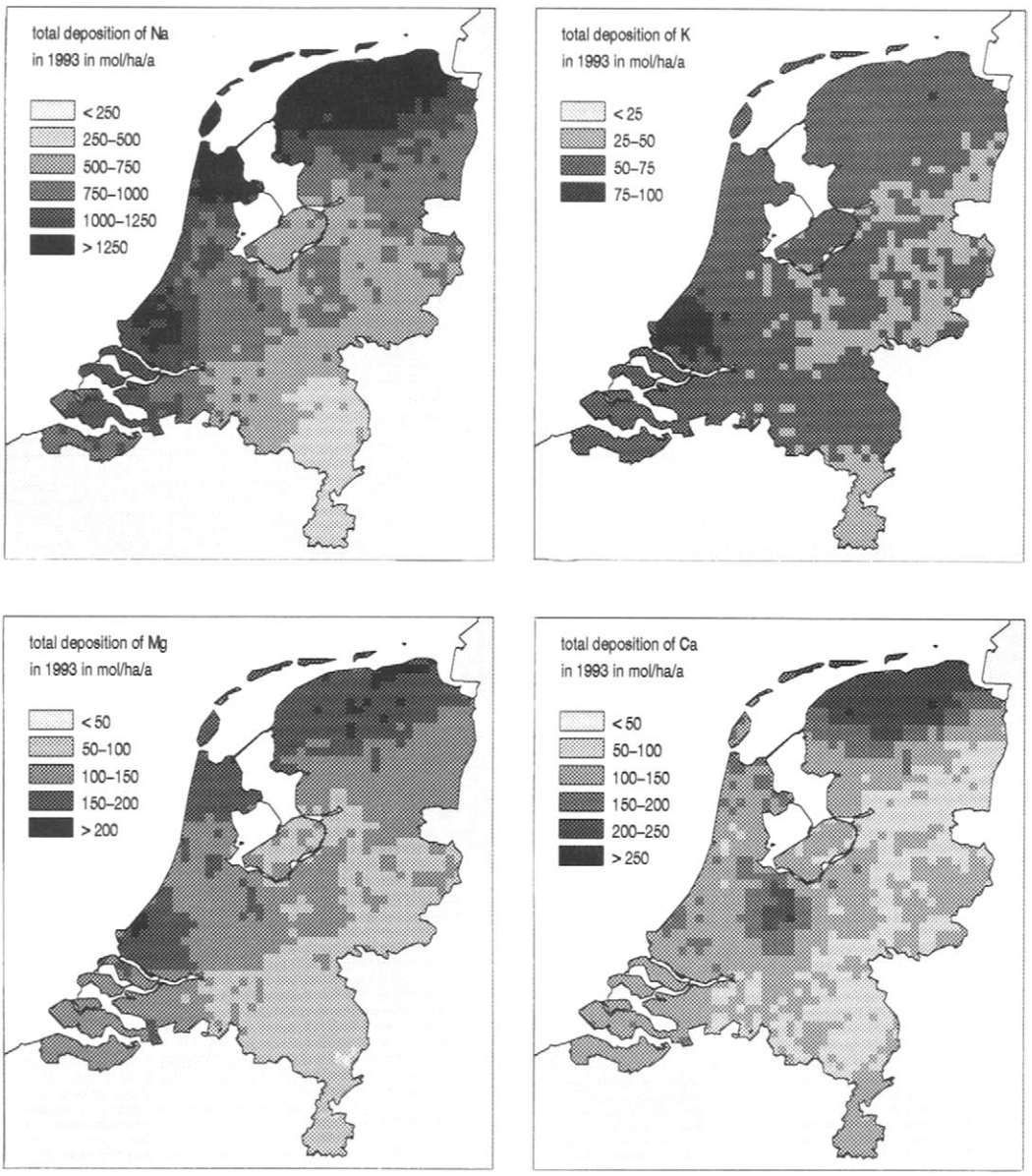

FIGURE 5.16 The spatial distribution of the deposition of Na^+, K^+, Mg^{2+} and Ca^{2+} in 1993 (mol ha^{-1} a^{-1}).

5.3 DEPOSITION MODELLING IN EUROPE

5.3.1 EDACS

The outline of the EDACS model to estimate local and regional scale deposition fluxes is presented in Figure 5.17. The basis for the two estimates is formed by calculations with the EMEP long-range transport model. With this model dry, wet and total deposition is estimated on a 150 x 150 km grid over Europe using emission maps for SO_2, NOx and NH_3 (Eliassen and Saltbones, 1983; Iversen *et al.*, 1991; Tuovinen *et al.*, 1994). The model results are used for estimating country-to-country budgets, as a basis of sulphur and nitrogen protocols, and for assessments. The local-scale approach used by RIVM depends strongly on LTRAP model results. Calculated ambient concentrations of the acidifying components (daily averages) and concentrations in precipitation (monthly averages) are used along with a detailed land-use map and meteorological observations to estimate small-scale dry deposition fluxes (Figure 5.17). By using calculated concentration maps, the relationship between emissions and deposition is maintained and scenario studies, budget studies and assessments can be carried out on different scales. Wet deposition is added to the dry deposition to estimate total local scale deposition in Europe. Wet deposition can either be obtained directly from the EMEP model, or from measurements made in Europe. The latter method is used here and will be described in the next section. The method for estimating dry deposition will be explained in section 5.3.3.

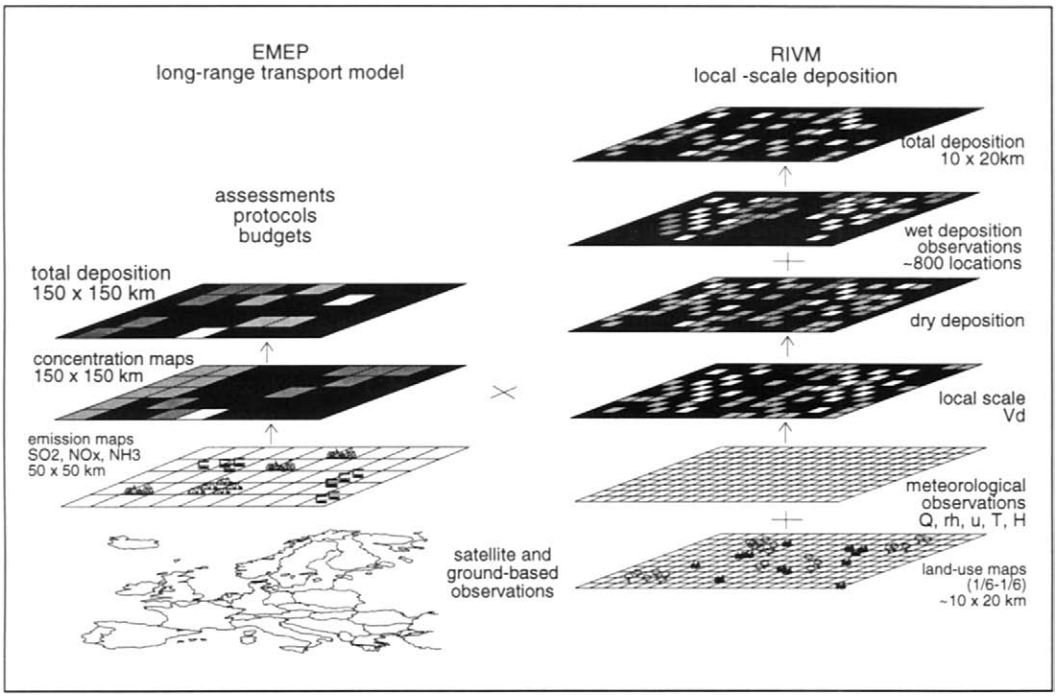

FIGURE 5.17 Outline of method to estimate local scale deposition fluxes.

5.3.2 WET DEPOSITION

Up to now, wet deposition maps on a European scale are based on long-range transport model results (e.g. the EMEP model; Iversen *et al.*, 1991), whereas for most components wet deposition maps based on measurements are only available on national scales. Although wet deposition is not a small-scale process, the resolution of the maps based on models is, for effect-related studies (e.g. the determination of the exceedances of critical loads), generally too small (e.g. 150 x 150 km blocks for the EMEP model) in comparison with local variations in deposition. Maps derived from measurements solve this problem as the resolution of these maps can be larger. Additionally, these measurement-based maps can be used to evaluate the long-range transport models. The first wet deposition map of NH_4^+ in Europe based on measurements was compiled by Buijsman and Erisman (1988). Van Leeuwen *et al.* (1995) recently used measurements in Europe to estimate the wet deposition in Europe.

In this section concentration and wet deposition maps of non-marine sulphate, nitrate, ammonium, hydrogen, sodium, chloride, magnesium, potassium and calcium based on the work by Van Leeuwen *et al.* (1995) are presented. These components, based on results of field measurements made at approximately 750 locations (the number of locations differs per

component), are mapped on a 50 x 50 km scale over Europe for 1989. Point observations are interpolated to a field covering the whole of Europe using the Kriging interpolation technique. An extensive uncertainty analysis is performed to assess the quality of the maps.

Data collection and data quality

The composition of precipitation is monitored in collectors throughout almost the whole of Europe. Information on concentrations of ions in precipitation in 1989 was obtained from the EMEP database (European Monitoring and Evaluation Programme) and from organisations responsible for wet deposition monitoring in their countries. The map of sites is presented in Figure 5.18; a list of monitoring networks is given in Table 3.2. The figure shows that the measurement sites are not evenly spread over Europe. Not all elements were analysed at all sites: the acidifying components SO_4^{2-}, NO_3^- and NH_4^+ were most frequently analysed. Concentrations measured with bulk samplers were corrected for the contribution of dry deposition onto the funnels of these samplers. Sulphate concentrations were corrected for the contribution of sea salt, because only non-marine sulphate contributes to the acidification process. By assuming that the ratio of sodium to sulphate in sea-spray is the same as in bulk sea water, and that all the sodium in a sample is of marine origin, it is possible to calculate non-marine sulphate. At about 200 sites only information about the sulphate concentration was available and the sodium concentration was not measured. At those sites interpolated values from the sodium map were used for correction.

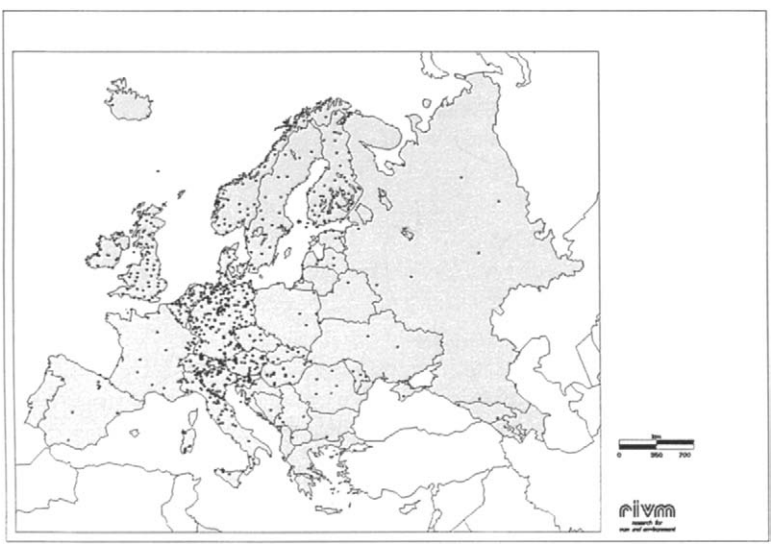

FIGURE 5.18 Location of wet deposition monitoring sites in Europe.

To obtain an idea on the quality of the data, two checks were carried out. First, a check on the ionic balance of the samples was performed. Of the total 824 measurement sites, all ions studied were measured at 478. About 52% of the 478 samples showed an ionic imbalance > 10%, and 13%, > 25%. In some cases a surplus of cations was observed, while in others anions dominate. The quality of the data was also checked by constructing X-Y plots of two elements that were highly correlated, e.g. NH_4-SO_4, NO_3-NH_4, SO_4-NO_3, Na-Mg, Cl-Mg and Na-Cl. No large outliers were observed.

Because data were skewly distributed, they were transformed to their common logarithms. Spatial structures of the concentration data were analysed using geostatistics based on Regionalised Variable Theory (Matheron, 1965). This spatial analysis revealed autocorrelation in all ions and reasonable bonded models were fitted to the experimental variograms. Data were interpolated using the Kriging interpolation technique. Using this technique, it is assumed that the sample data satisfy the intrinsic hypothesis (Cressie, 1993). A cross validation procedure was carried out to investigate whether the fitted variogram models describe the spatial structure of the data correctly. Generally, results were found to be satisfactory.

Interpolation
Because concentrations in precipitation are less variable in space and time than precipitation amounts, interpolation was performed on concentration data instead of fluxes. To obtain wet deposition fluxes, interpolated concentrations were multiplied by long-term mean precipitation amounts compiled by EPA (Environmental Protection Agency, USA). To create maps of all ions, estimates of the concentrations were made on a regular grid of 50 x 50 km by ordinary block Kriging. In some regions of Europe the distance between measurement sites is too large to obtain interpolated fields covering the whole of Europe. In the maps this can be seen in the concentric circles around some data points. Interpolation proceeds until the maximum distance of spatial correlation is reached.

Concentration data originated mainly from 1989. Because concentrations and precipitation amounts are physically linked, in principle, only precipitation amounts from 1989 should be used. As precipitation amounts can vary very much over short distances, a number of several thousands of sites is necessary to describe the variation to a reasonable extent. Therefore actual data measured in 1989 were necessary. For this purpose, data from the Observational Data Set (ODS), which is a product of ECMWF (European Centre for Medium-range Weather Forecasts), were investigated. The ODS dataset contains 1297 measurement sites spread over Europe. At each site amounts of rainfall were measured every 6-hour period. Data are invalidated and therefore highly uncertain (Potma, 1993), making these data not considered suitable for providing a map on amounts of precipitation for Europe.

Another dataset with interpolated values of long-term annual mean amounts of precipitation, based on several thousands of measurements (Legates and Willmott, 1990) was used at

RIVM. This EPA map (compiled at the Environmental Protection Agency, USA) is based on validated monthly mean precipitation amounts measured from 1920 to 1980. Data were corrected for gauge-induced biases to remove systematic errors caused by wind, wetting on the interior walls of the gauge and evaporation from the gauge. These corrected values were interpolated to a 0.5 degree of longitude by 0.5 degree of latitude grid. Areas with large precipitation amounts in coastal regions and in mountainous areas (due to orographic effects) can be recognised. Investigated was whether systematic differences between 1989 (ODS) data and long-term average (EPA) data could be found (Van Leeuwen *et al.*, 1995). As this did not happen, EPA data were used instead to determine wet deposition fluxes.

Description of spatial patterns

Several maps are presented in this section. These are flux maps of SO_4^{2-} (Figure 5.19), NO_3^- (Figure 5.20), NH_4^+ (Figure 5.21), H^+ (Figure 5.22) and total base cations (Mg^{2+}, Ca^{2+} and K^+) (Figure 5.23), as well as concentration maps of Na^+ (Figure 5.24), Cl^- (Figure 5.25), Mg^{2+} (Figure 5.26), Ca^{2+} (Figure 5.27) and K^+ (Figure 5.28). The non-marine sulphate, nitrate, ammonium and hydrogen maps clearly resemble European emission and climate patterns. Large emission sources can be recognised in the concentration maps, whereas in the flux maps climate patterns and orographic effects are also observed. In mountainous areas large fluxes due to orographic rains can be seen. Especially in former Yugoslavia the large long-term mean precipitation cause large fluxes in all flux maps. Besides originating from large amounts of rainfall, large fluxes can also arise from high concentrations in precipitation.

Considering the non-marine sulphate maps, large fluxes (400-1000 mol ha^{-1} a^{-1}) can be observed in Eastern and Central Europe (Germany, Poland, Czech and Slovak Republics, Austria, Hungary, northern Italy, The Ukraine and former Yugoslavia). Large sulphate concentrations are mainly caused by SO_2 emissions from industry and power stations. Concentrations and fluxes obtained in Turkey should be interpreted with care, as they are not based on measurements in Turkey itself but are solely the result of interpolation (in this case extrapolation) from surrounding countries. Nitrate arises mainly from NO_X emissions from industry, power stations and motor vehicle exhausts (i.e. burning processes). Spatial patterns in the nitrate maps resemble patterns found in the sulphate maps, but this time also in the Netherlands and southern Scandinavia rather large fluxes are observed (300-700 mol ha^{-1} a^{-1}). Again, large concentrations can be observed in the Black Triangle. In Russia nitrate concentrations and fluxes are low compared to sulphate concentrations and fluxes. Ammonia emissions arise mainly from livestock wastes, with smaller contributions from fertiliser application and the fertiliser-producing industry. Largest ammonium fluxes (400-1000 mol ha^{-1} a^{-1}) can therefore be observed in or near areas with intensive agricultural land use, e.g. Central Europe. In the Netherlands, for example, high ammonium fluxes are found due to intensive livestock breeding in this country.

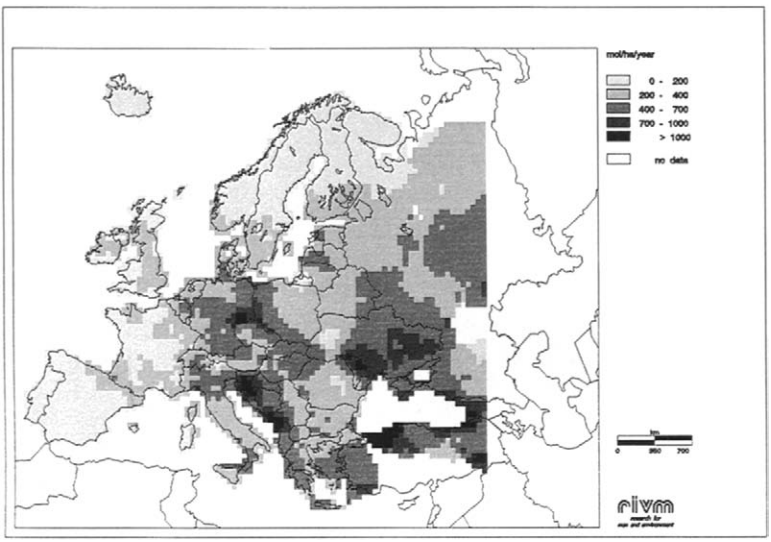

FIGURE 5.19 Wet deposition of SO_4^{2-} in Europe on a 50 x 50 km basis in 1989 in mol ha^{-1} a^{-1} (Van Leeuwen *et al.*, 1995).

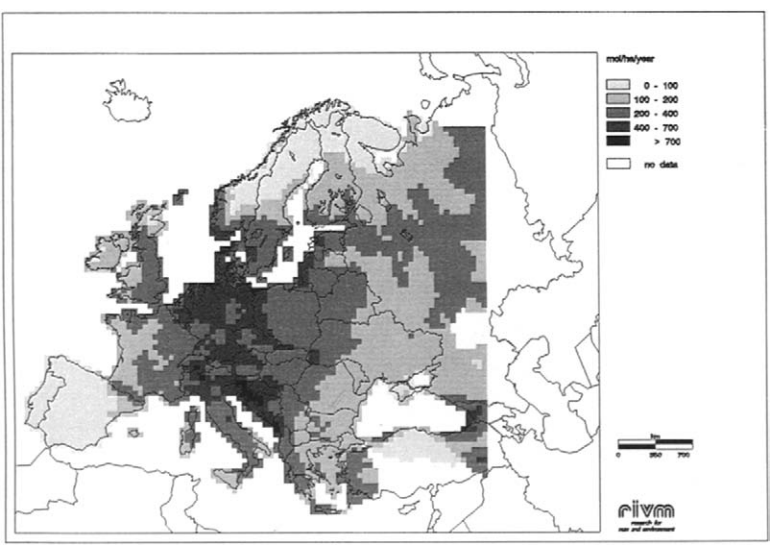

FIGURE 5.20 Wet deposition of NO_3^- in Europe on a 50 x 50 km basis in 1989 in mol ha^{-1} a^{-1} (Van Leeuwen *et al.*, 1995).

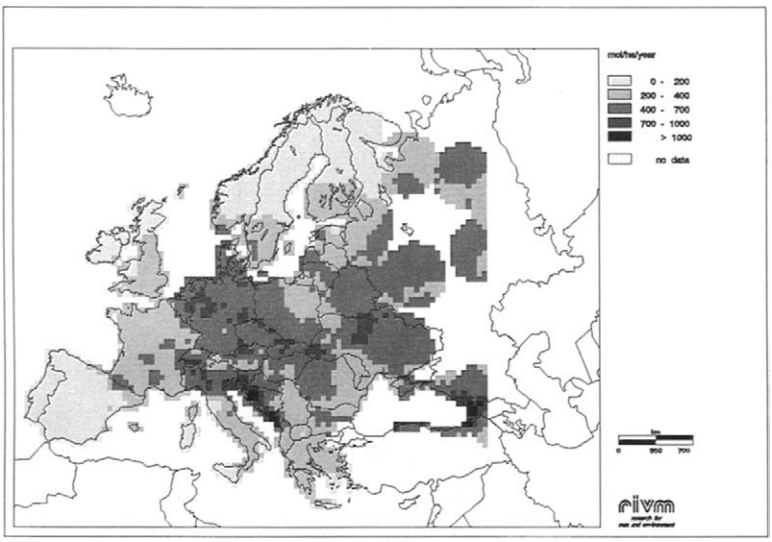

FIGURE 5.21 Wet deposition of NH_4^+ in Europe on a 50 x 50 km basis in 1989 in mol ha^{-1} a^{-1} (Van Leeuwen *et al.*, 1995).

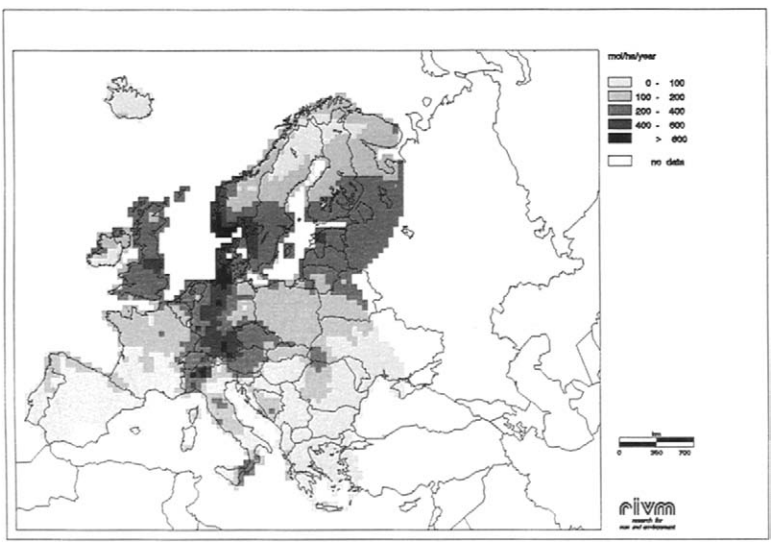

FIGURE 5.22 Wet deposition of H^+ in Europe on a 50 x 50 km basis in 1989 in mol ha^{-1} a^{-1} (Van Leeuwen *et al.*, 1995).

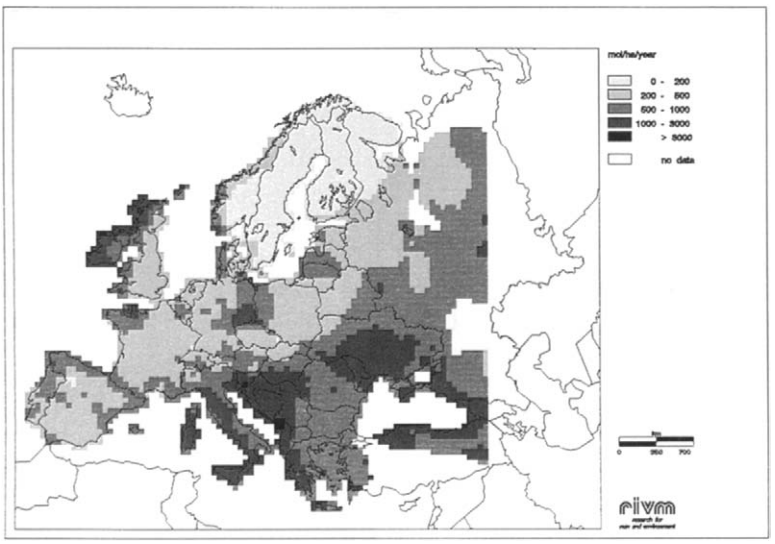

FIGURE 5.23 Wet deposition of total base cations (Ca^{2+}, Mg^{2+} and K^{+}) in Europe on a 50 x 50 km basis in 1989 in mol ha^{-1} a^{-1} (Van Leeuwen *et al.*, 1995).

In the hydrogen ion concentration map the largest acidity can be found in a small zone ranging from southern Scandinavia to northern Italy (Po Valley) and in Great Britain. The hydrogen ion concentration is a balancing term corresponding to the concentrations of the other three ions and is not related to any single factor. Lowest fluxes for all four components (< 200 mol ha^{-1} a^{-1}) can be found in northern Scandinavia, the Iberian Peninsula, and, to a lesser extent, France and Great Britain (except for the hydrogen ion). Note the spatial patterns of non-marine sulphate, nitrate and ammonium concentrations in Great Britain. The pattern clearly resembles increasing concentrations in eastern part of the country due to the influence of industry in the Midlands and the dominating westerly winds.

For base cations, a division can be made between components of marine origin (sodium, chloride and magnesium) and other elements (potassium and calcium), mainly originating from soils, agricultural activities, road dust and industry, as well as from marine sources. A clear pattern of decreasing fluxes with increasing distance to seas, in particular the Atlantic Ocean, can be observed for the elements of marine origin. This pattern is most distinct for sodium and chloride, especially along the Irish coast and the north coast of Great Britain, where fluxes are larger than 3000 mol ha^{-1} a^{-1}, caused by the combined effect of large concentrations with large precipitation amounts. The remainder of the European continent shows a fairly homogeneous pattern (fluxes varying from 0 to 800 mol ha^{-1} a^{-1}). The spatial variation in the magnesium fluxes is somewhat more differentiated than the variation in the

sodium and chloride fluxes. Besides near seas, large magnesium fluxes (> 100 mol ha^{-1} a^{-1}) can be observed in Hungary, The Ukraine and the former Soviet Union due to large concentrations. Note that the interpolated field in the former Soviet Union is based on only a few measurements. The potassium concentration and flux maps show homogeneous spatial variation almost all over Europe (fluxes varying between 0-75 mol ha^{-1} a^{-1}). Large fluxes (200-500 mol ha^{-1} a^{-1}) due to large concentrations can be observed in Ukraine and due to large rainfall amounts in Ireland and Great Britain. In the Ukraine large magnesium and calcium concentrations, and fluxes, can also be found. Particularly for calcium, this may be caused by the influence of locally emitted soil dust (especially in areas with alkaline soils), transport of desert dust from the Sahara and emissions of fly ash from the cement and concrete-processing industry. Besides in the Ukraine, the largest calcium fluxes (400-800 mol ha^{-1} a^{-1}) are found in Italy, Hungary and the Black Triangle. Calcium fluxes are lowest (0-100 mol ha^{-1} yr^{-1}) in Great Britain and Scandinavia.

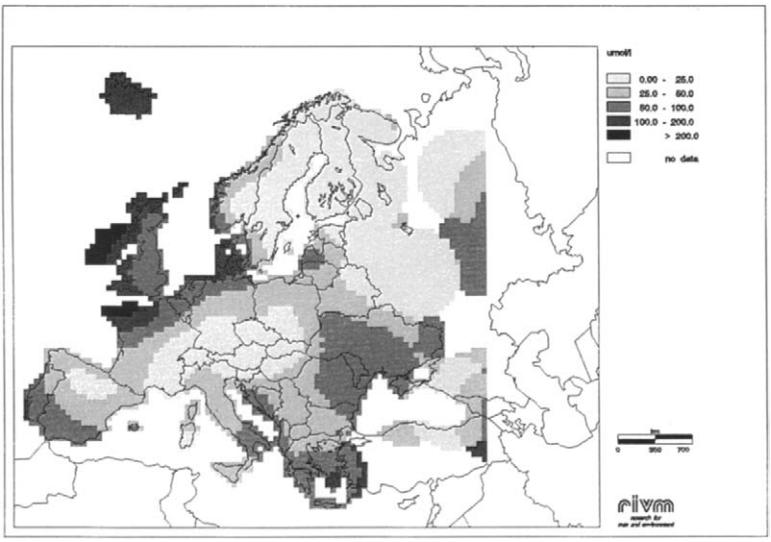

FIGURE 5.24 Concentration of Na^+ in Europe on a 50 x 50 km basis in 1989 in µmol l^{-1} (Van Leeuwen *et al.*, 1995).

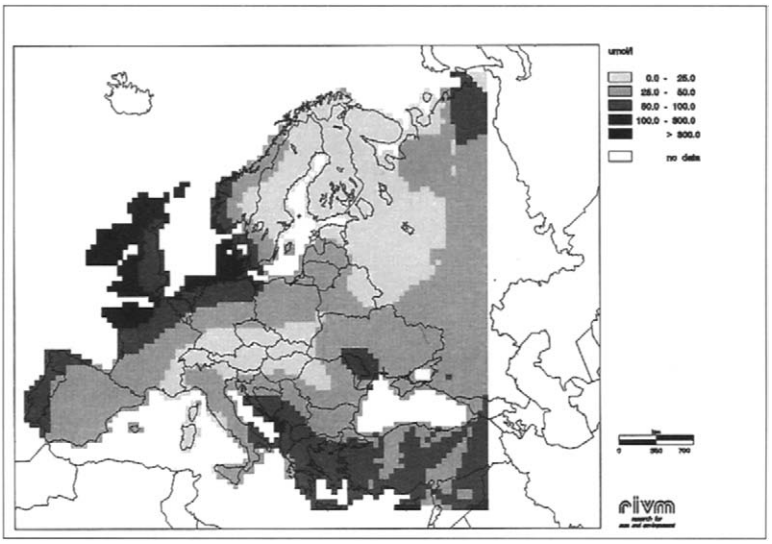

FIGURE 5.25 Concentration of Cl^- in Europe on a 50 x 50 km basis in 1989 in $\mu mol\ l^{-1}$ (Van Leeuwen *et al.*, 1995).

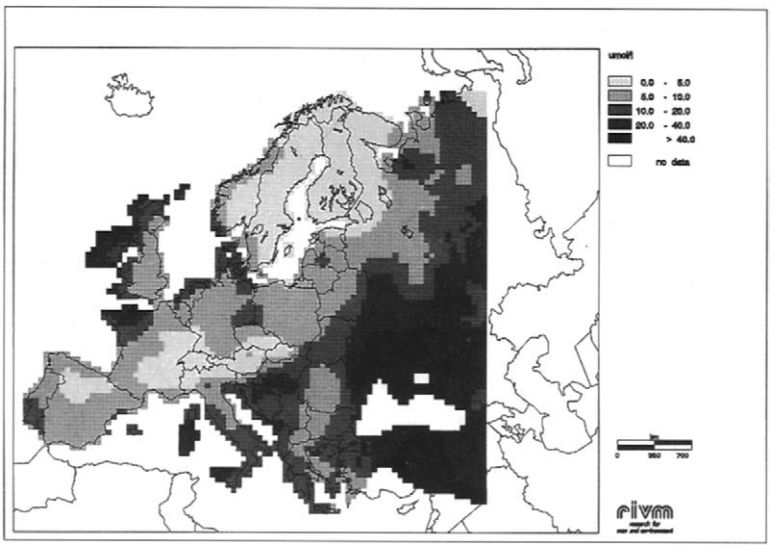

FIGURE 5.26 Concentration of Mg^{2+} in Europe on a 50 x 50 km basis in 1989 in $\mu mol\ l^{-1}$ (Van Leeuwen *et al.*, 1995).

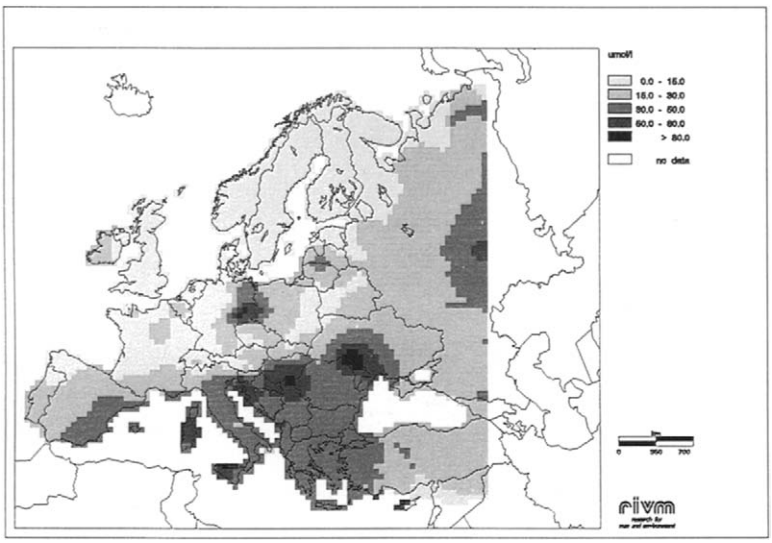

FIGURE 5.27 Concentration of Ca^{2+} in Europe on a 50 x 50 km basis in 1989 in µmol l^{-1} (Van Leeuwen *et al.*, 1995).

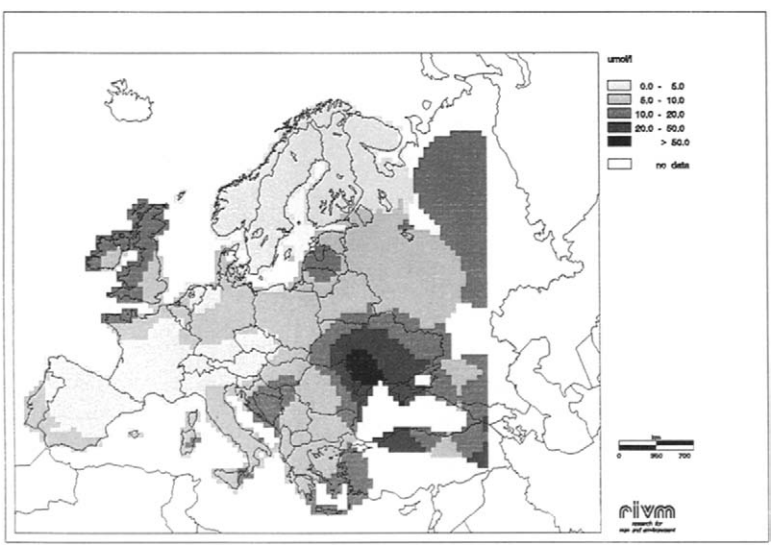

FIGURE 5.28 Concentration of K^+ in Europe on a 50 x 50 km basis in 1989 in µmol l^{-1} (Van Leeuwen *et al.*, 1995).

5.3.3 DRY DEPOSITION

Acidifying components

The method for dry deposition has been developed by Van Pul *et al.* (1992; 1994; 1995). Details can be found in these references. It is based on that used for the Netherlands and modelled in DEADM (Erisman, 1992; 1993a; see section 5.2.1). The main difference is that DEADM uses concentration measurements to determine the concentration distribution over the country (except for NH_3), while in EDACS, modelled concentrations are used. Dry deposition is inferred from the combination of long-range transport model concentrations provided by EMEP and parametrised dry deposition velocities (Hicks *et al.*, 1987; Van Pul *et al.*, 1995). Concentrations at 50 m above the surface (blending height) are used. At this height it is assumed that concentrations and meteorological parameters are not influenced by surface properties to a large extent. Dry deposition velocities of gases and particles at this height are calculated on a small scale using a land-use map, routinely available meteorological data and the inferential technique (Erisman *et al.*, 1994; Van Pul *et al.*, 1995) Resistances are modelled using observations for meteorological parameters in Europe and parametrisation of surface exchange processes. Parametrisations of the surface resistance used for different receptor surfaces and pollution climates in Europe were described in Chapter 4. Meteorological parameters are obtained from the ODS (Observational Data Set: Potma, 1994) every 6 h and interpolated over Europe on a $1/6^0$ x $1/6^0$ grid. Meteorological parameters consist of wind speed, friction velocity, radiation, temperature, humidity and precipitation.

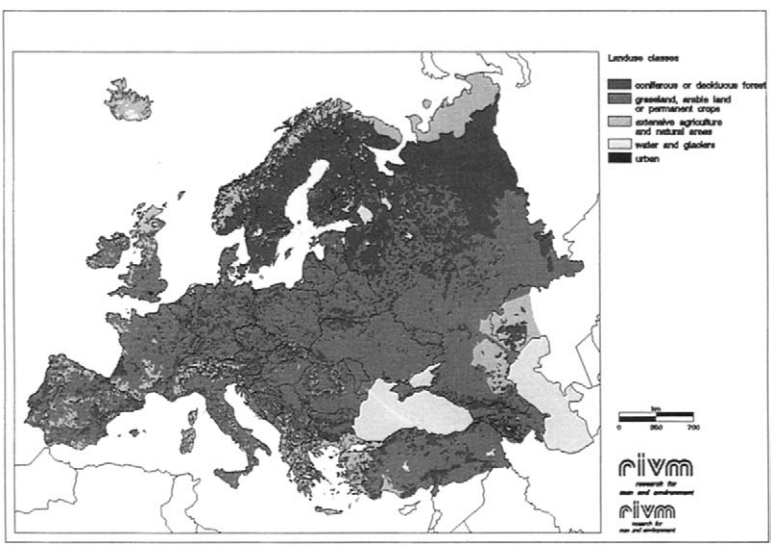

FIGURE 5.29 Land-use map on a $1/6^0$ x $1/6^0$ grid of Europe (Van Velde, 1994).

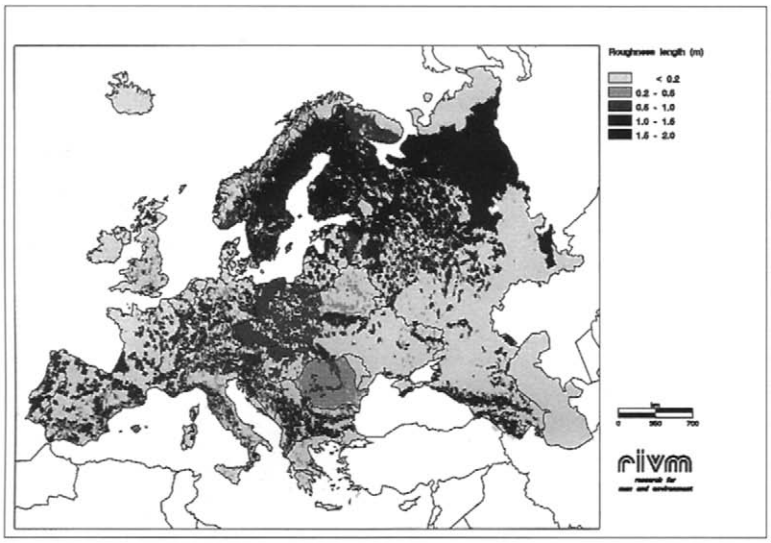

A

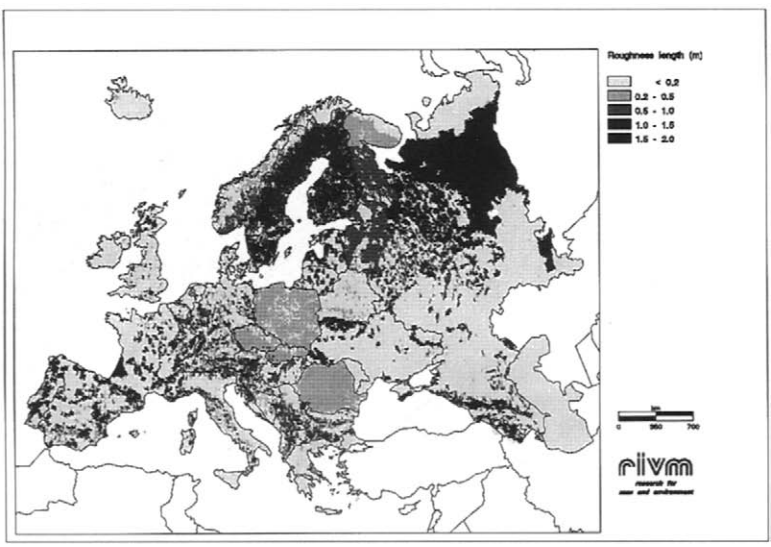

B

FIGURE 5.30 Summer (A) and winter (B) roughness length map of Europe on a $1/6^0$ x $1/6^0$ grid (in cm) (after Van Pul *et al.*, 1995).

The land-use map for Europe, based on a $1/6^0$ x $1/6^0$ (ca. 10 x 20 km), is constructed by RIVM from ground-based and satellite observations (Van Velde *et al.*, 1994). The map is shown in Figure 5.29. Figure 5.30 shows roughness length maps for the summer and winter seasons as derived from the land-use map. These maps were estimated according to the method described in section 5.2.2. The roughness length is used for estimating atmospheric transport to the surface. For each land-use class, the coverage within a grid cell and the deposition velocity are calculated. The average deposition velocity for a grid cell is then calculated by weighting the land-use specific deposition velocities with the surface area within that specific grid cell. Site-specific dry deposition might be calculated likewise, provided that detailed land-use and surface-roughness data of the site is available. Here aggregated estimates are presented.

Figure 5.31 to 5.33 show maps of the annual average dry deposition on a $1/6^0$ x $1/6^0$ scale of NOy, NHx and SOx in Europe. The effect of land use (roughness) and the difference in V_d is clearly shown. In areas with forested terrain (see Figure 5.29) the dry deposition is increased relative to the EMEP values, and, for example, in dry areas, the dry deposition is decreased as a result of a difference in V_d estimates. There is a clear sub-grid effect. The variation in dry deposition within EMEP grids is determined by variation in land use. This is the result of a variation in the resistance due to atmospheric transport due to differences in roughness (see Figure 5.29), or of a variation of the surface resistance due to differences in vegetation and surface conditions.

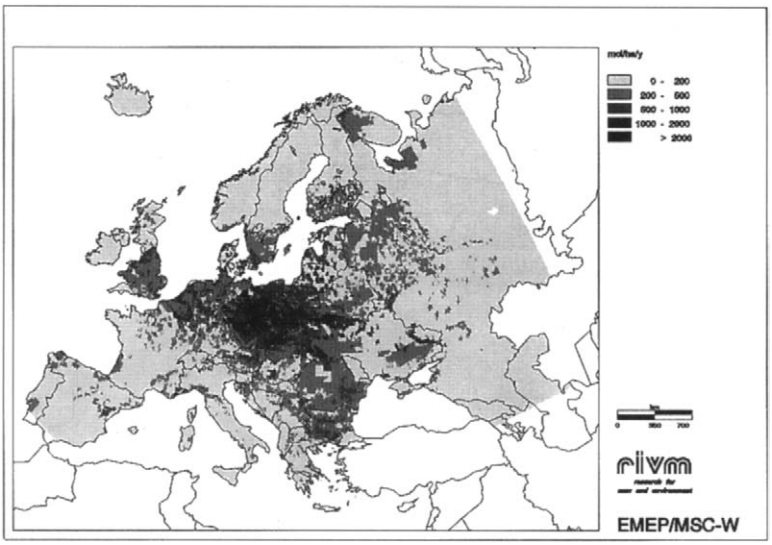

FIGURE 5.31 Dry deposition of SOx in Europe on a $1/6^0$ x $1/6^0$ scale in mol ha^{-1} a^{-1} (Van Pul *et al.*, 1995)

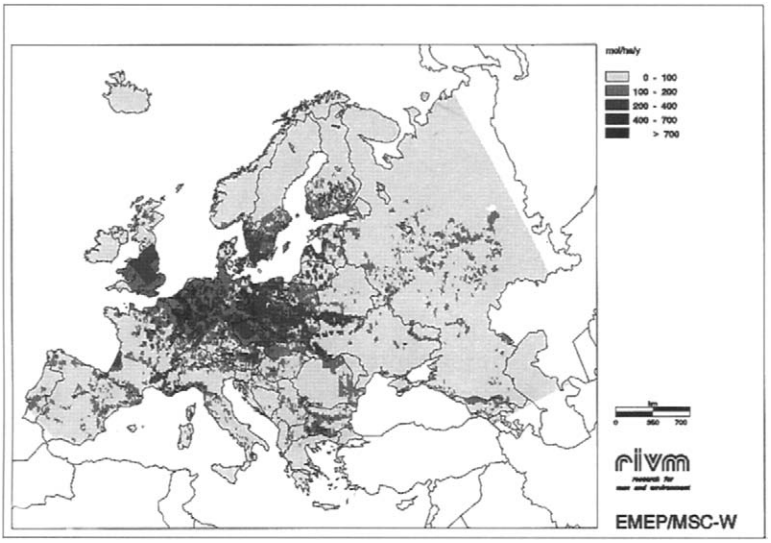

FIGURE 5.32 Dry deposition of NOy in Europe on a $1/6^0$ x $1/6^0$ scale in mol ha^{-1} a^{-1} (Van Pul *et al.*, 1995)

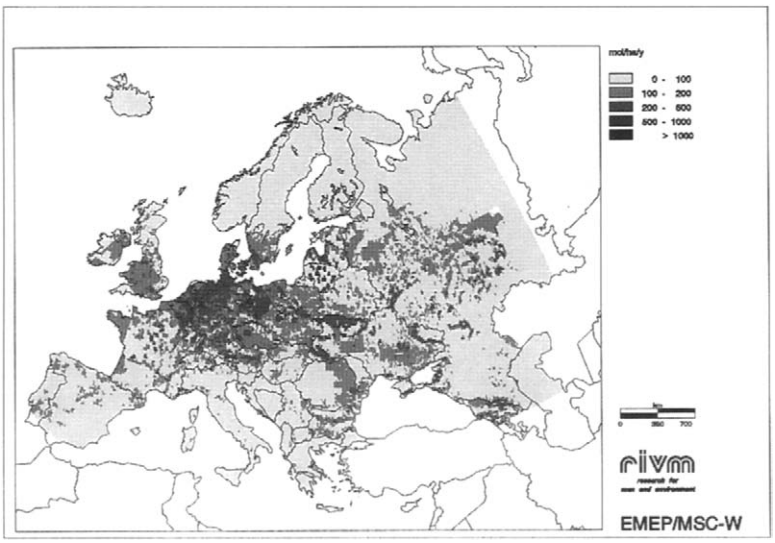

FIGURE 5.33 Dry deposition of NHx in Europe on a $1/6^0$ x $1/6^0$ scale in mol ha^{-1} a^{-1} (Van Pul et al., 1995)

Dry base cation deposition

The EDACS model is used to estimate the dry deposition of base cations in Europe. The dry deposition velocity is calculated for each land use class within the 1/6 x 1/6° grid cells for every six hours and averaged over the year. The deposition velocity is parametrised using the equations given in section 4.2.2. As is the case for the Netherlands, there is a serious lack of measured and modelled base cation concentrations in Europe. Therefore, the same method to estimate concentrations is used as that for the Netherlands (see section 5.2.3). The annual average base cation concentration maps are derived from the interpolated precipitation concentration maps given in Figure 5.24, 5.26, 5.27 and 5.28, and scavenging ratios of Eder and Dennis (1990) extended with the Speulder forest data. Correlations in time are not taken into account, because only annual data are available. Dry deposition maps of Na^+, Ca^{2+}, Mg^{2+} and K^+ are given in Figure 5.34 to 5.37. Figure 5.38 gives the total dry deposition of base cations (Mg^{2+}+Ca^{2+}+K^+), which is relevant for estimating critical loads. The spatial variation of the dry deposition of Na^+, Ca^{2+}, Mg^{2+} and K^+ is similar to that of precipitation concentrations. However, the influence of roughness is clearly shown in the figures. Data have not been compared with measurements because these first estimates for the small scale of Europe have been finished two minutes before printing this book. However, a quick glance at the data representative for the Speulder forest and some other sites in Europe shows that the agreement is reasonably good!

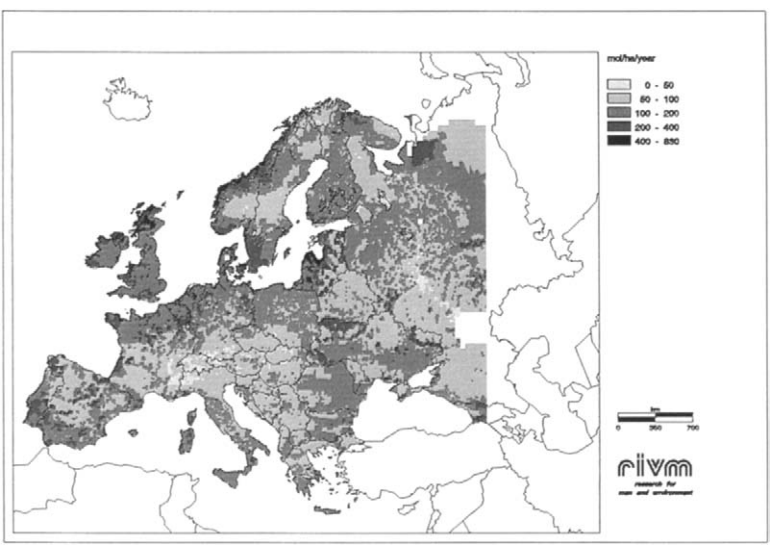

FIGURE 5.34 Dry deposition of Na^+ in Europe on a 1/6 x 1/6° scale in mol ha^{-1} a^{-1}.

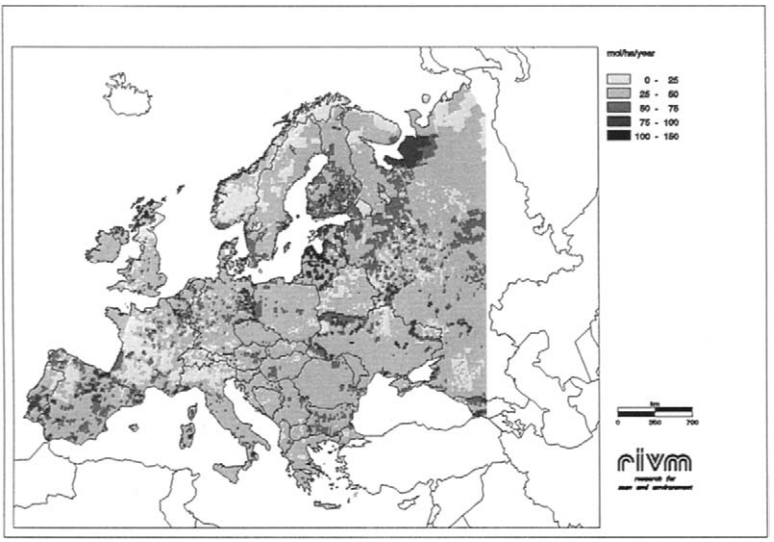

FIGURE 5.35 Dry deposition of Ca^{2+} in Europe on a 1/6 x 1/6° scale in mol ha^{-1} a^{-1}.

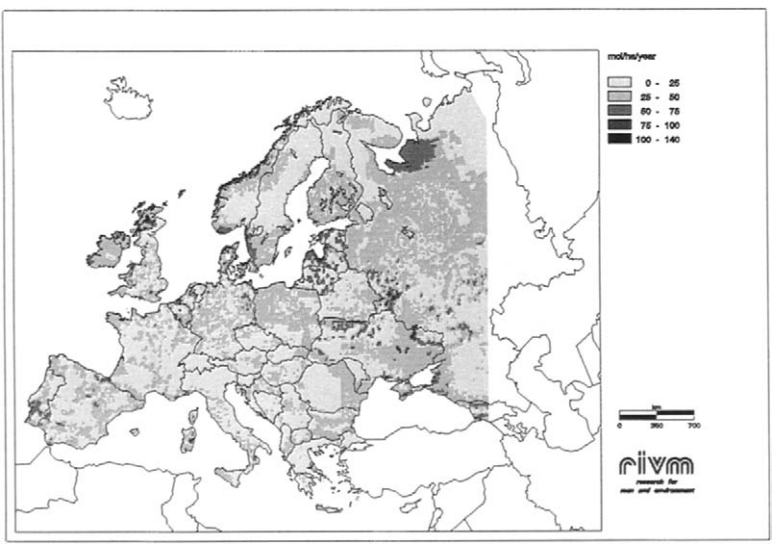

FIGURE 5.36 Dry deposition of Mg^{2+} in Europe on a 1/6 x 1/6° scale in mol ha^{-1} a^{-1}.

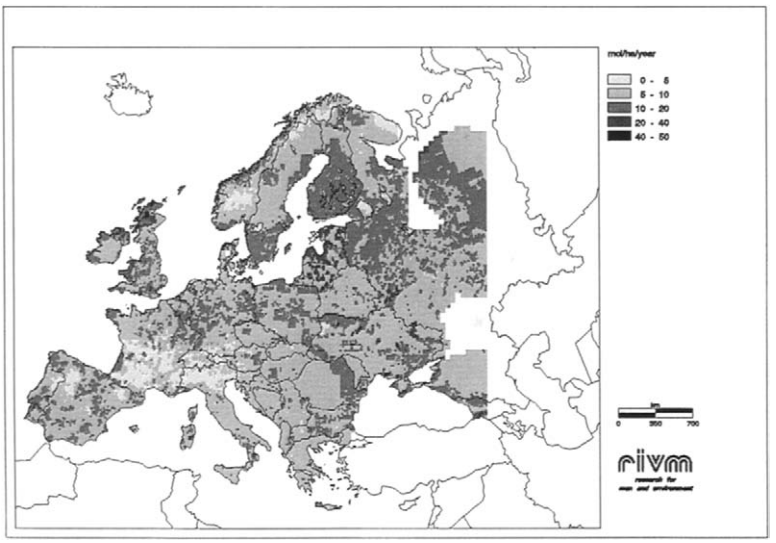

FIGURE 5.37 Dry deposition of K^+ in Europe on a 1/6 x 1/6° scale in mol ha^{-1} a^{-1}.

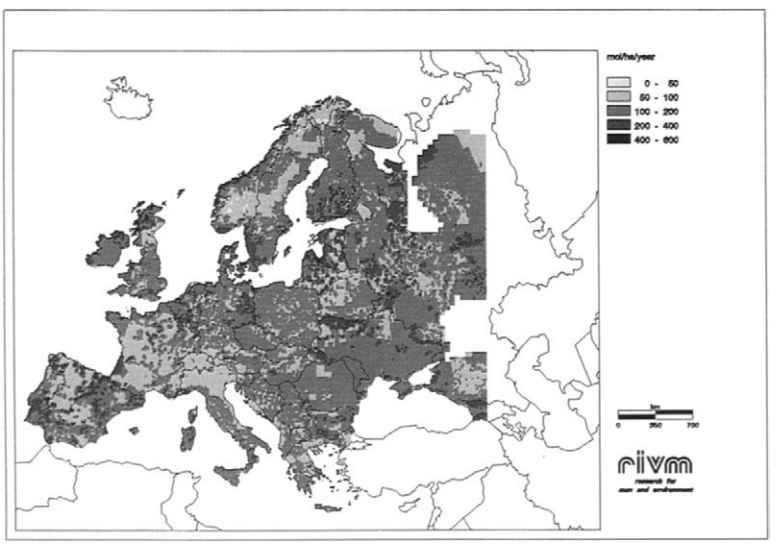

FIGURE 5.38 Dry deposition of base cations (Mg^{2+}+Ca^{2+}+K^+) in Europe on a 1/6 x 1/6° scale in mol ha^{-1} a^{-1}.

5.3.4 TOTAL DEPOSITION

Acidifying components

Total deposition of these components is given in Figures 5.39 to 5.41. Highest deposition of total sulphur occurs in the 'Black Triangle'. Relatively high sulphur fluxes are also found in parts of the Ukraine and former Yugoslavia. The highest deposition of total nitrogen is observed for the area including northern France, Belgium, The Netherlands, Germany, the Czech and Slovak Republics and Poland. Lower depositions are found over southwestern Europe, Ireland and northern Scandinavia. High deposition of oxidised nitrogen (>0.7 g N m^{-2} a^{-1}) is found in an area mainly covering the Netherlands, Germany and large parts of Poland, whereas high deposition of reduced nitrogen is also found over large parts of Ireland, Great Britain, France and Eastern Europe.

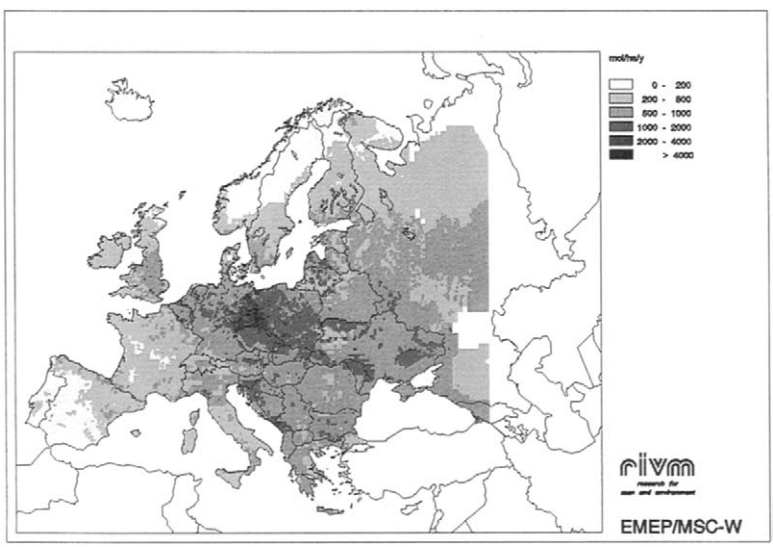

FIGURE 5.39 Total deposition of SOx in Europe on a 1/6 x 1/6° scale in mol ha^{-1} a^{-1} (Van Pul *et al.*, 1995)

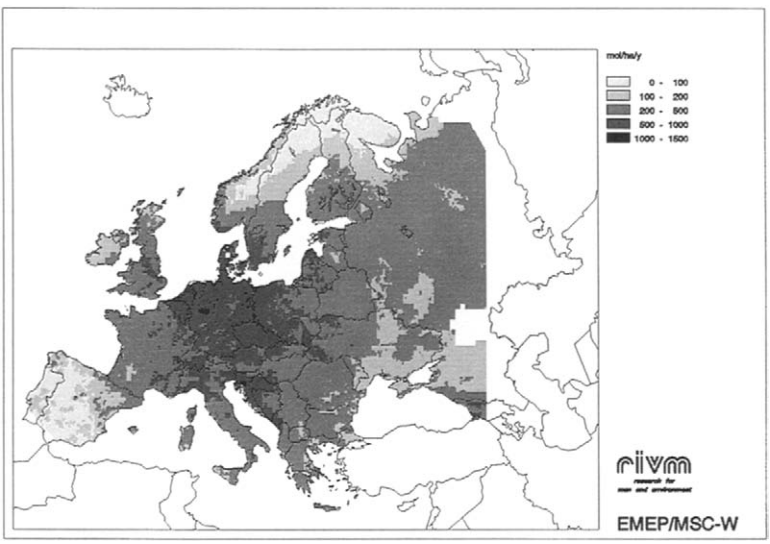

FIGURE 5.40 Total deposition of NOy in Europe on a 1/6 x 1/6° scale in mol ha^{-1} a^{-1} (Van Pul *et al.*, 1995)

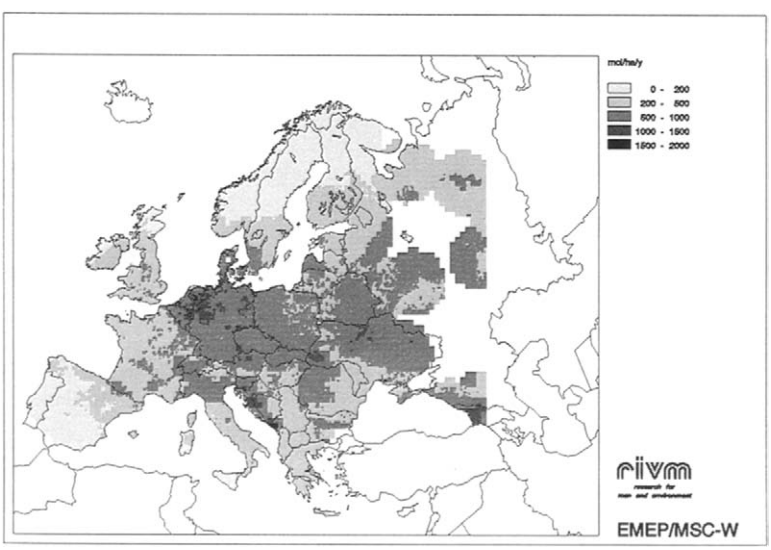

FIGURE 5.41 Total deposition of NHx in Europe on a 1/6 x 1/6° scale in mol ha^{-1} a^{-1} (Van Pul *et al.*, 1995)

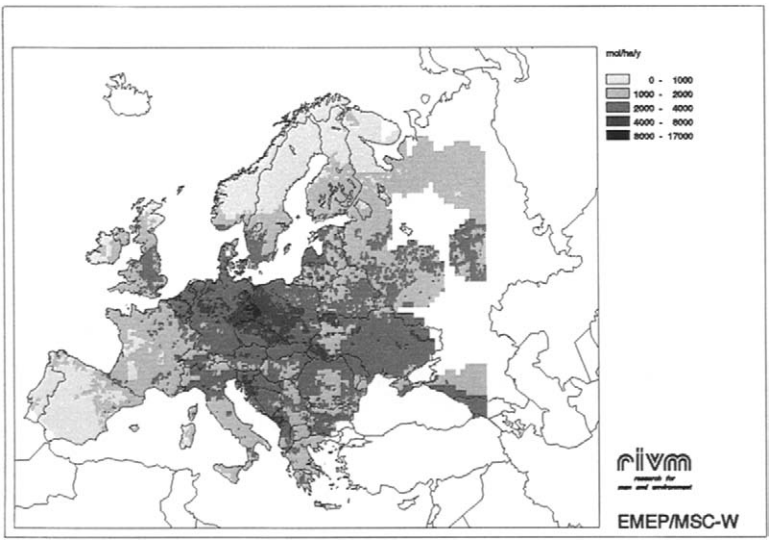

FIGURE 5.42 Total deposition of potential acid in Europe on a 1/6 x 1/6° scale in mol ha^{-1} a^{-1} (Van Pul *et al.*, 1995)

In all countries in Europe, only a fraction of the total deposition within the country originates from emission sources within the country itself. Figures 5.43 and 5.44 shows the emission and deposition of SOx, NOy and NHx per unit area per country or region in Europe in 1993 (data from Tuovinen *et al.*, 1994). These data may be somewhat different from those presented in this chapter because these are estimated using the long-range transport model results in which different deposition parametrisations are used. Furthermore, because of the large grid cells used as model resolution, the small countries, such as the Netherlands, are covered by grid cells, which also cover part of neighbouring countries. Moreover, the surface area of countries used to determine the average fluxes per unit area is different, leading, for example, to lower fluxes in the Netherlands than reported in section 5.2.

Figures 5.43 and 5.44 show which component contributes most to the potential acid emission or deposition in each country. Furthermore, they show where the potential acid emission or deposition is highest in Europe, and that in many countries of Europe sulphur is the most important component contributing to the potential acid emission and deposition. Nitrogen oxides always have the lowest contribution to the potential acid emission and deposition, only for Belgium, Norway, Sweden, Germany, the Czech Republic and the United Kingdom, the emission of NOx is higher than that of NH_3. In the Netherlands, France, Iceland, Ireland, Switzerland, Turkey, Latvia, Lithuania and Macedonia, the NH_3 emissions dominate over the other two components. The highest sulphur deposition is found in the Czech Republic, being

about 2700 mol H^+ ha^{-1} a^{-1}. The lowest sulphur deposition per unit area is found in Iceland (35 mol H^+ ha^{-1} a^{-1}), except for the oceans and seas. The highest nitrogen oxide and reduced nitrogen deposition per unit area are found in the Netherlands, being 750 and 1770 mol H^+ ha^{-1} a^{-1}, respectively. The lowest fluxes of NOx and NHx are found in Iceland, being 35 and 16 mol H^+ ha^{-1} a^{-1}, respectively.

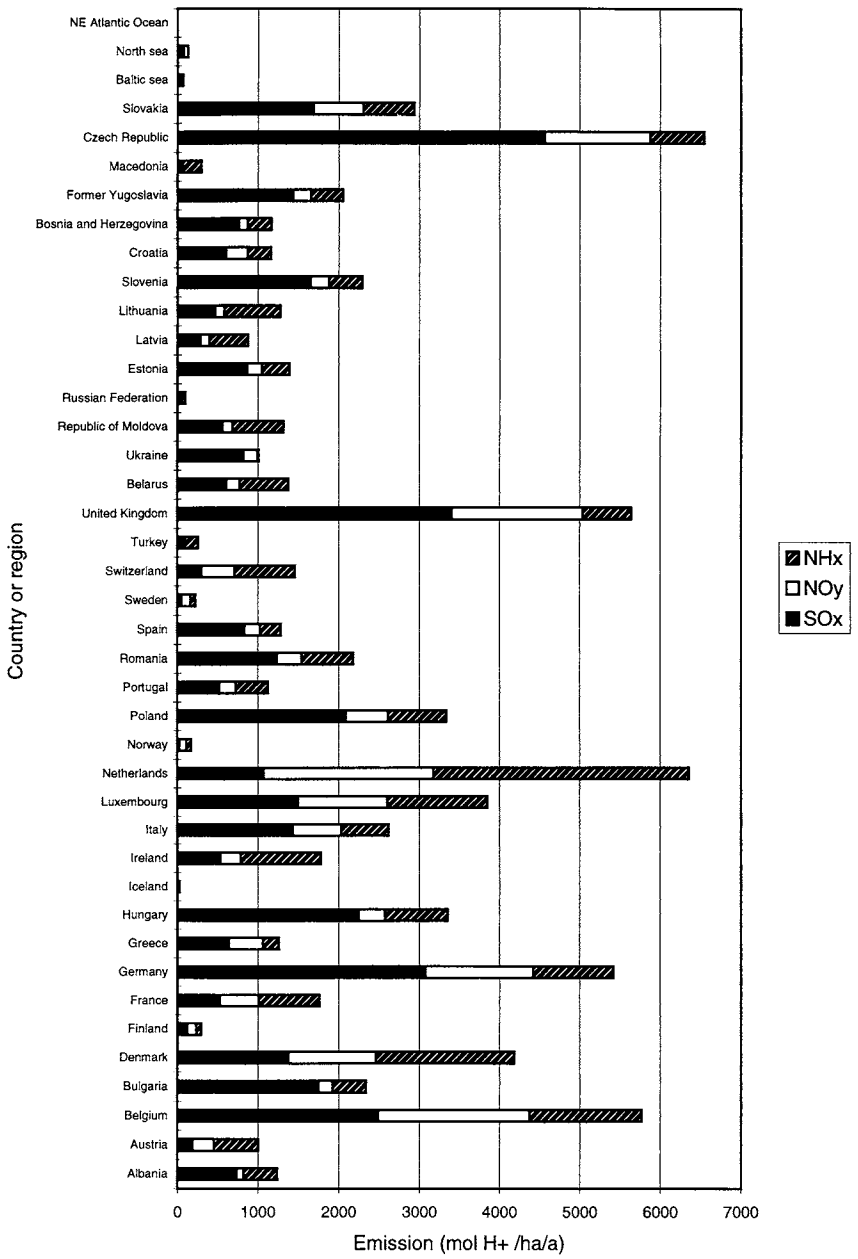

FIGURE 5.43 Emission of SOx, NOy and NHx per country or region in Europe in 1993 expressed in mol H^+ ha^{-1} a^{-1} (Tuovinen *et al.*, 1994).

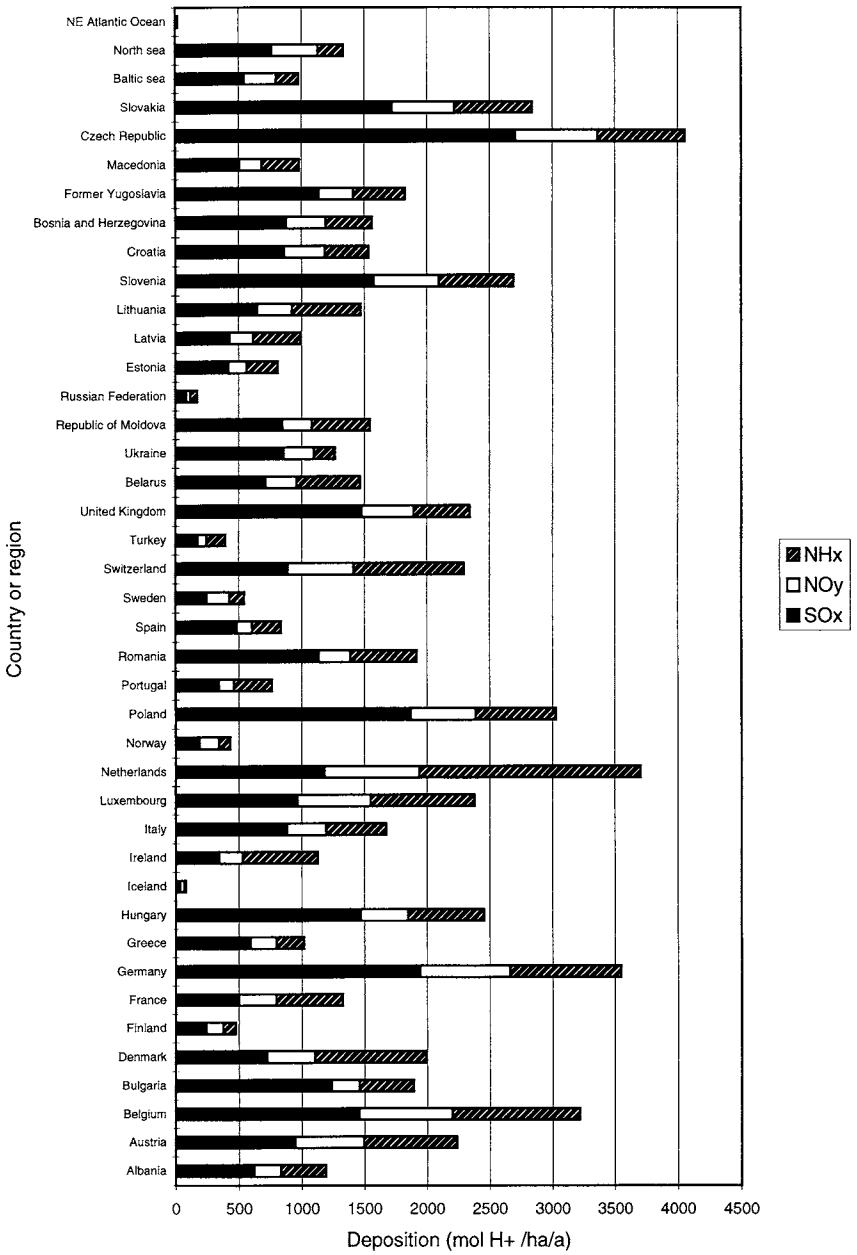

FIGURE 5.44 Deposition of SOx, NOy and NHx per country or region in Europe in 1993 expressed in mol H^+ ha^{-1} a^{-1} (Tuovinen *et al.*, 1994).

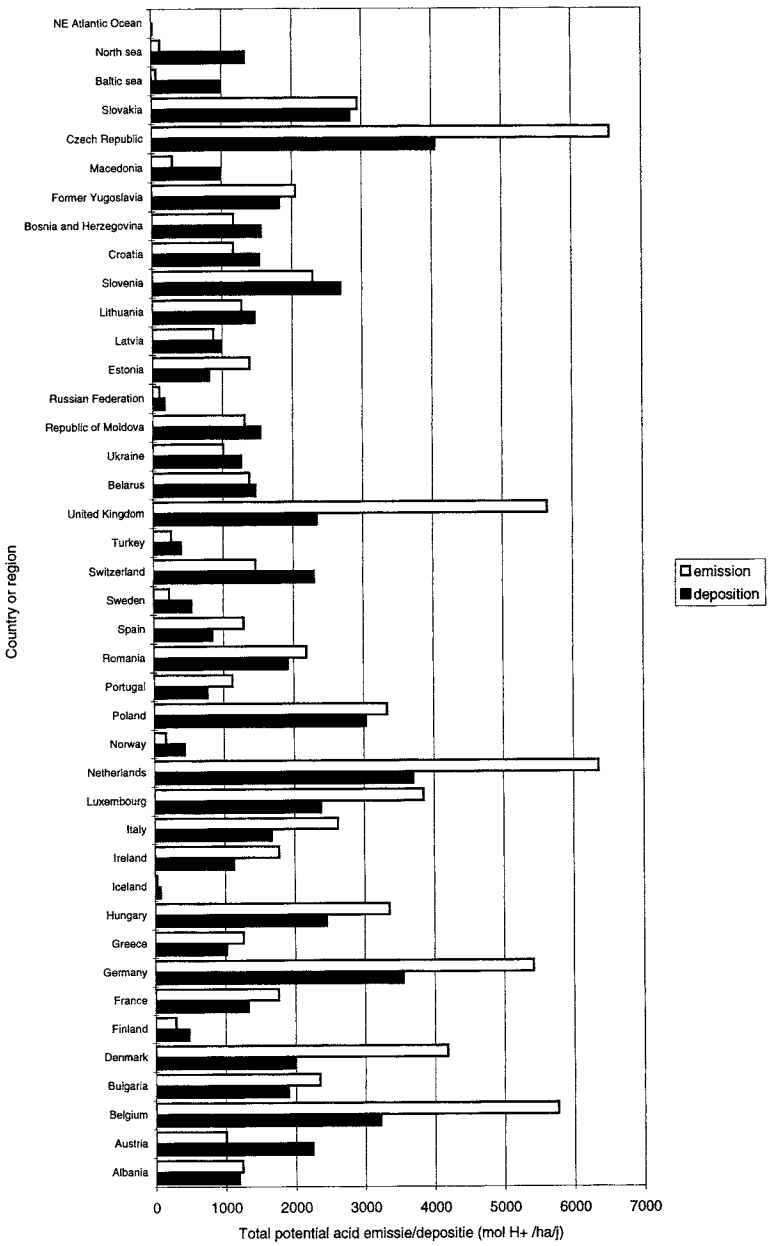

FIGURE 5.45 Emission and deposition of potential acid per country or region in Europe in 1993 in mol H^+ ha^{-1} a^{-1} (Tuovinen *et al.*, 1994).

Figure 5.45 shows the total potential emission next to the deposition in each country, expressed as average flux in the country. From this figure it can be deduced whether a country is a net-importer or exporter of acidic deposition and which country receives the highest fluxes per unit area. The figure shows that the largest emitters are the Czech Republic, the United Kingdom, The Netherlands, Germany, Denmark and Belgium. The largest fluxes are received by the Czech Republic, Poland, The Netherlands, Germany and Belgium. Relatively large net exporters of acidic pollutants are the United Kingdom, Germany, the Czech Republic, The Netherlands, Luxembourg, Italy, Denmark and Belgium. Relatively large net importers are the oceans and sees, Macedonia, Sweden, Norway, Finland, Switzerland and Austria. The extent of transboundary exchange of pollutants is a very complex function of the atmospheric residence time of the pollutant, the relative size of the country, location of emission sources within the country, the relative magnitude of domestic sources and sources outside the country, the strength and direction of dominant winds, and many other factors.

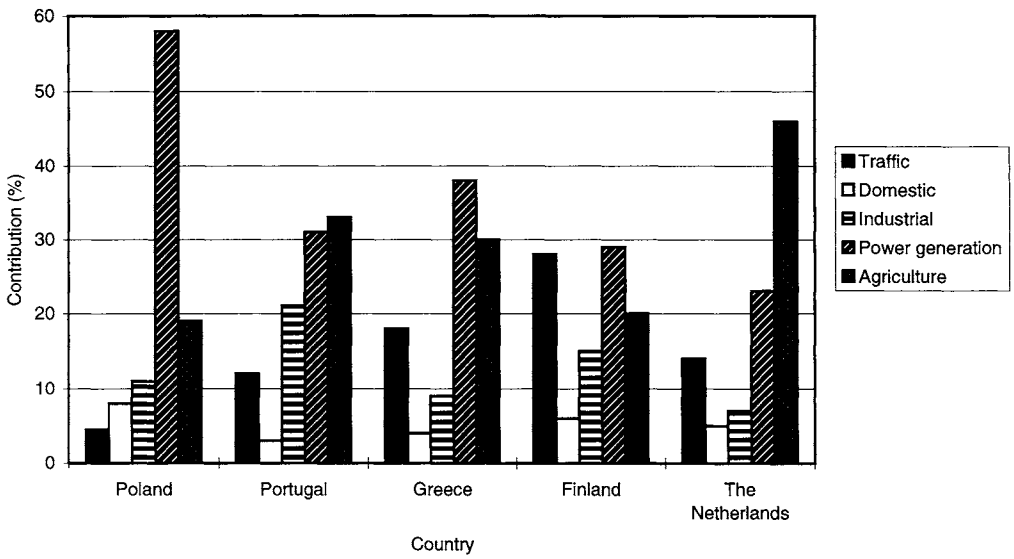

FIGURE 5.46 Contribution (%) of different source categories to the total potential acid deposition for 5 different countries in Europe in 1990.

Contribution of source categories to the deposition

The contribution of different source categories to the deposition varies to a large extent for different regions in Europe. This can be illustrated with Figure 5.46 where the contribution of different categories to the deposition in different countries is given. These data are calculated with the EMEP model (Tuovinen *et al.*, 1994) and are representative for the situation in 1990. Figure 5.46 shows that for Poland power generation is the main source of deposition, whereas the contribution of agriculture is highest in the Netherlands. Traffic and power generation are the main contributors to the deposition in Finland. In Portugal domestic and power generation is equally important. Industry is not dominating in either of these countries. Highest contribution of industry to deposition is found in Portugal (20%). The data for these 5 countries only serve as an example of differences in source contribution for different regions in Europe. It shows that the abatement strategies will have a different focus in different countries.

Base cations

No maps of base cation deposition in Europe have been available up to now. Nevertheless, information on base cation deposition is important as base cations influence the acidity of air and precipitation and in certain areas may significantly neutralise acid deposition. First maps of total base cation deposition are presented in Figure 5.47 to 5.50. Total deposition is estimated as the sum of wet and dry deposition. With the exception of forested areas, the contribution of wet deposition to the total deposition of base cations is higher than dry deposition. Highest sodium fluxes are found in coastal areas, reflecting sea salt being the main source. For Ca^{2+}, Mg^{2+} and K^{+} relatively high fluxes are estimated e.g. in the Ukraine, in the former Yugoslavia and the southern and eastern part of Europe. Main sources of high input can be combustion processes, calcareous soils and high rainfall. Figure 5.41 shows the total base cation deposition which to some extent is available for neutralising acid deposition ($Ca^{2+}+Mg^{2+}+K^{+}$). Note that the lowest input is found in regions where the buffering capacity of the soil is already relatively low, e.g. in Scandinavia. Highest fluxes are found near the coast of Ireland and Scotland, in the 'Black Triangle', Ukraine, former Yugoslavia and some parts of Italy.

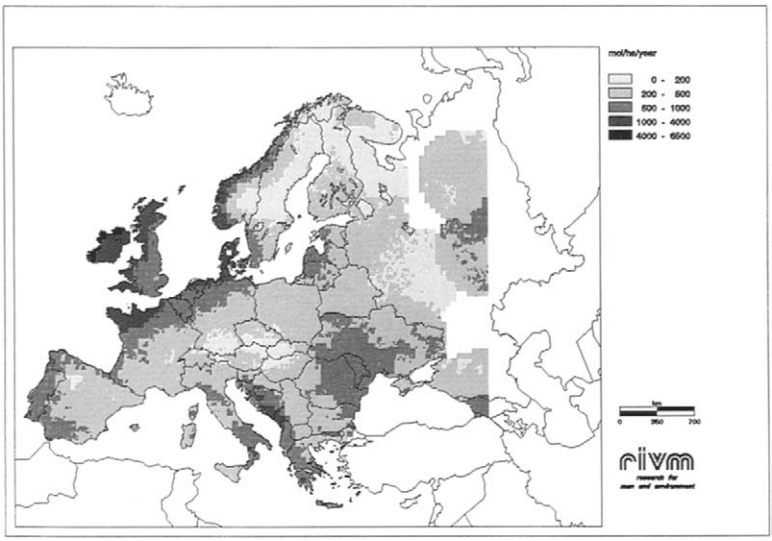

FIGURE 5.47 Total deposition of Na^+ in Europe on a 1/6 x 1/6° scale in mol ha^{-1} a^{-1}.

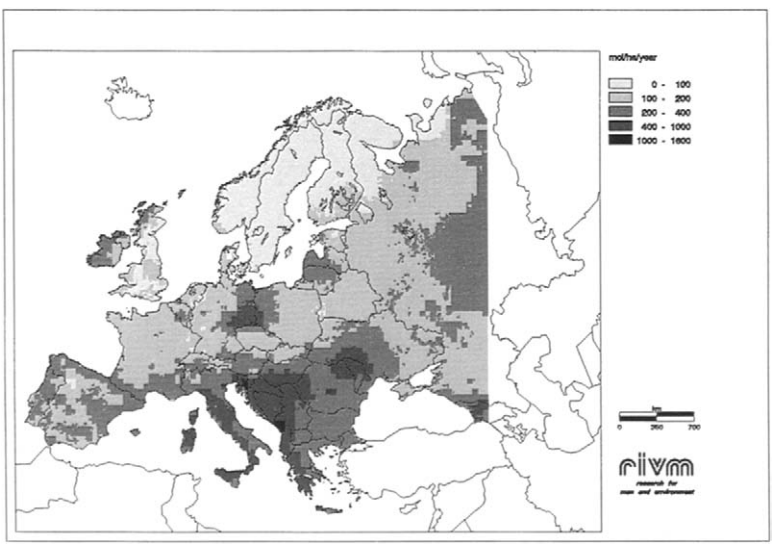

FIGURE 5.48 Total deposition of Ca^{2+} in Europe on a 1/6 x 1/6° scale in mol ha^{-1} a^{-1}.

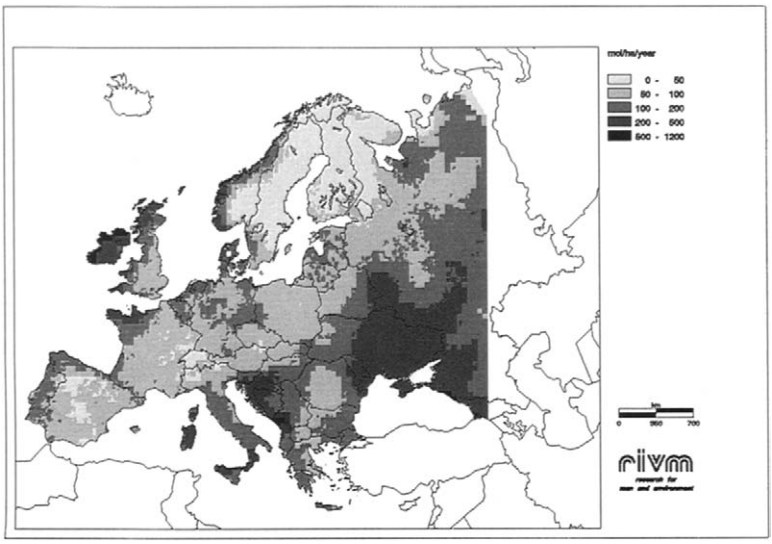

FIGURE 5.49 Total deposition of Mg^{2+} in Europe on a 1/6 x 1/6° scale in mol ha^{-1} a^{-1}.

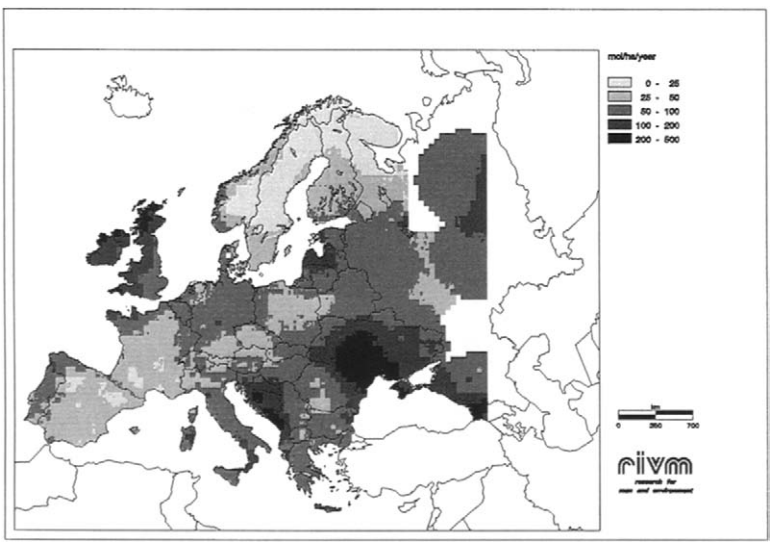

FIGURE 5.50 Total deposition of K^{+} in Europe on a 1/6 x 1/6° scale in mol ha^{-1} a^{-1}.

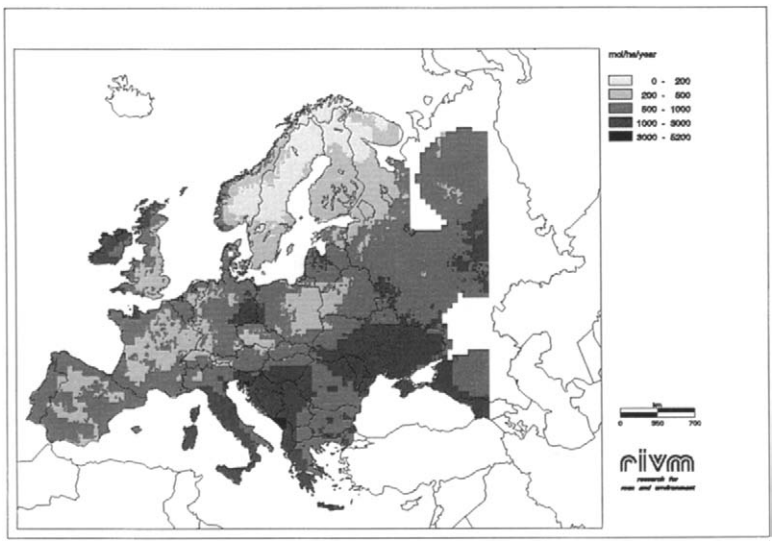

FIGURE 5.51 Total deposition of base cations ($Ca^{2+}+Mg^{2+}+K^{+}$) in Europe on a 1/6 x 1/6° scale in mol ha^{-1} a^{-1}

5.4 VARIATION IN DEPOSITION OVER SEVERAL YEARS

There are three ways of determining long-term trends in atmospheric input. First of all, it is possible to estimate trends using estimates of emissions, which in turn are used as input for long-range transport models to estimate atmospheric input using long-term average meteorological statistics (Mylona, 1993). There are several limitations to such a study: it is difficult to accurately determine long-term trends in emissions because usually data are scarce and differ strongly in quality. Furthermore, the long-term average meteorology used in long-range transport models is usually based on the most recent 10 to 30 years and may thus differ from longer-term data. Finally, non-linearities in deposition processes and atmospheric chemistry are not taken into account in current models.

The second option is to use historical measurements to determine long-term trends. The problem with this method is that the quality of data is sometimes not known and/or difficult to assess. Analysis of samples, sample strategy in relation to disturbing factors (sources, obstacles, etc.) are of varying quality and sometimes even unknown. Despite this, historical measurements are of enormous value for obtaining insight in the development in the pollution climates.

A third option is that a combination of long-term emission estimates with long-range transport model calculations and historical measurements are used. With this method, model calculations might be evaluated or calibrated using historical measurements, e.g. to test meteorological statistics and/or non-linearities in processes related to atmospheric input.

5.4.1 DEPOSITION AS A RESULT OF NATURAL SOURCES

If stringent emission reductions are realised in the future, the background deposition will become relatively more important. Natural sources of acidifying components can be the soil, volcanoes, oceans, lightning, wild animals and fires.

On the basis of precipitation measurements in remote areas of the world seen in the GPCP network (Global Precipitation Chemistry Project), it was found that the background pH is closer to 5.0 than 5.6, the latter being theoretically derived and assumed up to now (Sisteron *et al.*, 1989). The same data suggest that apart from a sea-salt background, a volume weighted concentration of SO_4^{2-}, NO_3^- and NH_4^+ of 10.6, 4.5 and 3.4 meq l^{-1}, respectively, was found as background. Sisteron *et al.* speculate that these values might be representative for the natural background. These data are somewhat higher than those reported by Locht and Van Aalst (1988), who found ranges for SO_4^{2-}, NO_3^- and NH_4^+ of, respectively, 2.2 - 7.3, 1.3 - 4.3 and 1.1 - 4.2. Using a long-term average amount of precipitation of 800 mm in the Netherlands, the values from Sisteron *et al.* (1989) would lead to background wet deposition fluxes in the Netherlands as listed in Table 5.8.

For NO_3^- and NH_4^+ these fluxes are in agreement with estimations made by Locht and Van Aalst (1988), i.e. 36 mol NOy ha^{-1} a^{-1} and 27 mol NHx ha^{-1} a^{-1}. Only the SOx flux is estimated as being lower by Locht and Van Aalst (25 mol SO_x ha^{-1} a^{-1}). Locht and Van Aalst (1988) estimated non-anthropogenic fluxes of acidifying components by two methods. A box model, where emissions were taken equal to depositions for a large area was used, and a transport model, along with emission estimates. Their estimates for the dry deposition of acidifying components from natural sources are also listed in Table 5.8. The total potential acid deposition is, in the present-day situation (1993), 1 order of magnitude greater than the background deposition estimates in Table 5.8. The deposition due to natural emissions can therefore presently be neglected. In this estimate, species such as H_2S and PAN have not been taken into account. These may also contribute to background deposition.

TABLE 5.8 Background wet, dry and total deposition in the Netherlands (mol H^+ ha^{-1} a^{-1}).

Component	Wet deposition	Dry deposition	Total deposition
SOx	74	24	98
NOy	32	13	45
NHx	24	48	72
Halogen	3	3	6
RCOOH	300	30	60
Potential acid	160	120	280

5.4.2 HISTORICAL MEASUREMENTS OF WET DEPOSITION

Section 1.2 provides a short overview of the historical development of atmospheric deposition measurements. Some of the data referred to in that chapter will be used here to assess the development in deposition in the former century up till now. More recent data in the Netherlands and Europe will be used to assess the trend in deposition after the maximum emissions of sulphur occurred in the seventies and nitrogen in the eighties.

Nitrogen compounds

The longest time series of wet deposition measurements in Europe to our knowledge were made in Paris (Montsouris) France by Albert Levy in 1876 to 1907 and in Rothamsted (England) between 1850 and 1980. The data from Montsouris comprise wet deposition measurements of oxidised and reduced nitrogen in precipitation. Sulphate was also analysed, but the main (agricultural) interest was focused on nitrogen (Ulrich and Williot, 1993). The data for ammonium and nitrate from Rothamsted and Montsouris are given in Figure 5.52. Also plotted in this figure are the estimates of the natural background deposition (section 5.4.1). These were considered to be representative for the years before 1850. Also shown in

the graph are the data from Eriksson (1952) and Miller (1905) for several locations in Europe. An assessment of the quality of data is reported in Brimblecombe and Pitman (1980) for Rothamsted, and in Ulrich and Williot (1993) for Montsouris and other French data. The data have not been corrected for dry deposition to the funnels of the samplers and other disturbing factors (Eriksson, 1952; Buijsman and Erisman, 1988). The dry deposition contribution could be 25% and 15% for ammonium and nitrate, respectively. The dry deposition contribution to the Montsouris and Rothamsted samples could be even higher because relatively large collecting funnels (3-5 m^2) were used in order to collect enough daily sample for analysis.

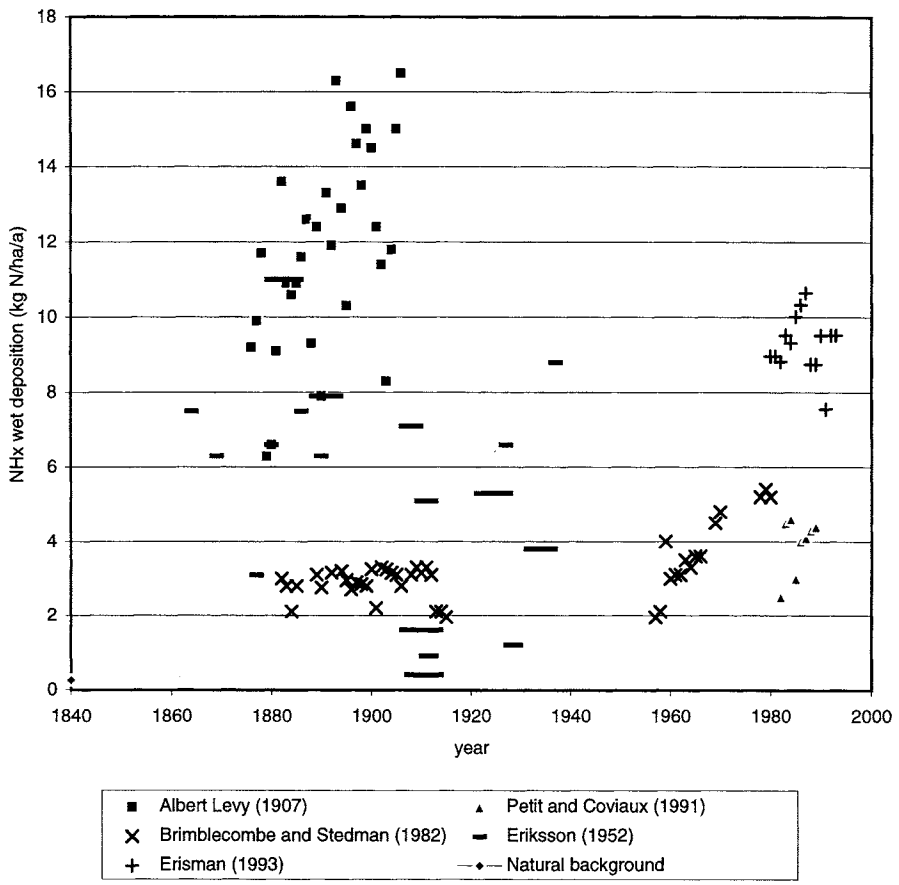

FIGURE 5.52 Wet deposition of ammonium at Rothamsted (UK) and Montsouris (France) (in kg N ha^{-1} a^{-1})

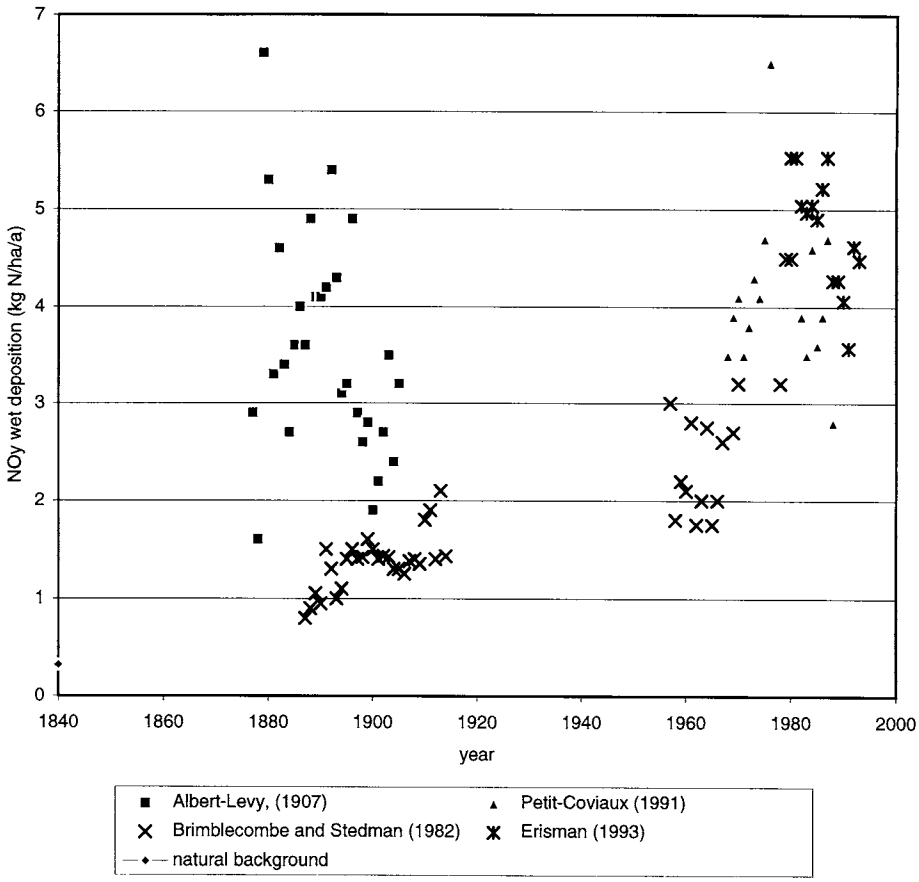

FIGURE 5.52 *(continued)* Wet deposition of nitrate at Rothamsted (UK) and Montsouris (France) (in kg N ha^{-1} a^{-1}

It is striking to see the very high NH_4^+ wet deposition values in Montsouris between 1876 and 1907. The values are in the same range of the current wet deposition data in the Netherlands, considered to be the highest in Europe (see Chapter 5). The first reaction is to suspect the measurements. However, this is one of the best documented and executed methods of that time. The quality of data was investigated by Ulrich and Williot (1993) who concluded that the reproducibility of the method was good and that the quality of data was acceptable. It must, however, be noted that ammonia-free laboratories did not exist then and it was not known that both human breath and sweat contains ammonia. Assuming that the data measured

in Montsouris are to some extent influenced by these error sources, the data still show very high values. Another explanation for this could be that the city of Paris, in which the monitoring site was situated, acted as a source of ammonia found in wet deposition. Indeed, Albert Levy, who was the first to make continuous measurements of ambient NH_3, measured average concentrations of 17 $\mu g\ m^{-3}$ at the same site. This is comparable to concentrations measured at sites located in high ammonia emission areas in the Netherlands nowadays (Erisman and Boermans, 1995). These high concentrations may be due to the excretion of animals in or near to the city, but also to the emission of NH_3 from coal combustion (Smith, 1872, Freyer, 1978). Müller (1888) showed with his snow measurements in and outside the city in Braunsweig (Germany), that the NH_4^+ concentration in snow depends on the population density, and more specific, on the flue gas emissions. Furthermore, measurements made by Bineau in 1853 (Bineau, 1855) in and outside Lyon showed that NH_4^+ concentrations were higher in winter than in summer in the city, whereas they were higher in summer than in winter in the rural areas outside Lyon. This also suggests that in the city the NH_4^+ content in precipitation was mainly determined by burning of coal which was much more intense in winter, whereas outside the city concentrations were mainly determined by emissions from animal waste, because animal waste emissions are higher in summer than in winter (Asman, 1992). The other French, German and British data, collected in the same period as those sampled by Albert-Levy, large variations are shown, with concentrations comparable to or much lower than the Montsouris data.

The recent measurements at Montsouris, made by Petit and Coviaux (1991), show much lower values than those measured in 1876-1907. The NO_3 data in Montsouris also seem to be very high, comparable to levels found nowadays. Again, this might be due to the influence of local emissions from Paris. The levels are comparable to those measured by Petit and Coviaux (1991) in Paris nowadays. The sources have changed in and around the city, but this does not necessarily mean that the emission levels have changed.

The Rothamsted NH_4^+ data show a gradual increase from 1881 to 1960, and a steeper increase between 1960 to 1980. This is in line with the emission increase during these periods (see Chapter 2). Nitrate at Rothamsted shows a gradual increase from about 1 kg $ha^{-1}\ a^{-1}$ in 1884 to about 3 kg $ha^{-1}\ a^{-1}$ in 1980. The steep increase in nitrate levels after 1960 reflect the change in NOx emissions (see Chapter 2).

The natural background values estimated by Locht and Van Aalst (1988) are much lower than the lowest ammonium and nitrate levels measured, except for the NH_4 levels measured around 1910 in Stornaway in the far north of Scotland and at other lighthouses in the Hebrides and in Iceland (Russell and Richards, 1919). When leaving out the Montsouris data, the data in Figure 5.52 indicates that wet deposition of NO_3^- increased from 0.3 kg N $ha^{-1}\ a^{-1}$ in the period before 1850 to about 4 kg N $ha^{-1}\ a^{-1}$ in the 1980s, for NH_4^+ these figures are 0.25 to 4 - 10 kg N $ha^{-1}\ a^{-1}$, depending on the location. This is an increase by a factor of 10 - 15 for NO_3^- and 15 to 40 for NH_4^+.

Sulphur

Average sulphur concentrations in precipitation over several years are displayed in Figure 5.53. Concentrations are given because for most sites no precipitation amounts were given. The data arise from different sources (Liesegang, 1927; Rodhe and Granat, 1984; Smith, 1872; Eriksson, 1952; Lawes, 1883; Locht and Van Aalst, 1988) and are not corrected for dry

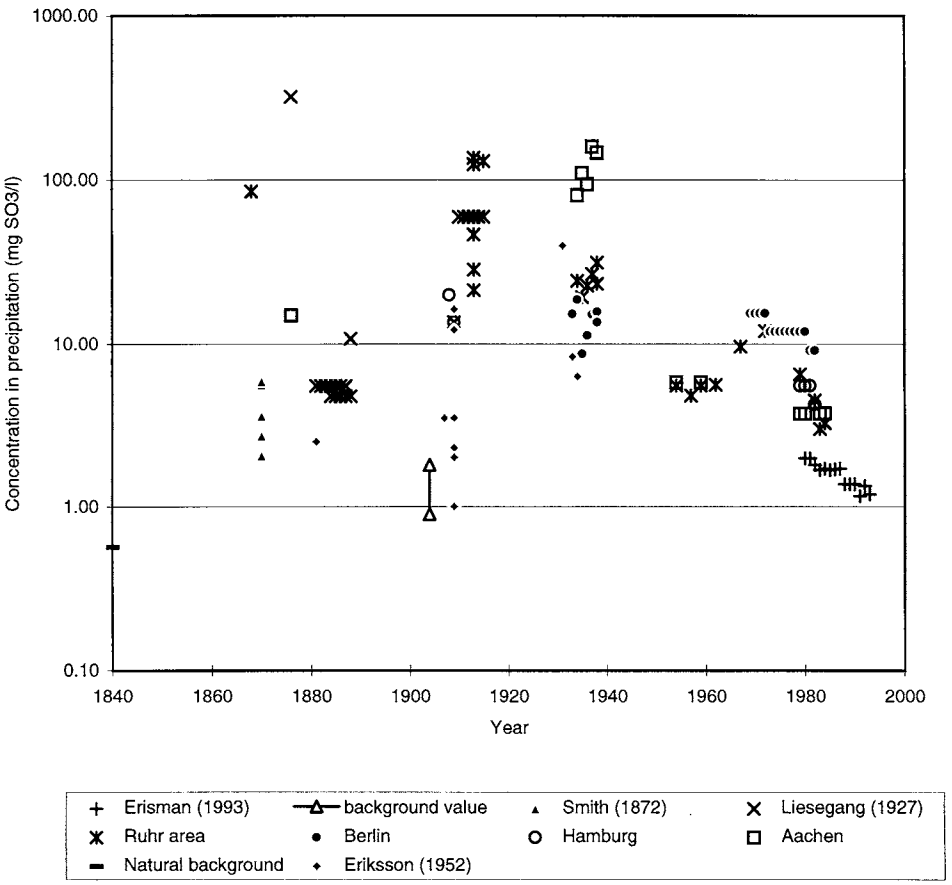

FIGURE 5.53 Concentrations of sulphur measured in precipitation at several locations in Europe (mg SO_3 l^{-1}).

deposition to the funnels of the bulk samplers. Most of the measurements were made in different areas in Germany, mostly near industrialised areas, such as the Ruhr area, Hamburg and Berlin. The data after 1960 comprise only those in Germany, in order to allow comparison

deposition to the funnels of the bulk samplers. Most of the measurements were made in different areas in Germany, mostly near industrialised areas, such as the Ruhr area, Hamburg and Berlin. The data after 1960 comprise only those in Germany, in order to allow comparison with other data. The Dutch data from 1980 to 1993 are also given for comparison. The data marked as Smith (1872) represent area averages obtained from measurements at several sites in the UK in the winter of 1870. The natural background is taken from estimates by Locht and Van Aalst (1988) (section 5.4.1). The other 'background values' are obtained from Liesegang (1927). These represent measurements in the rural areas of Tharand and Grillenburg in Germany.

Figure 5.53 displays several enormous concentrations in precipitation, up to 400 mg l^{-1} measured in the Ruhr area in Germany at the end of the eighteenth century. The scale in Figure 5.53 is logarithmic. The German data show an increase in concentration from 1870 to 1920. Between 1920 and 1940 concentrations remained the same, decreased after 1940 and increased again from the sixties to the seventies. After the seventies, the concentrations decreased again. These variations are similar to the variation in emissions in Germany between 1880 and 1990 (Mylona, 1993). Assuming a range of 700 to 1000 mm of precipitation at the sites, the bulk wet deposition of sulphur in Germany ranged from 50 - 70 mol ha^{-1} a^{-1} before 1850, to about 800 - 1100 mol ha^{-1} a^{-1} around 1900, 2000 to 3000 mol ha^{-1} a^{-1} in 1940, and 400 to 600 mol ha^{-1} a^{-1} in 1980.

Base cations

Dry deposition of base cations is estimated from wet deposition measurements via scavenging ratios. For those components for which scavenging ratios are obtained from a linear relationships between air concentrations and concentrations in precipitation (i.e. for all base cations at the low concentration ranges generally found in Europe), dry deposition is linear related to wet deposition. Temporal variations in dry deposition are therefore similar to those in wet deposition. Wet deposition of base cations is found to gradually decrease during the last 10 to 20 years in several parts of Europe and North America (Hedin *et al.*, 1994). The decline is related to the decrease in anthropogenic base cation emissions of fuel combustion processes and industrial processes as well as the reduction in emissions from unpaved roads. The decline of total base cation deposition was dominated by Ca^{2+}, which contributed about 80% to the total base cation decline (Hedin *et al.*, 1994; Buishand and Montfort, 1989). There is some evidence that in some parts of Europe the decline in base cation deposition have countered the effects of SO_2 emission reductions. Figure 5.54 shows the changes in concentrations of Na^+, Ca^{2+} and Mg^{2+} relative to the 5 year average concentrations (1932 - 1937) measured at Leiduin as reported by Leeflang (1938). The data in the figure illustrate the decline in Mg^{2+} and Ca^{2+} concentrations which are to some extent influenced by anthropogenic sources. Sodium, which is primarily emitted from the sea shows temporal variations, but no decline. Hedin *et al.* (1994) estimated a decline in base cation concentrations between 30 and 50% for different sites in the Netherlands between 1978 and 1987. Data in Figure 5.54 suggest that the

base cation concentrations decreased with 70% since 1932. The picture might be obscured by measuring errors or uncertainty in analysis in the Leeflang data. However, the Leeflang data are well documented and the uncertainty is expected to be low.

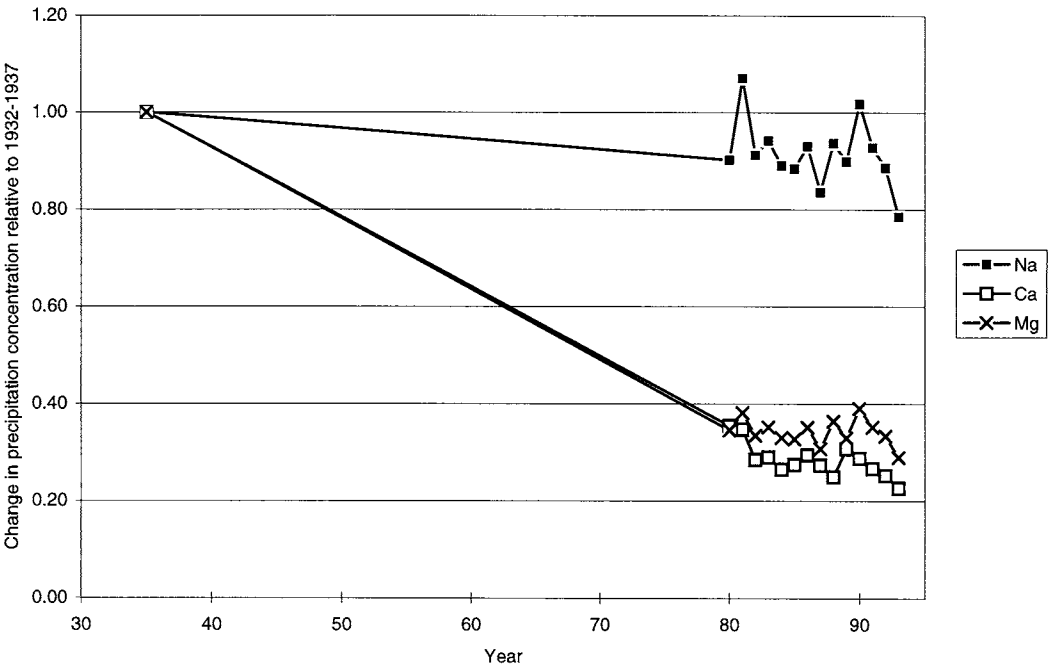

FIGURE 5.54 Changes in Na^+, Ca^{2+} and Mg^{2+} concentrations in precipitation (mg l^{-1}) measured at Leiduin near the Dutch coast.

The Netherlands

The first rainwater analysis in the Netherlands were made in Utrecht in 1825 by Mulder (1825). Van Ancum determined iodine concentrations somewhere in the Netherlands around 1850 (cf Ludwig, 1862). After these no reports are found on rainwater analysis until about 1900. The first systematic measurements in the Netherlands we found dated from around 1900. They comprise the determination of the chlorine content in precipitation sampled at Den Helder (Jorissen, 1906). Furthermore, Van der Sleen made measurements in the dunes near Haarlem around 1912 (cf. Leeflang, 1938). However, the first extensive research was published by Leeflang (1938). He published results of precipitation sampled every three months at several distances from the North Sea coast from 1932 to 1937. The quality of these measurements can be determined as the methods used are reasonably well described. His

measurements show a gradient from the coast land inward for Na^+, Ca^{2+}, Mg^{2+} and Cl^-, with highest concentrations at the coast and lowest at the Veluwe, about 86 km from the coast (Figure 5.55). The components which are related to inland (anthropogenic) sources, such as SO_4^{2-}, NH_4^+ and NO_3^- show a different horizontal gradient, with increasing concentrations with distance from the coast.

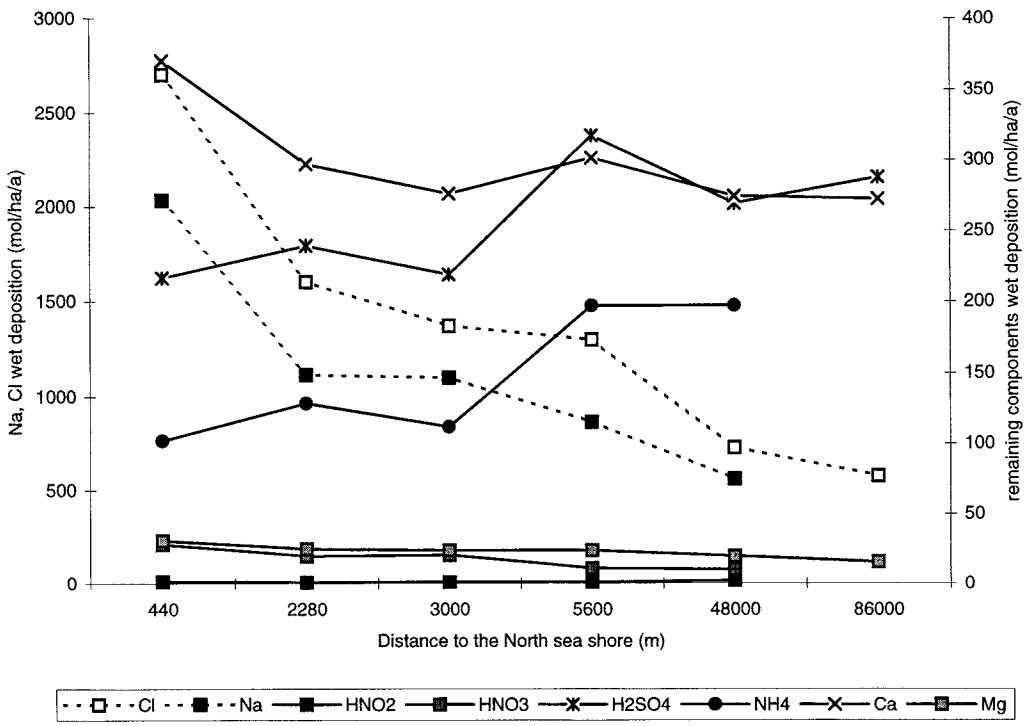

FIGURE 5.55 Horizontal gradient of wet deposition from the coast land inward as reported by Leeflang (1938). Data are averages of 5 years (1932 - 1937).

After the thirties, the measurements reported date from the fifties up till now. Ridder (1978) presents an overview of all the measurement sites where wet deposition was measured after the fifties in the Netherlands. About 200 different measurement sites were in use, most of them operated simultaneously in the seventies. Long-term measurements are available from the European Rossby monitoring network (1956 - 1970), in which wet deposition was made at three sites in the Netherlands: De Bilt, Den Helder and Witteveen, by KNMI and RIVM. TNO made measurements between 1959 and 1974 at Heijplaat and Oostvoorne. Figure 5.56 shows time series of concentrations measured at the five locations. Concentrations show a gradual

increase in SO_4^{2-}, NH_4^+ and NO_3^- concentrations during the fifties, sixties and seventies. Values are much lower in the eighties for SO_4^{2-} and NO_3^-. NH_4^+ levels are highest in the eighties. The values measured in the eighties are obtained from the LMR network which is the precipitation network still operating (Buijsman, 19??; RIVM, 1994). Figure 5.57 shows the deposition as measured at Witteveen during the years 1958 to 1993. Also plotted in this figure are the 5 year average values measured by Leeflang near the coast. The national emissions are also plotted in the figure. For SO_4^{2-} and NH_4^+ the variation in emissions and wet depositions are similar, with highest SO_2 emission and SO_4^{2-} deposition in the fifties and sixties (see also Figure 5.56), and highest NH_3 emission and NH_4^+ deposition in the eighties. Lowest emissions and depositions are observed in the thirties. For NO_3^- emission and deposition show different variations. The increase in deposition in the earlier years are similar to the emission increase. However, the measurements in the eighties are lower than those in the sixties and seventies, whereas they are expected to be higher based on the increase in emission.

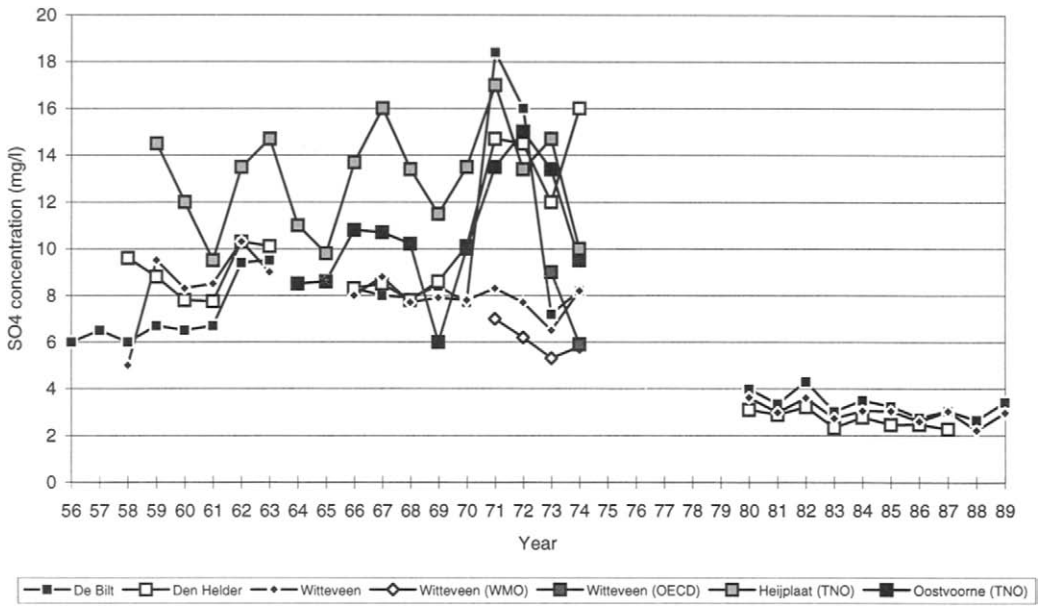

FIGURE 5.56 Time series of SO_4^{2-} concentration measurements in precipitation made at several sites in the Netherlands (mg l^{-1}

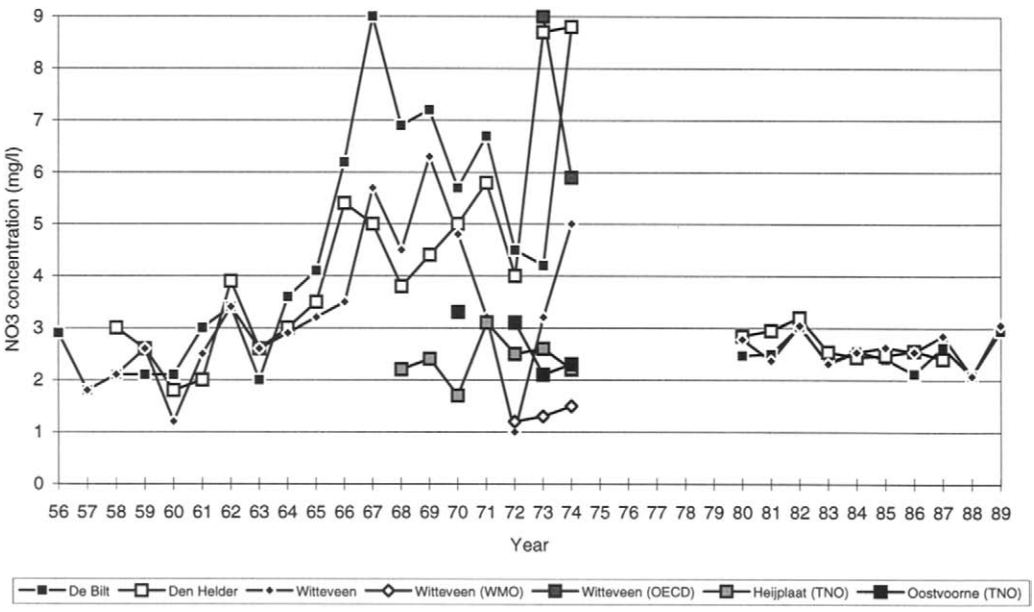

FIGURE 5.56 *(continued)* Time series of NO_3^- concentration measurements in precipitation made at several sites in the Netherlands (mg l^{-1})

A discussion on the uncertainties in measurements is needed here. Ridder (1978) analysed the data measured at several sites in order to assess the quality of the data. He found several sources of errors, especially related to the Rossby network. He found for example that samples obtained from unrelated sites (i.e. separated several hundreds of kilometres) analysed by the same laboratory showed high correlations, whereas data obtained at nearby sites, analysed by different laboratories showed no correlation at all. Furthermore, he found years where enormous amounts of precipitation were reported, as the result of administrative errors. He also found errors in the conversion of units resulting in reporting of values which are a factor of 20 too high. Furthermore, changes in the application of different sampling methods and procedures or analytical techniques could clearly be identified. The introduction of computers in 1967 did result in erroneous data handling because the punch capacity appeared to be too small.

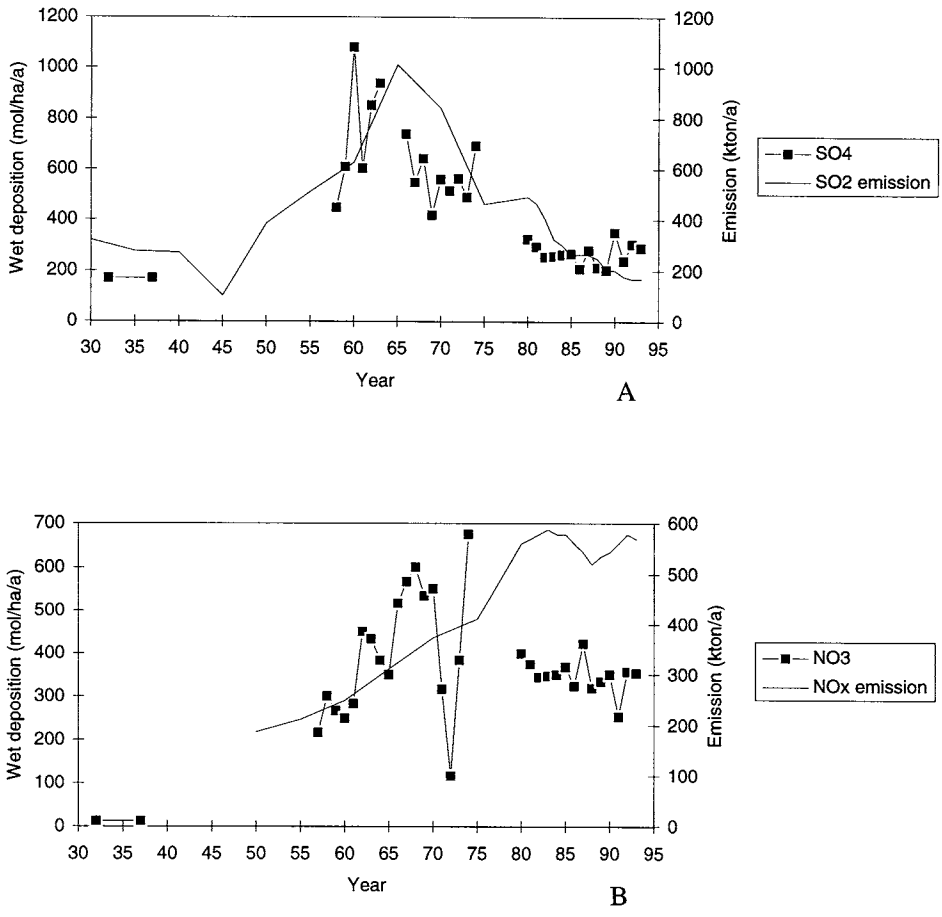

FIGURE 5.57 Time series of wet deposition measurements for (A) SO_4^{2-} and (B) NO_3^- made at Witteveen (mol ha^{-1} a^{-1}).

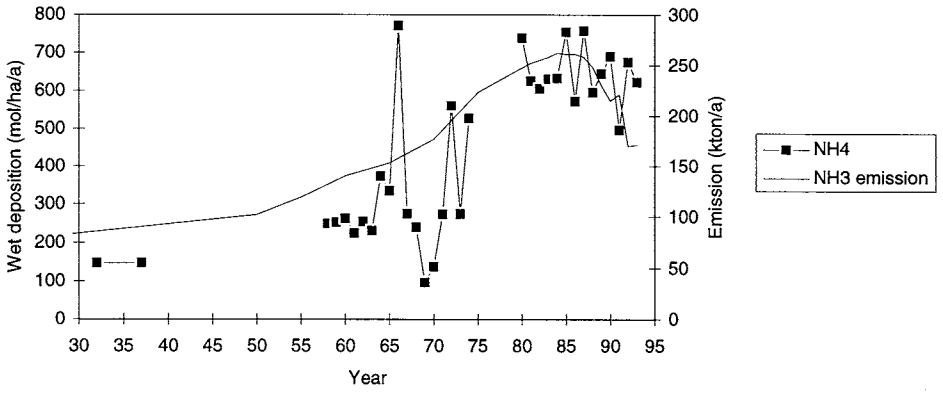

FIGURE 5.57 *(continued)* Time series of wet deposition measurements for NH_4^+ made at Witteveen (mol ha^{-1} a^{-1}).

The conclusion of Ridder was that in networks data handling should be done much more careful, that regular intercomparisons should be organised and all sorts of checks should be introduced. Most of the errors just mentioned were corrected for by Ridder when enough information was available to do so. His conclusion regarding the data as presented in Figure 5.56 and 5.57 was that the increase in NO_3^- deposition in the period 1965 - 1972 presumably refers to a real effect, though strongly enlarged by incorrect measurements. Furthermore, he states that the time series of annual average SO_4^{2-} data can be regarded as reasonably accurate. This can be derived from the fact that the variations at different sites are similar. He does not comment on the NH_4^+ data. However, Buijsman (1989) states that there is a large uncertainty in these data. This is e.g. shown by comparing data in years where two or more samplers were used at the same location. The fact that the emission variation and deposition variation in Figure 5.57 are similar could be a coincidence, but it could also be that despite the large uncertainty in the data, the increase in deposition is larger than the uncertainty and thus the difference is real.

5.4.3 NON-LINEARITIES IN TEMPORAL VARIATIONS

It has been found by Fricke and Beilke (1992) in Germany that the decrease in emissions of sulphur in western Europe from 1980 onwards has resulted in much larger decreases in observed concentrations of SO_2 in ambient air compared to the decrease in ambient SO_4^{2-}

aerosol concentrations and SO_4^{2-} precipitation concentrations. This result indicate that non-linearities play a role in determining source receptor relations. Non-linearities may be of importance when abatement strategies are based on models in which a linear relationship between emission and deposition changes in time is assumed (Hov *et al.*, 1987). Figure 5.58 shows the relative change in measured ambient SO_2 and SO_4^{2-} aerosol concentrations, rainwater SO_4^{2-} concentrations in the southern part of the Netherlands, and the estimated total SO_2 emission in the Netherlands and in Europe, between 1955 and 1990. The year 1955 was taken as the reference situation. The figure shows similar results as found by Fricke and Beilke (1992), i.e. the relative decrease in the observed SO_2 concentration is larger than that observed in SO_4^{2-} concentrations in aerosol and precipitation. The direction of the changes in sulphur concentrations in air and rain is similar to the changes in SO_2 emission but the magnitude is different. The emission in 1990 is only 40% of that in 1955, the SO_2 concentration is 54% of that in 1955, the SO_4 concentration 69%, the rainwater SO_4^{2-} concentration 76%. The measurements are effected by measuring errors and meteorological variation during the different years. However, these facts cannot explain the systematic difference in magnitude and the difference in SO_2 and SO_4^{2-} concentrations (Figure 5.58).

Several explanations for these non-linearities might be given. First of all, the concentrations in air, aerosol and precipitation are of a different origin and transported over different distances (Van Jaarsveld, 1989). The emission in the Netherlands might, therefore, not be representative for the changes in concentrations. It is estimated that only 30% of the concentration of sulphur is determined by sources in the Netherlands, the other 70% coming from abroad, mainly from Germany, Belgium, France and the UK. The changes in European emissions is also displayed in Figure 5.58. This variation, being much different from that in the Netherlands, indicates that the relative change in emission to be used in a comparison like this needs to be derived in another way. The change in emissions determining the concentrations should be compared to the measurements. Van Jaarsveld (1989) explains the difference or non-linearities by the fact that SO_2 and SO_4^{2-} (aerosol and precipitation concentrations) originate from different sources in different areas. Non-uniform changes in emissions and source characteristics would thus lead to different changes in SO_2 and SO_4^{2-} concentrations with time.

The second explanation might be that there is a non-linearity in atmospheric chemistry and cloud processes (Hov *et al.*, 1987). Cloud processes can be non-linear as the result of the nature of cloud formation but also because of cloud chemistry. Atmospheric or cloud chemistry can cause non-linearities when the components or mechanisms which lead to conversion of SO_2 to SO_4^{2-} are limiting, e.g. when the oxidising precursors are exhausted or when clouds are evaporated (H_2O_2, O_3), the pH of droplets falls below 4. In this respect, the role of ammonia might be of importance. NH_3, being an alkaline gas, provides the neutralising capacity of precipitation and aerosols and might provide an 'alkaline environment' when deposited at comparable amounts or in excess over acid-forming components.

The important role of NH_3 can clearly be shown in trends of wet and dry deposition of SO_2 in the Netherlands. Through a strong decrease in SO_2 emission during the past years in western Europe, SO_2 concentrations also show a strong decline. In most areas this has led to a decline in dry deposition of SO_2 (see Figure 5.59). However, wet deposition does not show the same decline (Figure 5.59). This might be explained by ammonia emissions which did not decrease to a large extent during the period 1955 to 1990. Ammonia can neutralise SO_2/SO_4^{2-} in the atmosphere, forming $(NH_4)_2SO_4$ particles. Before the steep decline of SO_2 emissions after 1987, SO_2 was in excess over NH_3. NH_3 was probably then the limiting factor in aerosol formation. After the emission decline, SO_2 and NH_3 are equally present in the atmosphere (see Figure 5.60), which means that aerosol formation might be limited by one or the other. The aerosol formation has not decreased, thus the availability of condensation nuclei [e.g. $(NH_4)_2SO_4$ particles] and scavenging of aerosols has not decreased. The only decrease in wet deposition of SO_4^{2-} is the decrease in below-cloud scavenging of SO_2. This is however not the most important factor determining wet deposition of SO_4^{2-}.

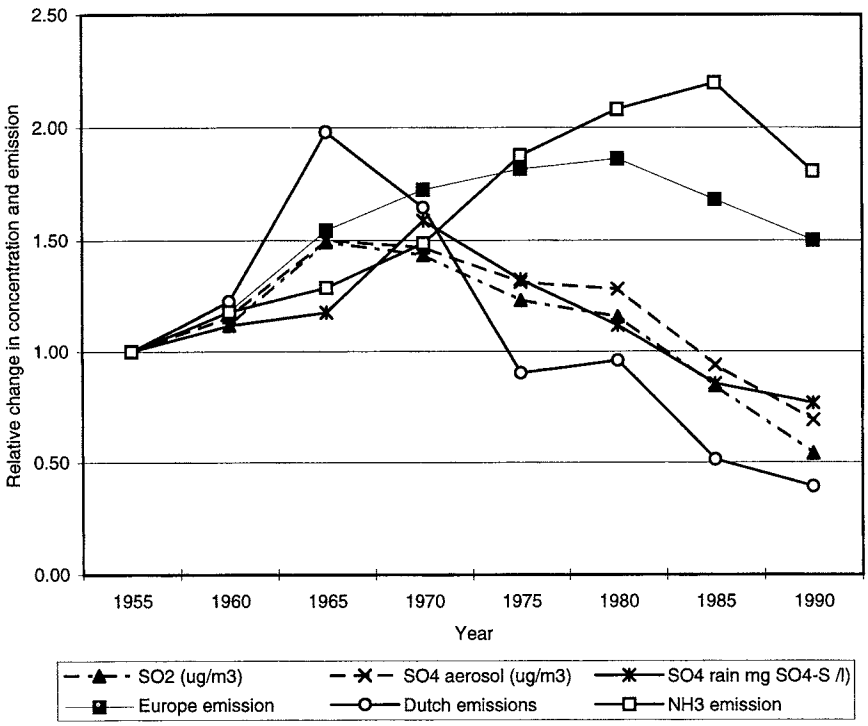

FIGURE 5.58 Relative change between 1955 and 1990 in measured concentrations of sulphur in air, aerosol and precipitation, and in estimated sulphur emissions in the Netherlands and in Europe, and in ammonia emissions in the Netherlands.

The other role of NH_3 is to provide an 'alkaline environment' when deposited. In this respect it is important to know if there is an excess of SO_2 over NH_3 in terms of deposition fluxes. Again, before the steep emission change in 1987, SO_2 was in excess of NH_3 in the Netherlands (Onderdelinden *et al.*, 1985; Erisman *et al.*, 1988). In this case, SO_2 dry deposition is limited to some extent because the surface becomes acid through which uptake of SO_2 in water layers, for example, is limited (see also discussion on co-deposition in Chapter 4). During the years after 1987 NH_3 became relatively more important in the Netherlands (see Figure 5.60), thus increasing the effect of co-deposition and increasing the SO_2 dry deposition velocity relatively to the SO_2 excess situation before 1987. This non-linear effect leads to a relative stronger decrease in SO_2 concentrations through the increase in dry deposition velocity and points in the same direction as the aerosol formation.

These results indicate that when simultaneous emission reductions in SO_2 and NH_3 are implemented, resulting in similar ratios of one gas over the other, non-linearities most probably do not play an important role.

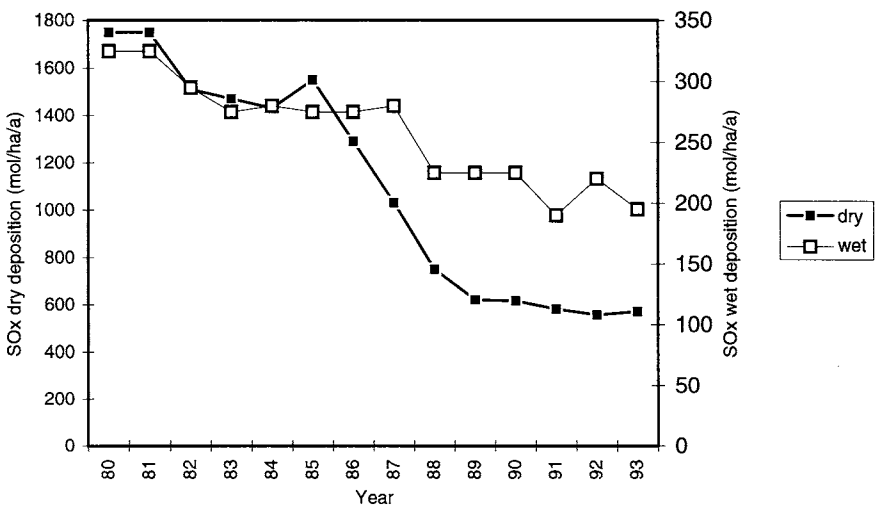

FIGURE 5.59 Wet and dry deposition of sulphur in the Netherlands over the period 1980-1993 (mol ha^{-1} a^{-1}).

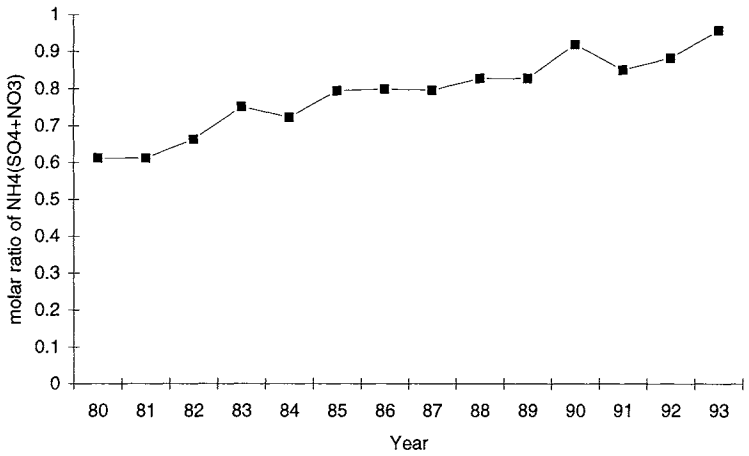

FIGURE 5.60 Ratio of NH_4^+ over (SO_4^{2-} plus NO_3^-) in precipitation in the Netherlands over the period 1980-1993.

5.5 SYNTHESIS

Inferential models were used to estimate atmospheric deposition of acidifying compounds and base cations in the Netherlands and Europe. In these models wet deposition is estimated using interpolated wet deposition measurement results. Dry deposition is estimated from interpolated air concentration measurement or model results, and land-use specific dry deposition velocities inferred using the resistance analogy. Deposition was estimated on a 5 x 5 km grid scale for the Netherlands and on a 10 x 20 km grid for Europe.

In the Netherlands, total deposition of SOx, NOy, NHx, and potential acid amounted in 1993 on average 760, 740, 2000 and 4280 mol ha^{-1} a^{-1}, respectively. Deposition of potential acid was highest in the south of the country, up to 9000 mol ha^{-1} a^{-1}. Very high values were also recorded in areas with many forests present. The deposition decreased since 1980 with 41%, mainly as the result of decreasing sulphur emissions in western Europe. Base cation deposition relevant for neutralising the acid input (Mg^{2+}, Ca^{2+} and K^{+}) amounted on the average 660 mol ha^{-1} a^{-1}. In contrast to the deposition of potential acid, base cation fluxes were highest in the north and at the west coast of the country. During recent years the base cation deposition decreased as the result of reductions in industrial emissions.

In Europe, total deposition of SOx, NOy, NHx, and potential acid in 1989 amounted on average 540, 300, 440 and 1820 mol ha^{-1} a^{-1}, respectively. Highest deposition of potential acid was found in former eastern Germany and Poland (the Black Triangle) for SOx (7000 mol ha^{-1} a^{-1}) and in the eastern part of the Netherlands and the western part of Germany for NOy (1300 mol ha^{-1} a^{-1}) and NHx (2500 mol ha^{-1} a^{-1}). Deposition of potential acid was highest in the Black Triangle, up to 16.500 mol ha^{-1} a^{-1}. Lowest values of deposition are found in the northern part of Europe, including Iceland. Deposition of SOx, NOy, NHx and total potential acid amounts 40, 20, 10 and 110 mol ha^{-1} a^{-1}, respectively in these regions. Base cation deposition in Europe relevant for neutralizing acid input amounted 730 mol ha^{-1} on average and ranged between 70 to 5160 mol ha^{-1} a^{-1}.

Natural background deposition of SOx, NOy, NHx, and potential acid was estimated around 100, 45, 70 and 280 mol ha^{-1} a^{-1}, respectively. In the Netherlands, nowadays these values are exceeded by a factor of 10, 22, 46 and 22, respectively. In some parts of Europe the natural background deposition is exceeded with a factor 20 or more.

Ancient measurements suggest that NH_4^+ and NO_3^- concentrations in rain water and ambient NH_3 air concentrations were very high in and near the large cities at the end of the 19th century, comparable to those found nowadays. NH_4^+ and NO_3^- concentrations in rainwater measured at the more rural site of Rothamsted (UK) show a gradual increase from 1880 to 1960, and a more steep increase between 1960 and 1980. Very high SO_4^{2-} concentrations were found in the (industrial) Ruhr area at the end of the 18th century. Other ancient German

measurements suggest that SO_4^{2-} concentrations in precipitation increased from 1870 to 1920. Between 1920 and 1940 concentrations remained the same, they decreased after 1940 and increased again from 1960 to 1980. After the seventies, SO_4^{2-} concentrations in precipitation decreased again. The temporal variations in wet deposition are similar to those in estimated emissions (see Figure 2.1).

Non-linearities between emission and deposition changes over time have been found. This was attributed to differences in origin, atmospheric chemistry and transport distance of the component.